

AN ASSESSMENT OF TAXOL-INDUCED APOPTOSIS  
IN MCF-7 AND MDA-MB-231 HUMAN BREAST  
ADENOCARCINOMA CELLS

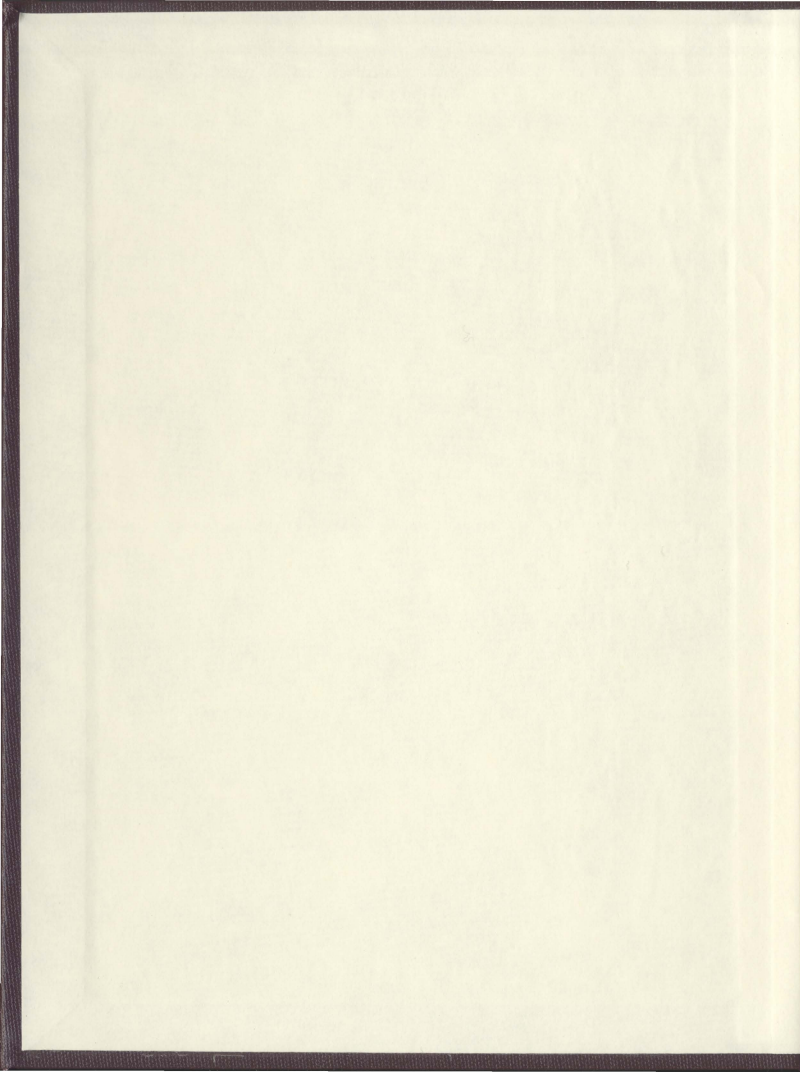
CENTRE FOR NEWFOUNDLAND STUDIES

---

**TOTAL OF 10 PAGES ONLY  
MAY BE XEROXED**

(Without Author's Permission)

KRISTA BUTT







**An Assessment of Taxol-Induced Apoptosis in MCF-7 and  
MDA-MB-231 Human Breast Adenocarcinoma Cells**

**By  
Krista Butt**

A thesis submitted to the  
School of Graduate Studies  
in partial fulfillment of the  
requirements for the degree of  
Master of Science

School of Pharmacy  
Memorial University of Newfoundland  
April 2004



St. John's

Newfoundland

*This Thesis is dedicated in loving memory of my Dad, whose  
attitude and strength were inspirational to all who knew him*

## ABSTRACT

The ability of taxol to induce apoptosis was compared in phenotypically dissimilar MCF-7 and MDA-MB-231 human breast adenocarcinoma cells. To assess this, morphological examination, PARP cleavage, and TUNEL assay was employed. Treatment of these cells with 100 nM taxol led to chromatin condensation, DNA fragmentation, and apoptosis-associated morphological changes after 3-24 hours exposure. Additionally, proteolytic cleavage of poly (ADP-ribose) polymerase was detected in MCF-7 but not MDA-MB-231 cells. To further elucidate these findings, the expression of certain apoptotic regulatory genes was also examined by western blot analysis. In MCF-7 cells, levels of Bcl-2 and p53 increased after 24 hours and 72 hours, respectively, whereas no significant change in levels of cytochrome c was found. Conversely, in MDA-MB-231 cells, levels of Bcl-2 and p53 decreased after 72 hours, whereas cytochrome c levels increased after 72 hours. These data suggest that 100 nM taxol induces apoptosis in MCF-7 and MDA-MB-231 cells, probably via a p53-dependent and independent pathway, respectively. Bcl-2 and cytochrome c, however, did not play clear roles. Increased understanding of taxol-induced apoptosis may lead to the development of more effective taxol-based chemotherapy regimens and improved clinical responses.

## ACKNOWLEDGEMENTS

I am deeply indebted to my supervisors, Drs. Lili Wang and Hu Liu, for believing in me and giving me the opportunity to study in this interesting research field. I sincerely appreciate their kindness and continuous encouragement. I also wish to thank my committee member, Dr. Philip Davis for his comments and suggestions throughout my course of study.

I am very grateful to Ms. Jieying Xiong for her invaluable support and technical assistance. I would also like to thank my colleagues, Zhili Kang, Wei Yang, Jerry Wang, Anas El-Aneed and Ravi Devraj for their friendship and support. Special thanks also to the Faculty and Staff of the School of Pharmacy for creating such a wonderful working environment.

I also wish to acknowledge the financial support provided by the School of Pharmacy and School of Graduate Studies, Memorial University of Newfoundland and MRC (now CIHR).

Finally, I feel gratitude beyond what I can express in words to my family, especially my husband Chris, for their patience, understanding and unwavering support. They have inspired me to make my good better and my better best. This work would not have materialized without their love and encouragement.

## TABLE OF CONTENTS

ABSTRACT .....	III
ACKNOWLEDGEMENTS .....	IV
TABLE OF CONTENTS .....	V
LIST OF TABLES.....	VII
LIST OF FIGURES .....	VIII
LIST OF ABBREVIATIONS.....	X
CHAPTER 1: INTRODUCTION .....	1
1.1 Cancer .....	1
1.2 Breast Cancer.....	3
1.3 Cancer Chemotherapy.....	3
1.3.1 Alkylating Agents .....	5
1.3.2 Antimetabolites.....	6
1.3.3 Antitumor Antibiotics .....	7
1.3.4 Plant-Derived Agents.....	7
1.4 Taxol.....	8
1.4.1 Chemistry of Taxol .....	9
1.4.2 Taxol Formulation and Dosing.....	10
1.4.3 Taxol-Mechanisms of Action .....	11
1.4.4 Drawbacks of Taxol .....	14
1.5 Apoptosis.....	17
1.6 Techniques to Assess Apoptosis.....	20
1.6.1 Morphological Assessment .....	21
1.6.2 Annexin V Assay .....	24
1.6.3 DNA Fragmentation.....	27
1.6.4 PARP Cleavage Assay .....	30
1.7 Regulation of Apoptosis.....	33

1.7.1	p53.....	33
1.7.2	Cytochrome c.....	36
1.7.3	Bcl-2.....	40
<b>CHAPTER 2: RESEARCH OBJECTIVES .....</b>		<b>43</b>
<b>CHAPTER 3: MATERIALS AND METHODS .....</b>		<b>45</b>
3.1	<b>Materials.....</b>	<b>45</b>
3.2	<b>Methods.....</b>	<b>46</b>
3.2.1	Cell Culture.....	46
3.2.2	Preparation of Taxol Working Solutions.....	47
3.2.3	Assessment of Cytotoxicity.....	48
3.2.4	Morphological Examination.....	51
3.2.5	TUNEL Assay.....	53
3.2.6	Extraction of Protein from MCF-7 and MDA-MB-231 Cells.....	54
3.2.7	Bio-Rad DC Protein Assay.....	55
3.2.8	Western Blot.....	56
3.2.9	Statistical Analysis.....	59
<b>CHAPTER 4: RESULTS.....</b>		<b>60</b>
4.1	<b>Cytotoxicity of DMSO and Taxol in MCF-7 and MDA-MB-231 Cells .....</b>	<b>60</b>
4.2	<b>Morphological Changes Evaluated by Light Microscopy .....</b>	<b>67</b>
4.3	<b>Chromatin Condensation Analyzed by Fluorescence Microscopy.....</b>	<b>80</b>
4.4	<b>DNA Fragmentation Assessed by TUNEL Assay .....</b>	<b>93</b>
4.5	<b>Apoptosis-Related Proteolytic Cleavage of PARP .....</b>	<b>109</b>
4.6	<b>Expression of p53 in MCF-7 and MDA-MB-231 Cells .....</b>	<b>112</b>
4.7	<b>Expression of Bcl-2 in MCF-7 and MDA-MB-231 Cells .....</b>	<b>117</b>
4.8	<b>Expression of Cytochrome c in MCF-7 and MDA-MB-231 Cells .....</b>	<b>122</b>
<b>CHAPTER 5: DISCUSSION AND CONCLUSIONS .....</b>		<b>127</b>
<b>CHAPTER 6: REFERENCES .....</b>		<b>133</b>

## LIST OF TABLES

Table 1.1. Differential Features and Significance of Necrosis and Apoptosis .....	19
Table 4.1. IC <sub>50</sub> Values of Taxol in MCF-7 and MDA-MB-231 Cells .....	66

## LIST OF FIGURES

Figure 1.1. Multistage Progression to Malignancy .....	2
Figure 1.2. Chemical Structure of Taxol .....	9
Figure 1.3. Mechanism of Action of Taxol .....	12
Figure 4.1. Cytotoxicity of DMSO in MCF-7 Cells .....	62
Figure 4.2. Cytotoxicity of DMSO in MDA-MB-231 Cells .....	63
Figure 4.3. Cytotoxicity of Taxol in MCF-7 Cells.....	64
Figure 4.4. Cytotoxicity of Taxol in MDA-MB-231 Cells.....	65
Figure 4.5. Representative Photomicrographs Demonstrating Morphological Changes of MCF-7 Cells Undergoing Apoptosis Induced by 100 nM Taxol.....	68
Figure 4.6. Representative Photomicrographs Demonstrating Morphological Changes in MDA-MB-231 Cells Undergoing Apoptosis Induced by 100 nM Taxol.....	74
Figure 4.7. Representative Fluorescence Photomicrographs of MCF-7 Cells Stained with Hoechst 33342.....	81
Figure 4.8. Representative Fluorescence Photomicrographs of MDA-MB-231 Cells Stained with Hoechst 33342.....	87
Figure 4.9. Representative Fluorescence Photomicrographs of MCF-7 Cells Stained Using the TUNEL Procedure.....	95
Figure 4.10. Representative Fluorescence Photomicrographs of MDA-MB-231 Cells Stained Using the TUNEL Procedure.....	101
Figure 4.11. Percentage of Apoptotic MCF-7 Cells Determined Utilizing the TUNEL Procedure.....	107

Figure 4.12. Percentage of Apoptotic MDA-MB-231 Cells Determined Utilizing the TUNEL Procedure.....	108
Figure 4.13. Assessment of PARP Cleavage in MCF-7 Cells.....	110
Figure 4.14. Assessment of PARP Cleavage in MDA-MB-231 Cells.....	111
Figure 4.15. Expression of p53 in MCF-7 Cells.....	113
Figure 4.16. Expression of p53 in MDA-MB-231 Cells.....	115
Figure 4.17. Expression of Bcl-2 in MCF-7.....	118
Figure 4.18. Expression of Bcl-2 in MDA-MB-231 Cells.....	120
Figure 4.19. Expression of Cytochrome c in MCF-7 Cells.....	123
Figure 4.20. Expression of Cytochrome c in MDA-MB-231 Cells.....	125

## LIST OF ABBREVIATIONS

AIDS	acquired immunodeficiency syndrome
ANT	adenine nucleotide translocator
APAF	apoptosis-activating factor
APS	ammonium persulfate
ATP	adenosine triphosphate
BH	Bcl-2 homology
BSA	bovine serum albumin
Caspases	cysteine-aspartic acid specific proteases
DAPI	4', 6-diamidino-2-phenylindole
DIC	differential interference contrast
DMEM	Dulbecco's modified Eagle's medium
DMSO	dimethyl sulfoxide
DNA	deoxyribonucleic acid
DTT	dithiothreitol
ECL	enhanced chemilumiscence
EDTA	ethylenediamine tetraacetic acid
FBS	fetal bovine serum
FDA	Food and Drug Administration
FITC	fluorescein isothiocyanate
HMW	high molecular weight
IC <sub>50</sub>	concentration of drug causing 50% cell growth inhibition

IgG	immunoglobulin G
kbp	kilobase pair
kDa	kilodalton
mAb	monoclonal antibody
MDR	multidrug resistant
MTT	3-(4,5-dimethylthiazol-2-yl)-2,5-diphenyltetrazolium bromide
NCI	National Cancer Institute
O.D.	optical density
PAGE	polyacrylamide gel electrophoresis
PARP	poly(ADP-ribose)polymerase
PBS	phosphate-buffered saline
PI	propidium iodide
PMSF	phenylmethylsulfonyl fluoride
PS	phosphatidylserine
PTP	permeability transition pore
RNA	ribonucleic acid
ROS	reactive oxygen species
SD	standard deviation
SDS	sodium dodecyl sulfate
TdT	terminal deoxynucleotidyl transferase
TEMED	N,N,N',N'-tetramethylethylenediamine
TMR	tetra-methyl rhodamine

- TUNEL      terminal deoxynucleotidyl transferase mediated d-UTP nick end  
              labeling
- VDAC        voltage dependent anion channel

## CHAPTER 1: INTRODUCTION

### 1.1 Cancer

Cancer is a devastating disease, claiming the lives of thousands of people each year. An estimated 139,900 new cases of cancer and 67,400 deaths from cancer will occur in Canada in 2003 (National Cancer Institute of Canada, 2003). Furthermore, an average of 2,690 Canadians will be diagnosed with cancer and 1,296 will die of cancer every week. Cancer is also the leading cause of premature death in Canada, being responsible for almost 31% of all potential years of life lost.

It has been recognized for many years that cancer is a genetic disease (MacDonald, F., *et al.*, 1997; Nowell, P.C., 1976). Cancer arises from a single cell that has undergone a mutation, which gives the cell some heritable form of growth advantage. The initial mutation will cause the cells to divide to produce a genetically homogenous population of cells. Further mutations will in turn occur, enhancing the cell's growth potential. These mutations give rise to subclones with different properties within the tumor. Consequently, most tumors are heterogenous.

Cancer development exhibits a multistage nature (MacDonald, F., *et al.*, 1997; Nowell, P.C., 1976). In 1949, Berenblum and Shubik concluded that carcinogenesis was at least a two-stage process. In 1954, Armitage and Doll took this observation a step further and concluded that carcinogenesis was at least a six or seven stage process. Furthermore, in 1957, Foulds showed that tumor progression occurred in a stepwise fashion. From these observations, it is clear that malignancy occurs via a multistage progression, although each of the steps cannot always be defined in an individual tumor

(Figure 1.1.). The initial step of the multistage progression to malignancy is thought to be caused by some form of genotoxic agents such as radiation or a chemical carcinogen. The cells at this stage are phenotypically normal, although they have altered deoxyribonucleic acid (DNA). Further mutations lead to the emergence of clones with additional properties associated with tumor cell progression. Finally, additional changes allow the outgrowth of clones with metastatic potential. Animal models of carcinogenesis have enabled these steps to be classified as initiation, promotion, malignant transformation and metastasis.

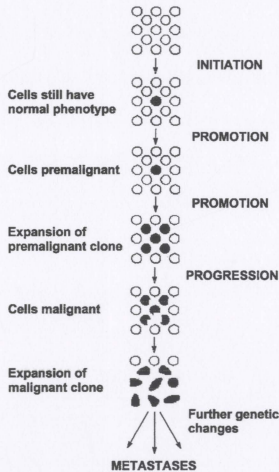


**Figure 1.1. Multistage Progression to Malignancy**

(MacDonald, F., *et al.*, 1997; Nowell, P.C., 1976)

## 1.2 Breast Cancer

Breast cancer is the most frequently diagnosed cancer in Canadian women, accounting for almost 1 in 3 cancer diagnoses ([www.cancer.ca/ccs](http://www.cancer.ca/ccs)). The Canadian Cancer Society estimates that in 2003, an estimated 21,200 women will be diagnosed with breast cancer and 5,300 will die of the disease.

Despite these grim statistics, the etiology of breast cancer remains poorly understood. It is known that a complex interplay between hereditary and environmental factors initiate and/or promote the disease. Factors associated with an increase risk include early age of menarche and late stage of menopause, nulliparity, late age of first time pregnancy, family history of breast cancer and having the mutated breast cancer genes BRCA1 or BRCA 2 (Campbell, J.B., 2002; Arver, B., *et al.*, 2000; Carolin, K.A., *et al.*, 2000; Hsieh, T., *et al.*, 1999). The effects of diet, physical activity, obesity, alcohol, hormone replacement therapy and smoking are under study.

## 1.3 Cancer Chemotherapy

There are a number of effective treatment modalities for cancer, including surgery, radiation therapy and chemotherapy. Surgery is often the first step in cancer treatment because it's used to both diagnose and treat cancer (Merrick, H.W., 1995; Skeel (a), R.T., 1995). Surgery is often utilized to obtain representative tissue so that accurate diagnosis can be made. Once a cancer diagnosis is confirmed, surgery is often chosen as the treatment modality if the cancer is limited to one area and it's anticipated that all the cancer cells can be removed without harming vital structures. Surgery is also used to

reduce the size of large tumors so that follow-up treatment by radiation therapy or chemotherapy will be more effective. In addition to curing cancer, surgery is used as a preventive measure by removing precancerous conditions. Furthermore, surgery may be recommended as a palliative measure to help reduce pain and other symptoms.

Radiation therapy is also used for the treatment of local disease. It may be employed when surgery cannot remove all the cancer or there is potential to compromise normal structures and functions (Skeel (a), R.T., 1995). Radiation therapy can be used in conjunction with other treatment options such as surgery. Doctors may use radiation before surgery to shrink a tumor, thus making it easier to remove. In addition, radiation therapy may be used after surgery to stop the growth of cancer cells that may remain. Furthermore, radiation therapy may be recommended as a palliative measure to shrink tumors and reduce pressure, pain, and other symptoms of cancer. Once cancer has metastasized to other areas of the body, however, both radiation therapy and surgery are ineffective. In such instances, chemotherapy is often chosen.

The primary role of chemotherapy is in the treatment of cancer that is no longer confined to one area and has spread systemically (Cella, D.F., 1995; Skeel (a), R.T., 1995). If possible, chemotherapy is used to cure the cancer. If a cure is not possible, chemotherapy is used to control the disease, by shrinking the tumor mass or by reversing or slowing the rate of progression, in order to extend the life of the patient. Sometimes control is unlikely, particularly if the cancer is in an advanced stage. In this case, chemotherapy is used as a palliative measure to relieve symptoms of cancer. Furthermore, chemotherapy is used in conjunction with other treatment modalities. For

instance, it may be used to shrink a tumor before surgery or radiation therapy.

Chemotherapy can also be employed to destroy any cancer cells that may be remaining after surgery and/or radiation therapy. In some cases, chemotherapy can make other treatment modalities such as radiation therapy more effective.

Chemotherapeutic agents comprise a wide variety of drugs. They are customarily divided into several classes and within each class there are several types of agents. Examples of the classes of chemotherapeutic agents include alkylating agents, antimetabolites, antitumor antibiotics and plant-derived agents.

### **1.3.1 Alkylating Agents**

The alkylating agents are a diverse group of polyfunctional compounds that have the ability to substitute alkyl groups for hydrogen ions (Skeel (b), R.T., 1995; May, D.M., *et al.*, 1994). These compounds react with a number of nucleophilic groups, such as phosphate, amino, hydroxyl, sulfhydryl, carboxyl and imidazole groups. At neutral or alkaline pH, alkylators ionize and generate positively charged ions that attach to susceptible nuclear proteins, particularly the N-7 position of guanine. This alkylation reaction leads to abnormal base pairing, cross-linking of DNA, interference with DNA replication and ribonucleic acid (RNA) transcription. Consequently, these effects result in interruption in cell's normal functions.

The alkylating agents are cell cycle phase-nonspecific in that they exert their activity regardless of the specific phase of the cell cycle (Skeel (b), R.T., 1995; May, D.M., *et al.*, 1994). Alkylating agents include nitrogen mustards, ethylenimine

derivatives, alkyl sulfonates, triazine, nitrosoureas and metal salts. They are important in such cancers as acute and chronic leukemias, Hodgkin's disease, non-Hodgkin's lymphoma, multiple myeloma, primary brain tumors, malignant melanoma and carcinomas of the breast, ovaries, testes, lungs, bladder, cervix, head, and neck.

### **1.3.2 Antimetabolites**

The antimetabolites are a group of low molecular weight compounds that interfere with metabolic processes vital to the physiology and proliferation of cancer cells (Skeel (c), R.T., *et al.*, 1995; DeLap, R.J., 1994). They exert these effects due to their structural or functional similarity to naturally occurring metabolites involved in nucleic acid synthesis. Almost all of the currently used antimetabolites inhibit the synthesis of purine or pyrimidine nucleotides and/or directly inhibit the enzymes of DNA replication. Many antimetabolites also interfere with RNA and ribonucleotide synthesis, amino acid metabolism and protein synthesis.

Because of their primary effect on DNA synthesis, antimetabolites are cell cycle phase-specific (Skeel (c), R.T., 1995; DeLap, R.J., 1994). They include folic acid analogs, pyrimidine analogs and purine analogs. Antimetabolites are used in the treatment of various cancers including carcinomas of the breast, bladder and colon, acute and chronic leukemias, and non-Hodgkin's lymphoma.

### 1.3.3 Antitumor Antibiotics

The antitumor antibiotics constitute a heterogenous group of chemotherapeutic agents that affect the function and synthesis of nucleic acids through various mechanisms including DNA strand scissions, topoisomerase II-dependent cleavage, DNA intercalation, cross-linking of DNA strands, and inhibition of RNA synthesis (Skeel (d), R.T., 1995; Kobayashi, K., *et al.*, 1994).

The antitumor antibiotics include anthracyclines (doxorubicin, daunorubicin and idarubicin), mitomycin C, bleomycin, dactinomycin and plicamycin (Skeel (d), R.T., 1995; Kobayashi, K., *et al.*, 1994). They are important in the treatment of a wide variety of cancers, including carcinomas of the breast, lung, thyroid and stomach, as well as Hodgkin's disease, non-Hodgkin's lymphoma, myeloma, acute lymphocytic and myelogenous leukemia, and sarcomas of various sites.

### 1.3.4 Plant-Derived Agents

Plants are considered a valuable resource for the discovery and development of novel, naturally derived agents. To date, several plant-derived anticancer drugs are administered as part of standard chemotherapeutic regimens, including etoposide, the vinca alkaloids and taxol (Agarwala, S.S., 1994). Plant-derived agents exert their neoplastic effects through several mechanisms including inactivation of topoisomerase II, promotion of microtubule assembly and binding of tubulin. These agents are widely used in the therapy of the leukemias, Hodgkin's disease, non-Hodgkin's lymphoma, testicular

cancer, small cell lung cancer, breast cancer, refractory ovarian carcinoma and childhood tumors.

#### 1.4 Taxol

Taxol is one of the most intriguing anticancer drugs to enter the clinical arena in many years. It was discovered as part of the new cancer drugs screening and discovery program of the U.S. National Cancer Institute (NCI) in the 1960s (Panchagnula, R., 1998). In this program, the NCI collected and screened more than 35,000 plant specimens from around the world with the hope of discovering new cytotoxic entities (Bissett, D., *et al.*, 1993). Among these was the crude extract from the bark of the *Taxus brevifolia* (Pacific or Western Yew). This extract showed antitumor activity against several cancer cell lines and the chemical structure of the active ingredient was identified as taxol (Panchagnula, R., 1998). Despite its novel structure, and apparent *in vitro* activity, little interest was shown in developing taxol further at that time due to its scarcity, problems with formulation and the mistaken assumption that its mechanism of action was similar to that of other microtubule-affecting agents, such as the vinca alkaloids (Panchagnula, R., 1998; Bissett, D., *et al.*, 1993). However, following the discovery of taxol's unique mechanism of action in 1979, interest was rekindled and the first clinical trials began in 1983. Since then, taxol has been approved by the U.S. Food and Drug Administration (FDA) to treat ovarian, breast and non-small lung carcinomas as well as acquired immunodeficiency syndrome (AIDS) related Kaposi's sarcoma (He, L., 2001; Rowinsky, E.K., 1997).

### 1.4.1 Chemistry of Taxol

The chemical name of taxol is 5 $\beta$ , 20-epoxy-1, 2 $\alpha$ , 4, 7 $\beta$ , 10 $\beta$ , 13 $\alpha$ -hexahydroxytax-11-en-9-one 4, 10-diacetate-2-benzoate 13-ester with (2R, 3S)-N-benzoyl-3-phenylisoserine (Panchagnula, R., 1998). It occurs as a white to off-white crystalline powder with the empirical formula C<sub>47</sub>H<sub>51</sub>NO<sub>14</sub> and a molecular weight of 853.9 daltons (Kohler, D.R., *et al.*, 1994). Structurally, taxol differs from other currently available anticancer drugs (Gregory R.E., *et al.*, 1993; Kingston, D.G.I., 1991). It is a complex diterpene molecule with a taxane ring structure fused with a four-membered oxetane ring, an ester side chain at C-13 and a benzoyl side-chain at the C-2 position (Figure 1.2.) (Burris, H.A. 3<sup>rd</sup>, 1994). Structure-activity relationships have determined that both the intact taxane ring and the ester side-chain are essential for cytotoxicity (Kingston, D.G.I., 1994; Guéritte-Voegelein, F., *et al.*, 1991; Kingston, D.G.I., 1991).

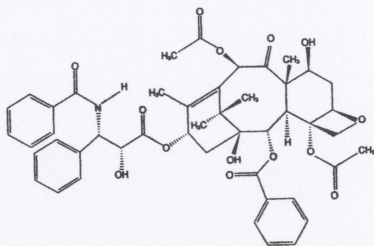


Figure 1.2. Chemical Structure of Taxol

(Burris, H.A. 3<sup>rd</sup>, 1994)

#### 1.4.2 Taxol Formulation and Dosing

A major problem encountered in the development of taxol for clinical use was its insolubility in water (Dorr, R.T., 1994). As a result, taxol is formulated in 50% cremophor EL and 50% ethanol for intravenous administration (Bissett, D., *et al.*, 1993). Cremophor EL, a non-ionic surfactant, is a polyoxyethylated castor oil that has been used to dissolve several other water-insoluble drugs, including cyclosporine, teniposide and diazepam (Dorr, R.T., 1994). Despite its widespread use as a vehicle for many drugs, cremophor EL has been implicated in a variety of toxic side effects and is thought to be responsible for the hypersensitivity reactions seen in some patients undergoing taxol treatment (He, L., *et al.*, 2001; Rowinsky, E.K., 1997). As a result, premedication with corticosteroids and antihistamines is mandatory prior to chemotherapy with taxol and has reduced the incidence of serious hypersensitivity reactions to less than 5% (Bissett, D., *et al.*, 1993; Rowinsky, E.K., *et al.*, 1993; Weiss, R.B., *et al.*, 1990). In cases of severe hypersensitivity reactions, it has been advised that taxol should be discontinued immediately (Kohler, D.R., *et al.*, 1994; Gregory, R.E., *et al.*, 1993). Many efforts have been made through chemical modification to increase taxol's aqueous solubility while retaining cytotoxic activity, but as of yet these analogues have not clinically replaced the taxol:cremophor EL formulation.

Paclitaxel® (the only available formulation of taxol) is formulated as a clear, colorless to slightly yellow viscous and concentrated solution containing 6 mg/mL taxol, 527 mg/mL cremophor EL polyoxyethylated castor oil and 49.7% (v/v) dehydrated alcohol, USP (Panchagnula, R., 1998; Goldspiel, B.R., 1994). Taxol is packaged in a

single dose of 5 mL per vial containing 30 mg of taxol (Kohler, D.R., *et al.*, 1994). Prior to administration by intravenous infusion, taxol concentrate is diluted for injection with 0.9% sodium chloride injection or 5% dextrose injection or 5% dextrose and 0.9% sodium chloride injection, or 5% dextrose in Ringer's injection to a final taxol concentration of 0.3-1.2 mg/mL (Panchagnula, R., 1998). Taxol is then infused intravenously at a dose of 135 or 175 mg/m<sup>2</sup> as a 3- or 24-hour-infusion every 3 weeks. Larger doses and longer infusion periods have also been used. However, optimal dosage and schedule for taxol as a single agent and in combination chemotherapy has not yet been established (Goldspiel, B.R., 1994).

#### **1.4.3 Taxol-Mechanisms of Action**

Taxol has a unique mechanism of action that differs from that of other anticancer drugs. The target of taxol is microtubules, which are essential self-assembling and self-disassembling proteins that are involved in various cellular functions, such as motility, ingestion of food, regulation of cell form, sensory transduction and spindle formation during cell division (Panchagnula, R., 1998; Kohler, D.R., *et al.*, 1994; Horwitz, S.B., 1992; Manfredi, J.J., *et al.*, 1984). At any time during the course of the cell cycle, there is a constant state of dynamic equilibrium between microtubules and tubulin dimers, the structural units polymerized to form microtubules (Kohler, D.R., *et al.*, 1994). Taxol disrupts this dynamic equilibrium, shifting it toward microtubule assembly, by aiding the polymerization of tubulin dimers to form microtubules, even in the absence of factors that are normally required for microtubule assembly (e.g. guanosine 5'-triphosphate and

microtubule-associated proteins) and then stabilizes the microtubules against conditions favoring depolymerization, such as low temperature and high calcium concentrations (Figure 1.3.) (He, L., *et al.*, 2001; Panchagnula, R., 1998; Kohler, D.R., *et al.*, 1994). This results in the formation of abnormal cytoskeletal structures that are not only very stable but also dysfunctional (Rowinsky, E.K., *et al.*, 1995; Jordan, M.A., *et al.*, 1993). These *in vitro* activities are facilitated by the binding of taxol within the NH<sub>2</sub>-terminal 31 amino acids of  $\beta$ -tubulin (Rao, S., *et al.*, 1994). Although the precise mechanism of action of taxol is not entirely clear, it is thought that taxol induces cytotoxicity by blocking the cell cycle at G<sub>2</sub> or M phase, thereby inhibiting cell replication and mitosis (Panchagnula, R., 1998; Kohler, D.R., *et al.*, 1994).

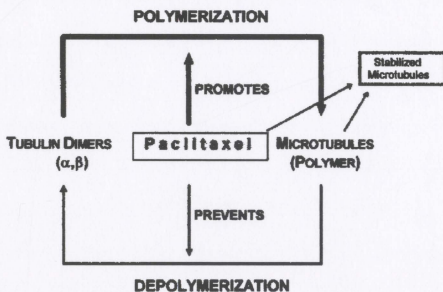


**Figure 1.3. Mechanism of Action of Taxol**

(Panchagnula, R., 1998)

Even though the principle cellular target for taxol is the tubulin/microtubule system, recent studies have demonstrated an increasing number of nonmicrotubule effects (Fojo, T., *et al.*, 2000). Taxol has been demonstrated to inhibit tumor angiogenesis, an event critical for supporting tumor growth and progression (Blajeski, A.L., *et al.*, 2001; Lau, D.H., *et al.*, 1999; Klauber, N., *et al.*, 1997; Belotti, D., *et al.*, 1996). In addition, taxol induces expression of tumor necrosis factor- $\alpha$ , activates early response genes and alters macromolecular trafficking through the nuclear pore complex (Blajeski, A.L., *et al.*, 2001; Theodoropoulos, P.A., *et al.*, 1999; Moos, P.J., *et al.*, 1998; Burkhart, C.A., *et al.*, 1994). Numerous studies have also demonstrated activation of a variety of signal transduction pathways, including Raf-1 and c-Jun N-terminal kinase following addition of taxol (Blajeski, A.L., *et al.*, 2001; Fojo, T., *et al.*, 2000; Shtil, A.A., *et al.*, 1999; Amato, S.F., *et al.*, 1998; Blagosklonny, M.V., *et al.*, 1996). Additionally, several laboratories have demonstrated that taxol is able to induce internucleosomal DNA fragmentation and other characteristic features of apoptosis (Blajeski, A.L., *et al.*, 2001; Fan, W., 1999; Saunders, D.E., *et al.*, 1997; McCloskey, D.E., *et al.*, 1996; Liu, Y., *et al.*, 1995). Furthermore, reports have indicated that taxol has numerous effects on proteins involved in apoptosis, such as the phosphorylation of Bcl-2, an event that abrogates its antiapoptotic activity (Blagosklonny, M.V., 2001; Cheng, S.C., *et al.*, 2001; Haldar, S., *et al.*, 1996; Blagosklonny, M.V., *et al.*, 1996). These results suggest that taxol possesses the ability to induce apoptosis. Specifically, research groups have reported that taxol can induce apoptosis in MCF-7 and MDA-MB-468 human breast cancer cells (Saunders,

D.E., *et al.*, 1997; McCloskey, D.E., *et al.*, 1996). Whether these are primary effects of taxol or secondary effects of other alterations remain to be elucidated.

#### **1.4.4 Drawbacks of Taxol**

##### **1.4.4.1 Development of Drug Resistance**

Two mechanisms of acquired resistance to taxol have been characterized (Kohler, D.R., *et al.*, 1994; Kuhn, J.G., 1994; Rowinsky, E.K., 1993). The first mechanism involves the development of altered  $\alpha$ - and  $\beta$ -tubulin proteins, which impair the ability of tubulin dimers to polymerize to form microtubules. These cells lack normal microtubules in their mitotic spindles when grown in the absence of taxol. Subsequently, these cells become partly or completely dependent on the presence of taxol for microtubule assembly to progress normally. As a result, this mechanism of resistance confers 2- to 3-fold taxol resistance. The second mechanism of acquired taxol resistance involves the multidrug resistance (MDR) phenotype, which gives varying degrees of cross-resistance to taxol and many other classes of drugs, including the vinca alkaloids, colchicines, doxorubicin, daunorubicin, and etoposide. The presence of this phenotype results in a decreased accumulation of drug within the cell due to an overexpression of P-glycoprotein, a transmembrane protein which functions as a drug efflux pump. Cell lines expressing the MDR phenotype have been developed that are 800-fold resistant to taxol.

#### 1.4.4.2 Availability of Taxol

Throughout its development, taxol has been greatly hampered by the limited supply of its source materials. Until recently, the only source of taxol was from the bark of the *Taxus brevifolia* (Pacific or Western Yew) (Blume, E., 1991). The Yew is a slow growing tree which dies once its bark is removed, thus making it difficult to obtain enough taxol to meet the demands (Panchagnula, R., 1998; Kohler, D.R., *et al.*, 1994). In recent years, improvements have been made in production technology to increase the supply of taxol from the Yew's bark (Panchagnula, R., 1998). But still, 3000 trees must be sacrificed in order to obtain 1 kg of taxol, enough to treat about 500 people (Panchagnula, R., 1998; Blume, E., 1989).

In an attempt to alleviate the drug supply problem, research programs were implemented to evaluate alternative sources of taxol (Kohler, D.R., *et al.*, 1994). A semisynthetic method using a precursor, baccatin III, extracted from the needles and twigs of more prevalent Yews, including ornamental and commercially cultivated varieties has been developed (Panchagnula, R., 1998; Kohler, D.R., *et al.*, 1994). Since twigs and needles are renewable and does not cause the death of the tree, this method provides a means to ensure continuing supplies of taxol. For example, Docetaxel (Taxotere®), a semisynthetic analogue of taxol, is produced by attaching a semisynthetic side-chain to 10-deacetylbaccatin III, which is readily available, in yields of about 1 kg per 3000 kg of needles, from *Taxus baccata* (European Yew) (Panchagnula, R., 1998). Docetaxel inhibits microtubule depolymerization in a similar manner to taxol and was

shown to have a broad spectrum of activity in preclinical studies (Ringel, I., *et al.*, 1991; Bissery, M.C., *et al.*, 1991).

*Taxus* cell culture, by a fungal endophyte, *Taxomyces andreanae*, is also a promising approach to meeting the growing demands for taxol (Panchagnula, R., 1998; Kohler, D.R., *et al.*, 1994; Stierle, A., *et al.*, 1993). Although the amount of taxol produced with this technique is low, studies have shown that the addition of methyl jasmonate, which plays an important role in signal transduction, can increase the production of taxol and baccatin III (Panchagnula, R., 1998). Sustained production of taxol by semicontinuous perfusion nodule cultures also appears to be another approach to produce large quantities. Although this is a relatively new research area, the results are very promising and the technique appears to be a bright prospect for increasing production of taxol and baccatin III.

Although the total synthesis of taxol has been achieved, its synthesis on an industrial scale is very difficult and may not be commercially feasible (Panchagnula, R., 1998; Nicolaou, K.C., *et al.*, 1994). Furthermore, taxol analogues are also a challenge due to the construction of the taxane framework with a four-membered oxetane ring and an ester side chain at C-13, both of which are essential for cytotoxic activity (Panchagnula, R., 1998). Thus, with today's technology, the replacement of natural sources of taxol with totally synthetic taxol does not seem to be commercially feasible. Consequently, major efforts are under way to develop taxol using the former approaches.

#### 1.4.4.3 Delivery Problems

Another major hurdle for successful treatment with taxol is its delivery. Since taxol is insoluble in water, it is formulated in 50% cremophor EL and 50% ethanol for intravenous administration (Panchagnula, R., 1998; Goldspiel, B.R., 1994; Bissett, D., *et al.*, 1993). However, it is obvious from the problems seen in present-day therapy, such as toxic side effects and hypersensitivity reactions, the necessity of developing an improved delivery system for taxol that is devoid of cremophor EL (Panchagnula, R., 1998).

Researchers are also searching for formulations that would allow production on a larger scale and stability for longer periods of time. Several attempts have been made to deliver taxol by newer drug delivery systems such as nanocapsules, liposomes, enzyme-activatable prodrugs in conjugation with antibodies, albumin conjugates, parenteral emulsion, water-soluble prodrugs, microspheres and cyclodextrins. However, these drug delivery systems have had only limited success. None of these have reached the stage of replacing cremophor-based vehicles in clinical situations. The search for newer drug delivery systems for taxol is an ongoing project.

### 1.5 Apoptosis

Based on morphological, biochemical, and molecular criteria, two distinct modes of cell death can be recognized: apoptosis and necrosis (Gorczyca, W., *et al.*, 1998; Kerr, J.F.R., *et al.*, 1972). Apoptosis, from the Greek word for, "dropping off" or "falling off" of petals from flowers or leaves from trees, is used to describe a process in which a cell actively participates in its own demise (Gorczyca, W., *et al.*, 1998; Yeh, E.T.H., 1998). It

is recognized to play crucial roles in a wide variety of normal physiological processes including embryogenesis, development, and tissue homeostasis of multicellular organisms (Pinton, P., *et al.*, 2001; Kerr, J.F.R., *et al.*, 1972). Moreover, dysregulation of apoptosis has broad ranging pathological manifestations and has been associated with Alzheimer's, Hodgkin's, transplant rejection, cancer and AIDS (Kitamura, Y., *et al.*, 1998; Lin, T., *et al.*, 1998; Wang, L., *et al.*, 1998; Lorenzen, J., *et al.*, 1997; Thompson, C.B., 1995; Carson, D.A., *et al.*, 1993). Consequently, apoptosis is a process of major biomedical interest.

Necrosis, which typically occurs as a result of gross injury to the cell, is distinct from apoptosis in a number of important ways (Darzynkiewicz, Z., *et al.*, 1997). Necrosis is a chaotic process and lacks the tight regulation and organization of apoptosis (Dixon, S.C., *et al.*, 1997). Furthermore, it's an unplanned, passive process as opposed to apoptosis, which is an active process requiring the participation of affected cells in their own death (Gorczyca, W., *et al.*, 1998). Another primary difference between these two modes of cell death is the physical and biochemical factors that either suppress or induce an inflammatory reaction (Dixon, S.C., *et al.*, 1997). Necrotic cell death begins with the swelling of the cell and mitochondrial contents, followed by rupture of the plasma membrane (Darzynkiewicz, Z., *et al.*, 1998; Majno, G., *et al.*, 1995). As a result, necrosis can trigger an inflammatory reaction in the surrounding tissue and often results in scar formation due to the release of cytoplasmic contents. In contrast, in apoptosis, the dying cells become fragmented into "apoptotic bodies" which are rapidly eliminated by phagocytic cells without eliciting inflammatory damage to surrounding cells. These and

other morphological, biochemical and pathological characteristics that differentiate these two modes of cell death are described in Table 1.1.

Necrosis	Apoptosis
<p><b>Morphological features</b></p> <ul style="list-style-type: none"> <li>Loss of membrane integrity</li> <li>Begins with swelling of cytoplasm and mitochondria</li> <li>Ends with total cell lysis</li> <li>No vesicle formation, complete lysis</li> <li>Disintegration (swelling of organelles)</li> </ul>	<ul style="list-style-type: none"> <li>Membrane blebbing, but no loss of integrity</li> <li>Aggregation of chromatin at the nuclear membrane</li> <li>Begins with shrinking of cytoplasm and condensation of nucleus</li> <li>Ends with fragmentation of cell into smaller bodies</li> <li>Formation of membrane bound vesicles (apoptotic bodies)</li> <li>Mitochondria become leaky due to pore formation involving proteins of the bcl-2 family</li> </ul>
<p><b>Biochemical features</b></p> <ul style="list-style-type: none"> <li>Loss of regulation of ion homeostasis</li> <li>No energy requirement (passive process, also occurs at 4°C)</li> <li>Random digestion of DNA (smear of DNA after agarose gel electrophoresis)</li> <li>Postlytic DNA fragmentation (= late event of death)</li> </ul>	<ul style="list-style-type: none"> <li>Tightly regulated process involving activation and enzymatic steps</li> <li>Energy (ATP)-dependant (active process, does not occur at 4°C)</li> <li>Non-random mono- and oligonucleosomal length fragmentation of DNA (Ladder pattern after agarose gel electrophoresis)</li> <li>Prelytic DNA fragmentation</li> <li>Release of various factors (cytochrome C, AIF) into cytoplasm by mitochondria</li> <li>Activation of caspase cascade</li> <li>Alterations in membrane asymmetry (i.e. translocation of phosphatidylserine from the cytoplasmic to the extracellular side of the membrane)</li> </ul>
<p><b>Physiological significance</b></p> <ul style="list-style-type: none"> <li>Affects groups of contiguous cells</li> <li>Evoked by non-physiological disturbances (complement attack, lytic viruses, hypothermia, hyposia, ischemia, metabolic poisons)</li> <li>Phagocytosis by macrophages</li> <li>Significant inflammatory response</li> </ul>	<ul style="list-style-type: none"> <li>Affects individual cells</li> <li>Induced by physiological stimuli (lack of growth factors, changes in hormonal environment)</li> <li>Phagocytosis by adjacent cells or macrophages</li> <li>No inflammatory response</li> </ul>

**Table 1.1. Differential Features and Significance of Necrosis and Apoptosis**

(Adapted from <http://www.roche-applied-science.com>)

In recent years, increasing evidence is beginning to establish that many and perhaps all chemotherapeutic agents affect tumor cell killing *in vitro* and *in vivo* through launching the mechanisms of apoptosis. This was first observed in a landmark study investigating the mechanism of action of etoposide, camptothecin and other cytotoxic anticancer drugs (Hannun, Y.A., 1997; Kaufmann, S.H., 1989). In this study, it was observed that treatment of human HL-60 and KG1A leukemia cells with etoposide resulted in the rapid induction of internucleosomal DNA fragmentation. This observation raised the possibility that etoposide caused apoptotic cell death. Since then, the spectrum of chemotherapeutic agents causing apoptosis has expanded progressively and includes inhibitors of protein and RNA synthesis, dihydrofolate reductase inhibitors, topoisomerase I and II targeting drugs, nucleoside analogues, microtubule poisons, alkylating agents, cisplatin, ionizing radiation and hydrogen peroxide (Hannun, Y.A., 1997; Fisher, D.E., 1994). This list continues to expand as more evidence supporting the role of apoptosis in chemotherapy continues to grow.

## **1.6 Techniques to Assess Apoptosis**

The earliest techniques to detect apoptosis were based mainly on morphology. However, during the last decade, techniques designed to identify, quantitate and characterize apoptosis have been extended to biochemistry, molecular biology and immunology as we learn more about the complex mechanisms that underlie this process. In the next sections, some of the different techniques utilized to assess apoptosis will be discussed.

### 1.6.1 Morphological Assessment

A cell undergoing apoptosis proceeds through three phases of morphological change. In the first, there is reduction in nuclear size, nucleolar disintegration and condensation of chromatin (Arends, M.J., *et al.*, 1991; Arends, M.J., *et al.*, 1990). The condensation begins at the margin of the nucleus with regions of condensed chromatin acquiring a concave shape resembling a half-moon, horseshoe or sickle (Daryznkiewicz, Z., *et al.*, 1997). Additionally, there is a loss of contact between apoptotic cells and their neighboring cells (Dixon, S.C., *et al.*, 1997). This detachment isolates the dying cells as they begin simultaneously shedding specialized surface elements such as cell-cell junctions and microvilli. Furthermore, the cell undergoes a rapid, yet selective, voiding of water and ions without a corresponding loss of macromolecules or organelles. This imbalance leads to condensation of the cytoplasm and compaction of organelles. The result is an overall shrinkage of cell volume and a sudden increase in intracellular density causing a change in cell shape and size. As a consequence, the cells may become elongated and generally are smaller.

In the second phase (which may overlap with the first), there is budding and separation of both nucleus and cytoplasm into multiple membrane-bound apoptotic bodies with intact organelles that may or may not contain nuclear fragments (Arends, M.J., *et al.*, 1991; Arends, M.J., *et al.*, 1990). These apoptotic bodies may be shed from epithelial surfaces or quickly phagocytosed *in vivo* by their nearest neighbor or by macrophages without triggering an immune reaction.

In the third phase, there is progressive breakdown of residual nuclear and cytoplasmic structures (Arends, M.J., *et al.*, 1991; Arends, M.J., *et al.*, 1990). In cultured cells, this is seen as a rupturing of the plasma membrane, resulting in permeability to vital dyes. Eventually, all membranes disappear, organelles become unrecognizable and the appearance is that of a lysosomal residual body.

Numerous methods can be employed to assess these morphological changes, however light microscopy still remains the “gold standard” (Gorczyca, W., *et al.*, 1998). Many morphological features of apoptosis, such as cell shrinkage, membrane blebbing, chromatin condensation, nuclear fragmentation and formation of apoptotic bodies can be seen through examination of cells by light microscopy. Electron microscopy can also be utilized to detect morphological changes on the subcellular level, thus increasing sensitivity and specificity (van Heerde, W.L., *et al.*, 2000). Furthermore, time-lapse videomicroscopy is an effective tool for assessing morphological features of apoptosis, particularly membrane blebbing (Hall, P.A., 1999).

Numerous dyes and stains are also utilized to assess apoptotic nuclear morphology by microscopy. Haematoxylin, thionin blue and eosin are examples of nuclear counterstains used for light microscopic examination (Wilson, J. W., *et al.*, 1999). Fluorescent nuclear stains, such as 4', 6-diamidino-2-phenylindole (DAPI) and Hoechst 33258 and 33342 are also commonly used to assess apoptosis. Hoechst 33342 is a dye that is readily incorporated into the nuclei of early apoptotic cells rather than the nuclei of non-apoptotic cells (Strobl, J.S., *et al.*, 1998; Eguchi, Y., *et al.*, 1997). As a result, the

Hoechst dye stains morphologically normal nuclei dimly blue, whereas apoptotic nuclei demonstrate condensed, smaller, and very intensely bright blue nuclei.

Changes in morphology of apoptotic cells can also be assessed using flow cytometry due to a change in light-scattering properties (van Heerde, W.L., *et al.*, 2000; van Engeland, M., *et al.*, 1996; Darzynkiewicz, Z., *et al.*, 1992). During the apoptotic process, cells shrink and subsequently condense, resulting in a shift in the cytogram from high forward/low side scatter to low forward/high side scatter. This technique can be employed on relatively large number of cells in a short period of time and thus is an excellent tool for assessment of apoptosis.

Despite the versatility of morphological assessment, there are several limitations associated with this technique. Firstly, flow cytometric analysis of morphology generally requires cells to be in suspension and thus limits its applicability for routine use whereas microscopic analysis is elaborate, time consuming and cumbersome for quantitative analysis (van Heerde, W.L., *et al.*, 2000; van Engeland, M., *et al.*, 1996). Also, a disadvantage of light microscopy is its low sensitivity, especially due to the speed of apoptosis and the rapid clearance of apoptotic cells from tissues by phagocytosis, which can be completed within 30-60 minutes from the onset of apoptosis (van Heerde, W.L., *et al.*, 2000). In addition, late apoptotic cells may not be detected by light microscopy due to their small size (Singh, N.P., 2000). Thus, it is very well possible that light microscopy may illustrate only the tip of the iceberg (van Heerde, W.L., *et al.*, 2000; Majno, G., *et al.*, 1995; Kerr, J.F.R., *et al.*, 1972). Finally, it may be difficult to detect the early stages

of apoptosis with little or no morphological changes, which may affect quantitative analysis and perceived apoptotic index (Singh, N.P., 2000; Au, J.L.S., *et al.*, 1997).

### 1.6.2 Annexin V Assay

Another measurable feature of apoptosis is the loss of plasma membrane asymmetry. The cell membrane is composed of four major phospholipids: phosphatidylcholine, phosphatidylethanolamine, sphingomyelin and phosphatidylserine (PS) (Blankenberg, F.G., *et al.*, 2000). These phospholipids are distributed asymmetrically throughout the plasma membrane, with phosphatidylcholine and sphingomyelin predominately on the outer leaflet and phosphatidylethanolamine and PS on the inner leaflet of the plasma membrane (van Engeland, M., *et al.*, 1998; Devaux, P.F., 1991). This phospholipid asymmetry is generated and maintained by membrane proteins called flippases, which facilitate the translocation of lipid molecules from one leaflet to the other (van Engeland, M., *et al.*, 1998; Higgins, C.F., 1994).

Early in apoptosis, before the loss of plasma membrane integrity, PS becomes translocated from the inner to the outer leaflet of the plasma membrane (Blankenberg, F.G., *et al.*, 2000; van Engeland, M., *et al.*, 1998; Vermes, I., *et al.*, 1995; van Engeland, M., *et al.*, 1996; Koopman, G., *et al.*, 1994; Fadok, V.A., 1992). While the exact mechanism by which PS becomes externalized is not entirely clear, it is thought to arise due to an inhibition of the aminophospholipid translocase and subsequent activation of scramblase, a plasma membrane protein which facilitates the rapid mobilization of PS to

the external leaflet of the plasma membrane upon elevation of internal  $\text{Ca}^{2+}$  concentration (Denecker, G., *et al.*, 2000).

The exposure of PS to the external surface of the cell is a general feature of apoptosis (Blankenberg, F.G., *et al.*, 2000). It is thought to serve as a signal to neighboring cells that PS-expressing cells are undergoing apoptosis. It is also thought to play a functional role in the recognition and removal of apoptotic cells by macrophages, which possess a PS receptor on their plasma membrane (Tzima, E., *et al.*, 2000; Fadok, V.A., 1998; Koopman, G., *et al.*, 1994; Fadok, V.A., *et al.*, 1992). This has important implications as the recognition and phagocytosis of apoptotic cells prior to cell lysis is crucial in the avoidance of tissue damage and inflammation associated with necrosis (Fadok, V.A., 1992; Wyllie, A.H., *et al.*, 1980).

In addition to PS externalization, the apoptotic cell undergoes other structural changes in its plasma membrane to signal its process of dying to the environment (van Engeland, M., *et al.*, 1996). These include a change in carbohydrate profile, a change in surface charge, and a shift from tightly to loosely packing of the plasma membrane phospholipids (van Engeland, M., *et al.*, 1996; Fadok, V.A., *et al.*, 1992; Savill, J.S., *et al.*, 1989; Duvall, E., *et al.*, 1985; Morris, R.G., *et al.*, 1984). The former two changes have not yet formed the basis of an apoptosis assay. However, the loose packing of phospholipids has been probed flow cytometrically by Merocyanine 540, which probably intercalates in these membranes (van Engeland, M., *et al.*, 1996; Mower, D.A. Jr., *et al.*, 1994).

Annexin V is a 35-36 kilodalton (kDa)  $\text{Ca}^{2+}$ -dependent, phospholipid-binding protein that has a high affinity for PS, and binds to cells with exposed PS (van Engeland, M., *et al.*, 1998; Vermes, I., *et al.*, 1995; Koopman, G., *et al.*, 1994). Based on these findings and the phenomenon that PS is exposed during apoptosis, a method using annexin V conjugated to fluorochromes, such as fluorescein isothiocyanate (FITC), to detect apoptosis was developed (Koopman, G., *et al.*, 1994). These formats retain their high affinity for PS and hence serve as sensitive probes for detection of apoptosis.

The exposure of PS to the external leaflet of the plasma membrane is not only unique to apoptosis, but also occurs during necrosis (Vermes, I., *et al.*, 1995). A major difference between the two is that in the early stages of apoptosis the cell membrane remains intact, whereas at the onset of necrosis, the cell membrane loses its integrity and becomes leaky. As a result, the annexin V assay must be performed in conjunction with a dye exclusion test in order to establish cell membrane integrity (Darzynkiewicz, Z., *et al.*, 2001; Vermes, I., *et al.*, 1995). Therefore, the simultaneous application of annexin V with a vital dye such as propidium iodide (PI) makes it possible to identify unaffected, nonapoptotic cells (annexin V negative/ PI negative) from early apoptotic cells (annexin V positive/PI negative) and late apoptotic as well as necrotic cells (annexin V positive/PI positive).

The annexin V assay is a widely used method to assess apoptosis facilitated by the observation that translocation of PS seems to be a universal phenomenon during apoptosis (van Engeland, M., *et al.*, 1998). It has been detected in mammalian, insect, and plant cells under the action of most, if not all, triggers of apoptosis. Furthermore, the

annexin V assay can identify apoptotic cells at an earlier stage than assays based on morphological as well as nuclear changes, since loss of plasma membrane asymmetry is a rather early phenomenon in the apoptotic process.

Despite these advantages, there are limitations associated with the annexin V assay. One weakness is its limited applicability (van Engeland, M., *et al.*, 1999). For example, in frozen and paraffin-embedded tissue sections, annexin V also detects PS on the inner leaflet of the plasma membrane. Therefore, in these situations another apoptosis detection system has to be employed. Additionally, the annexin V assay cannot differentiate between necrotic cells and cells that have already undergone apoptosis, because in both cases the dead cells will stain with annexin V (positive) and PI (positive) (Darzynkiewicz, Z., *et al.*, 2001). This in turn, may affect quantitative analysis and perceived apoptotic index.

### **1.6.3 DNA Fragmentation**

One of the most characteristic features of apoptosis is DNA fragmentation, a process that results from the activation of endogenous endonucleases (Walker, P.R., *et al.*, 1999; Walker, P.R., *et al.*, 1997; Walker, P.R., *et al.*, 1994). These endonucleases cleave DNA in a two-step process, characterized by the size-classes of DNA fragments produced. In the first step, DNA is cleaved into high molecular weight (HMW) fragments of 50-300 kilobase pairs (kbp). This cleavage is sufficient to destroy the normal pattern of chromosome organization, resulting in partial condensation of chromatin. The second step of DNA fragmentation, which does not occur in all cell types,

involves the subsequent cleavage of the HMW fragments to smaller fragments and the classical oligonucleosome DNA "ladder". Significantly, only the first step of DNA fragmentation is considered essential for cell death, as some cells, such as MCF-7, never produce DNA "ladders" although they show the classic morphological features of apoptosis. Moreover, in cells that usually do produce DNA "ladders", blocking the second step of DNA fragmentation does not prevent either chromatin condensation or apoptosis.

Currently, numerous techniques are available to assess DNA fragmentation. Internucleosomal DNA fragmentation can readily be detected by agarose gel electrophoresis (Darzynkiewicz, D., *et al.*, 2001; Al-Rubeai, M., 1998; Gong, J., *et al.*, 1994; Arends, M.J., *et al.*, 1990). Activation of endonucleases during apoptosis leads to the generation of discontinuous DNA fragments representing nucleosomal- and oligonucleosomal-sized DNA sections. These fragments generate a characteristic "ladder" pattern during agarose gel electrophoresis. In contrast, DNA fragments produced during necrosis are not as extensive and are heterogenous in size, resulting in a smear on agarose gels. Thus, due to the characteristic "ladder" pattern revealed by agarose gel electrophoresis, this technique is widely used to assess apoptosis.

*In situ* DNA strand breaks generated during apoptosis can also be detected and identified using two techniques (Darzynkiewicz, Z., *et al.*, 1997; Li, X., *et al.*, 1996). The first technique is based on measurement of cellular DNA content; cells are permeabilized or prefixed, hydrated, stained with any DNA-specific fluorochrome and subjected to DNA content analysis (Darzynkiewicz, Z., *et al.*, 1997; Li, X., *et al.*, 1996; Walker, P.R.,

*et al.*, 1994). In apoptotic cells, however, cell permeabilization or alcohol fixation does not fully preserve the degraded DNA. Consequently, this fraction of DNA leaks out during the hydration and staining steps. Hence, apoptotic cells contain reduced amounts of DNA and therefore stains less intensely with any DNA fluorochrome. As a result, apoptotic cells can be differentiated from live cells in DNA histograms as cells with DNA stainability ("sub-G<sub>1</sub>" peaks) often lower than that of G<sub>1</sub> cells. This approach offers the advantage of simplicity and applicability as it can be employed with any DNA fluorochrome or instrument. The second technique is based on specific labeling of DNA strand breaks that are generated during apoptosis. In this technique, cells are pre-fixed with a cross-linking fixative and the 3'-OH ends of the DNA strand breaks are detected by labeling with biotin- or digoxigenin-conjugated deoxynucleotides in a reaction catalyzed by exogenous terminal deoxynucleotidyl transferase (TdT) or DNA polymerase (nick translation). The former assay based on the use of TdT, commonly known as TUNEL (TdT-mediated deoxyuridine triphosphate-biotin nick-end labeling) offers a better discrimination between apoptotic and nonapoptotic cells than the nick translation assay.

There are numerous limitations associated with the various techniques to assess DNA fragmentation. Although the characteristic "ladder" pattern of DNA fragmentation is one of the most common methods to assess DNA fragmentation, it has several weaknesses. First, it should be noted that some cell types, such as MCF-7 and DU145, show almost no DNA fragmentation, although they show the classical morphological features of apoptosis (Oberhammer, F., *et al.*, 1992; Cohen, G.M., *et al.*, 1992). Second,

agarose gel electrophoresis detection of DNA fragmentation involves a DNA isolation procedure from millions of cells and thus the results obtained cannot be quantified (Singh, N.P., 2000). Third, agarose gel electrophoresis requires large numbers of apoptotic cells and thus is difficult to detect a small number of apoptotic events. A limitation of the DNA extraction method is its low specificity (Elstein, K.H., *et al.*, 1994). In addition to apoptotic cells, the sub G<sub>1</sub> peak can represent cells with lower DNA content, mechanically damaged cells or cells with different chromatin structure in which accessibility of DNA to the fluorochrome is restricted (Darzynkiewicz, Z., *et al.*, 1997). Furthermore, although the TUNEL assay is sensitive, this method is associated with a number of artifacts, as it labels DNA strand breaks from any insult, in both apoptotic and nonapoptotic cells (Singh, N.P., 2000; Kockx, M.M., *et al.*, 1998). In addition, the TUNEL assay frequently results in the loss of frail apoptotic cells during handling. Moreover, it requires elaborate handling of cells to incorporate hapten-labeled nucleotides at the sites of nicked DNA (van Engeland, M., *et al.*, 1996). Finally, the TUNEL assay does not discriminate between early and late stages of apoptosis and does not provide information on the integrity of the plasma membrane.

#### **1.6.4 PARP Cleavage Assay**

Poly(ADP-ribosylation) is a post-translational modification of proteins that is involved in many critical processes within the eukaryotic cell, including DNA repair and replication, transcription and cell death (Soldani, C., *et al.*, 2002; Soldani, C., *et al.*, 2001). One of the best-known poly (ADP-ribosylating) enzymes is poly (ADP-ribose)

polymerase (PARP), a 116 kDa zinc-finger nuclear enzyme involved in DNA repair and activated in response to DNA damage (Soldani, C., *et al.*, 2002; Soldani, C., *et al.*, 2001; Shall, S., *et al.*, 2000; Soldatenkov, V.A., *et al.*, 2000; Aoufouchi, S., *et al.*, 1999; Duriez, P.J., *et al.*, 1997). At a site of DNA breakage, PARP binds very tightly to DNA strand breaks or nicks, and uses  $\beta\text{NAD}^+$  as a substrate for transferring ADP-ribose moieties to nuclear proteins including topoisomerases, histones and PARP itself.

Recently, it has been reported that PARP is a target of the cysteine-aspartic acid specific proteases (caspases) associated with apoptosis (Soldani, C., *et al.*, 2002; Aoufouchi, S., *et al.*, 1999; Duriez, P.J. *et al.*, 1997; Sallmann, F.R., *et al.*, 1997; Patel, T., *et al.*, 1996). Early in apoptosis, caspase-3 and caspase-7 cleave the intact 116 kDa PARP at the DEVD site between Asp214 and Gly215, to generate 85- and 25- kDa fragments. This process separates the amino-terminal DNA binding domain of the enzyme from the carboxy-terminal catalytic domain resulting in a loss of normal function of PARP. Although the exact role of PARP in apoptosis remains to be elucidated, PARP cleavage is considered a marker of apoptosis.

Numerous techniques can be employed to assess PARP cleavage. Monoclonal or polyclonal anti-PARP antibodies can be used for immunoblotting, immunoprecipitation, and immunohistochemical visualization of PARP or its fragments (Duriez, P.J., *et al.*, 1997). Autoimmune antisera that recognize PARP can also be utilized. Furthermore, the availability of the cDNA has permitted synthesis of radioactive PARP for *in vitro* cleavage assays. Radioactive PARP allows the simultaneous detection of all fragments of PARP and alleviates the problems associated with specificity and epitope recognition that

can limit the detection capacity with antibodies. Moreover, fragments of PARP with the intact C-terminus can also be detected due to their enzymatic activity. Specifically, the 89-kDa apoptotic fragment can be detected through its capacity to make the polymer of ADP-ribose from radioactive or nonisotopic NAD. Finally, flow cytometric analysis of cells differentially stained for PARP p89 and DNA makes it possible to score and identify apoptotic cells and also allows one to correlate apoptosis with the cell cycle or DNA ploidy (Darzynkiewicz, Z., *et al.*, 2001).

Compared with other detection methods, PARP cleavage is a relatively simple and sensitive marker for apoptosis. It can be detected very early during apoptosis and even when very few cells in the total population are undergoing apoptosis (Duriez, P.J., *et al.*, 1997). For instance, PARP cleavage can be detected by immunoblotting within 15-30 minutes during etoposide-induced apoptosis of HL-60 cells, while internucleosomal degradation of DNA cannot be detected until after 2-3 hours.

Despite the advantages of using PARP cleavage in the assessment of apoptosis, there are limitations associated with this technique. In some models of apoptosis, PARP is not cleaved to form the signature 89-kDa fragment, such as the case during camptothecin-induced apoptosis of Hep 3B cells (Adjei, P.N., *et al.*, 1996). Furthermore, recent studies have demonstrated that PARP<sup>-/-</sup> cells exhibit a normal apoptotic response to various stimuli, including TNF- $\alpha$  and anti-FAS treatment, suggesting that PARP is dispensable in various apoptotic pathways (Leist, M., *et al.*, 1997; Wang, Z.-Q., *et al.*, 1997). Finally, in some cases, essentially due to technical drawbacks, PARP cleavage can

sometimes be detected in non-apoptotic cells (Budihardjo, I.I., *et al.*, 1998). For these reasons, apoptosis cannot be assessed by evaluating PARP cleavage exclusively.

## 1.7 Regulation of Apoptosis

Apoptosis is a highly regulated process that depends on the expression of a specific set of genes. In recent years, a large number of apoptosis regulators and gene families comprised mostly of cell death mediators have emerged (Mckenna, S.L., *et al.*, 1998). In addition, several oncogenes and tumor suppressor genes have also been implicated in the modulation of apoptotic pathways.

### 1.7.1 p53

The p53 tumor suppressor gene is a phosphoprotein barely detectable in the nucleus of normal cells (Soussi, T., 2000; Levine, A.J., 1997). In response to cellular stress, p53 protein accumulates in the cell nucleus, causing cells to undergo cell cycle arrest to enable DNA repair, or apoptosis to eliminate defective cells (Herr, I., *et al.*, 2001; Zörnig, M., *et al.*, 2001; Levine, A.J., 1997; Thompson, C.B., 1995). These functions are thought to be achieved due to the transactivational properties of p53, which activate a series of genes involved in cell cycle regulation (Herr, I. *et al.*, 2001; Shen, Y., *et al.*, 2001; Zörnig, M., *et al.*, 2001; Hainaut, P., *et al.*, 2000; Soussi, T., 2000; Mowat, M.R.A., 1998). Many of these p53 target genes have been identified, and their functions have been characterized. For instance, p53-induced cell cycle arrest is known to require

transactivation of p21<sup>Waf1/Cip1</sup>, GADD45 and cyclin G (Herr, I., *et al.*, 2001; Canman, C.E., *et al.*, 1995).

How p53 mediates apoptosis is less clear. However, several studies conducted using various p53 transactivation-defective mutants have shown that p53-induced apoptosis is dependent on its transcriptional transactivating activity (Herr, I., *et al.*, 2001; Shen, Y., *et al.*, 2001; Hainaut, P., *et al.*, 2000; Mowat, M.R.A., 1998). One such transcriptional target for p53-induced apoptosis is the Bax gene (Herr, I., *et al.*, 2001; Shen, Y., *et al.*, 2001; Hainaut, P., *et al.*, 2000; Mowat, M.R.A., 1998; Levine, A.J., 1997; Miyashita, T. *et al.*, 1995). Bax is a member of the Bcl-2 gene family that comprises both positive and negative regulators of apoptosis. Studies have shown that overexpression or induction of p53 up-regulates Bax and down-regulates Bcl-2, both of which insert into mitochondrial membranes to inhibit (Bcl-2) or facilitate (Bax) the opening of the mitochondrial permeability transition pores. In doing so, p53 is thought to promote mitochondrial leakage of apoptogenic signals. Other proapoptotic members of the Bcl-2 gene family, such as Bak and Noxa, are also up-regulated by p53. They are thought to function downstream of p53 and induce p53-related toxicity. Another potential target for p53 transactivation are death receptors such as Killer/DR5, APO1/fas/CD95 and TRID (Shen, Y., *et al.*, 2001; Hainaut, P., *et al.*, 2000; Mowat, M.R.A., 1998). These receptors are important regulators of apoptosis and are among the transactivational targets of p53, suggesting that p53 may play a role in death receptor-induced apoptosis. Another class of p53 transactivation targets includes many genes involved in signal transduction regulation, such as IGF-BP3, PTGF-*beta* and PERP. These genes are all involved in

promoting apoptosis, suggesting that p53 may mediate apoptosis by manipulating signal-transduction pathways. Finally, it has been suggested that some p53 target gene products regulate the production of reactive oxygen species (ROS), resulting in mitochondrial membrane changes and cytoplasmic release of apoptogenic signals (Herr, I., *et al.*, 2001; Shen, Y., *et al.*, 2001; Hainaut, P., *et al.*, 2000). Hence, p53 may signal apoptosis through the production of ROS.

Although p53 is mostly known to activate transcription, it can also repress gene transcription (Shen, Y., *et al.*, 2001; Hainaut, P., *et al.*, 2000; Mowat, M.R.A., 1998). Studies have shown that p53 represses the expression of a number of genes including c-fos, cyclin A, map 4, interleukin 6 and Bcl-2. Recent studies have also shown that in response to irradiation, p53 can up-regulate genes involved in cell-cycle arrest and DNA repair, while repressing genes involved in cell division.

p53 can also induce apoptosis through non-transcriptional mechanisms. For example, p53 can increase the expression of the cell surface death receptor, CD95 by facilitating its transport from the Golgi complex (Herr, I., *et al.*, 2001; Zörnig, M., *et al.*, 2001). This cell surface redistribution of cytoplasmic CD95 sensitizes cells to CD95-induced apoptosis and can occur without new RNA synthesis.

Additionally, p53 can contribute to apoptosis by direct signaling at the mitochondria (Zörnig, M., *et al.*, 2001). Following DNA or hypoxic damage, a small amount of stress-induced p53 protein is redirected from the nucleus to the mitochondria. This mitochondrial localization occurs before the release of cytochrome c and procaspase activation and is blocked by the overexpression of anti-apoptotic Bcl-2 proteins. Studies

have shown that redirecting p53 from the nucleus to the mitochondria by using mitochondrial import leader peptides is sufficient to induce apoptosis in p53-deficient mice, even with a transcriptionally inactive p53 mutant.

Taken together, apoptosis induced by or involving p53 consists of multiple transcriptional activation-dependent and independent pathways. Given the importance of p53 on the regulation of apoptosis, growth arrest and DNA repair, additional studies are required to further elucidate the role of p53 and its target genes on these cellular functions.

### 1.7.2 Cytochrome c

Cytochrome c is an electron transporting protein that normally resides in the space between the outer and inner membranes of the mitochondria where it plays a critical role in the process of oxidative phosphorylation and production of cellular adenosine triphosphate (ATP) (Zörnig, M., *et al.*, 2001; Boyer, P.D., *et al.*, 1977). In recent years, an increasing amount of interest has been directed toward the role which cytochrome c has been demonstrated to play in apoptotic processes. Following exposure to an apoptotic stimulus, cytochrome c is rapidly released from the mitochondria into the cytosol (Parone, P.A., *et al.*, 2002; Zörnig, M., *et al.*, 2001; Tsujimoto, Y., *et al.*, 2000; Chen, Q., *et al.*, 2000; Jiang, X., *et al.*, 2000). Once in the cytosol, cytochrome c binds its cytosolic partner, apoptosis-activating factor 1 (Apaf-1), via the C-terminal WD-40 repeat domain, and induces the oligomerization of Apaf-1/cytochrome c in the presence of ATP or dATP. This multimeric complex, called an apoptosome, is sufficient to recruit

procaspase-9 to the complex and induces auto-activation of the procaspase. Activated caspase-9 is then released from the Apaf-1/cytochrome c complex and activates downstream caspases such as caspase -3, -6 and -7, which are central executioners of the apoptotic pathway (Hengartner, M.O., 2000). In addition to triggering caspase activation and apoptosis, the release of cytochrome c from the mitochondria is thought to have several other consequences, such as a loss of oxidative phosphorylation and the generation of ROS (Goldstein, J.C., *et al.*, 2000; Green, D.R., *et al.*, 1998). These may contribute to cell death even if caspase function is inhibited.

Despite the importance of this key event in apoptosis, the mechanism by which cytochrome c is released into the cytosol is not entirely clear. However, several theories have been proposed (Parone, P.A., *et al.*, 2002; Zörnig, M., *et al.*, 2001; Tsujimoto, Y., *et al.*, 2000, Von Ahsen, O., *et al.*, 2000, Bossy-Wetzel, E., *et al.*, 1999). Two of these theories suggest that cytochrome c release is mediated by physical rupture of the mitochondrial outer membrane, resulting from mitochondrial swelling. In one theory, swelling is postulated to result from opening of the permeability transition pore (PTP). The PTP is a multiprotein complex formed at the contact sites between the inner and outer mitochondrial membrane. It is composed of many proteins including hexokinase, voltage dependent anion channel (VDAC), adenine nucleotide translocator (ANT) and cyclophilin D. Opening of the PTP leads to equilibration of solutes up to 1.5 kDa between the mitochondrial matrix and the intermembrane space. This results in a loss in mitochondrial inner membrane potential, uncoupling of the respiratory chain, mitochondrial swelling and rupture of the outer membrane, leading to the passive release

of cytochrome c from the mitochondria. This theory has been supported by studies where cytochrome c was shown to be released from isolated mitochondria by agents that open the PTP. A second theory for cytochrome c release suggests an initial hyperpolarization (increase in mitochondrial membrane potential) due to inhibition in mitochondrial ATP/ADP exchange as a result of closure of the VDAC. Altered mitochondrial metabolism is thought to result in an increased negative charge across the mitochondrial inner membrane. Consequently, this increased stress leads to an influx of water to the matrix followed by rupturing of the outer membrane and subsequent cytochrome c release from the mitochondria.

The Bcl-2 family of proteins is also thought to regulate the release of cytochrome c during apoptosis (Parone, P.A., *et al.*, 2002; Zörnig, M., *et al.*, 2001; Bossy-Wetzel, E., *et al.*, 1999). Pro-apoptotic Bcl-2 family members have been shown to induce release of cytochrome c from mitochondria, whereas anti-apoptotic Bcl-2 proteins prevent it. However, the precise biochemical mechanism for the regulation of cytochrome c release by the Bcl-2 family remains to be elucidated. Currently, three models have been proposed. Firstly, it has been suggested that Bcl-2 family members can form cytochrome c conducting channels. Studies have shown that Bax and Bak can insert into mitochondrial membranes and form oligomers or aggregates large enough to allow the passage of cytochrome c into the cytosol. This has been supported by an electron microscopy study that showed *in vivo* Bax and Bak coalesce in large aggregates on the surface of apoptotic mitochondria. It has also been suggested that Bax and tBid (caspase-8 cleaved form of Bid) can form large pores on the planar lipid bilayer or could form a

protein-lipid complex, which might be large enough to allow the passive release of cytochrome c to the cytosol. In such cases, it has been postulated that Bcl-2 proteins could prevent the release of cytochrome c by interfering with the formation of Bax or Bak pores. Another hypothesis for cytochrome c release suggests that pro-apoptotic Bcl-2 proteins, such as Bax, can cause the opening of large channels in the outer mitochondrial membrane. Studies have shown that pro-apoptotic Bcl-2 family proteins interact with the outer mitochondrial membrane channel, VDAC, and in doing so form a pore large enough for the release of cytochrome c. Conversely, anti-apoptotic Bcl-2 family members have been shown to inhibit the release of cytochrome c by preventing the opening of the VDAC/Bax pore. Finally, it has been postulated that Bcl-2 family members can control the release of cytochrome c by regulating the activity of the PTP. For example, Bax/Bak have been shown to open the PTP. Following opening of the PTP, water and solutes enter into the mitochondria. Consequently, the mitochondria swells and the outer membrane ruptures, allowing the passive release of cytochrome c and other apoptogenic factors. This theory has been supported by several studies which have shown that opening of the PTP results in the release of cytochrome c and apoptosis, both events being inhibited by pharmacological inhibitors of the PTP.

In summary, there are several hypotheses being advanced to explain the mechanism behind the release of cytochrome c during apoptosis. However, further work is necessary to elucidate the exact mechanism of cytochrome c release during apoptosis.

### 1.7.3 Bcl-2

Bcl-2 was first identified as an oncogene that was overexpressed in approximately 80% of patients with human follicular B-cell lymphoma because of a t(14;18) chromosomal translocation (Zörnig, M., *et al.*, 2001; Graham, S.H., *et al.*, 2000; Strasser, A., *et al.*, 1997). The translocation moves Bcl-2 from its normal position at 18q21 into the immunoglobulin heavy chain locus at 14q3, resulting in transcriptional dysregulation of the Bcl-2 gene and overexpression of the Bcl-2 protein. Functional studies of the effects of deregulated Bcl-2 on cultured lymphocytes indicated that Bcl-2 rendered lymphocytes resistant to apoptosis. Since then, it has been well established that overexpression of Bcl-2 can suppress apoptosis in response to a variety of stimuli, including serum and growth factor deprivation, glucocorticoids, radiation and chemotherapeutic agents.

In recent years, a rapidly expanding group of genes, structurally or functionally related to Bcl-2 has been discovered (Graham, S.H., *et al.*, 2000; Tsujimoto, Y., *et al.*, 2000; Strasser, A., *et al.*, 1997). Based on their biological function and sequence homology, these proteins are divided into three categories: (1) death-suppressor Bcl-2 family members that contain all of the conserved Bcl-2 homology (BH) regions (BH1, BH2, BH3 and BH4) such as Bcl-2, Bcl-x<sub>L</sub>, Bcl-w, Mcl-1, A1 (Bfl-1) and Boo; (2) death-promoter Bcl-2 family members that contain BH1, BH2 and BH3 domains but not the BH4 domain, such as Bax, Bak, Bad, Mtd (Bok), and Diva; (3) death-promoter Bcl-2 family members that contain only the BH3 domain, such as Bik, Bid, Bim, Hrk (Dp5), Blk and Bnip3, and Bnip3L.

The Bcl-2 gene family is a key regulator of the apoptotic pathway involving the mitochondria and cytochrome c (Liu, D., *et al.*, 2001; Graham, S.H., *et al.*, 2000; Tsujimoto, Y., *et al.*, 2000; Strasser, A., *et al.*, 1997). By controlling the release of mitochondrial apoptogenic factors such as cytochrome c, members of the Bcl-2 family can either suppress or activate apoptosis. Anti-apoptotic Bcl-2 family members are located at the outer mitochondrial membrane and act to promote cell survival by preventing the release of cytochrome c from the mitochondria. On the other hand, pro-apoptotic Bcl-2 family members are expressed and translocated to the mitochondria in response to various death signals, resulting in the release of cytochrome c from the mitochondria into the cytosol. Once in the cytosol, cytochrome c then binds to Apaf-1 in the presence of dATP. This activated complex then may produce activated caspase-9, which in turn may cleave downstream caspases such as caspase -3, -6 and -7, which are central executioners of the apoptotic pathway (Hengartner, M.O., 2000).

The exact mechanism by which Bcl-2 family members induce mitochondrial dysfunction and release of cytochrome c is controversial (Parone, P.A., *et al.*, 2002; Liu, D., *et al.*, 2001; Zörnig, M., *et al.*, 2001; Tsujimoto, Y., *et al.*, 2000; Bossy-Wetzel, E., *et al.*, 1999). Homo- and heterotypic dimmers observed among members of the Bcl-2 family are thought to play a key role. Through heterodimerization, anti-apoptotic and pro-apoptotic Bcl-2 family members can inhibit or neutralize the biological activity of their opposing partners. Hence, the relative ratio of these proteins and the different combinations of their complexes can determine the fate of a cell. In addition to the regulation of each other's activity through heterodimerization, some Bcl-2 protein

members can also function independently as observed in transgenic and knockout mice experiments. As discussed in section 1.7.2., some pro-apoptotic Bcl-2 family members such as Bad, Bak, Bax and Bid have been proposed to form pores or channels in the outer mitochondrial membrane through which cytochrome c can diffuse. Other models suggest that these proteins affect channels in the inner or outer mitochondrial membrane, such as the PTP, thereby inducing hyperpolarization and permeability transition. Both of these events have been proposed to cause the entry of water and solutes, matrix swelling, and rupture of the outer membrane, thus allowing the passive release of cytochrome c.

In summary, the Bcl-2 family consists of positive and negative regulators of the apoptotic pathway. Anti-apoptotic and pro-apoptotic members heterodimerize to suppress the activity of their partners and also function independently to directly regulate the release of mitochondrial apoptogenic factors, such as cytochrome c. Thus, elucidating the structure-function and detailed mechanisms of the Bcl-2 family is important for understanding some of the fundamental principles underlying the apoptotic pathway.

## CHAPTER 2: RESEARCH OBJECTIVES

Breast cancer is the most frequent malignancy among women worldwide, and its incidence is rising (Arver, B., *et al.*, 2000). Although there are numerous treatment modalities currently available, new therapeutic approaches are needed, as age-adjusted mortality has not changed significantly for fifty years (Wingo, P.A., *et al.*, 1995).

Utilization of apoptotic pathways is one potential approach.

Apoptosis is an active form of cell death that occurs in most multicellular organisms and is necessary for numerous fundamental life processes. Apoptosis also occurs in tumor cells treated with a variety of chemotherapeutic agents. The ability of these agents to induce apoptosis in tumor cells has now become a rationale for therapeutic approaches and entertains the possibility that apoptosis may be enhanced in tumors for therapeutic benefit.

Taxol is one of the most promising agents used for the clinical treatment of breast cancer (Rowinsky, E.K., *et al.*, 1995; Holmes, F.A., *et al.*, 1991). It is known for its unique ability to stabilize microtubules, thus preventing the completion of mitosis. Studies have also shown that taxol exerts its cytotoxic effects via the induction of apoptosis (Kaufmann, S.H., *et al.*, 2000; Fan, W., 1999; McCloskey, D.E., *et al.*, 1996; Bhalla, K., *et al.*, 1993). The first objective of this project was to assess taxol-induced apoptosis in MCF-7 and MDA-MB-231 human breast adenocarcinoma cells. Increased understanding of taxol-induced apoptosis may lead to the development of more effective taxol-based chemotherapy regimens and improved clinical responses.

Currently, the number of techniques designed to identify, quantitate and characterize apoptosis is escalating as we learn more about the complex mechanisms, which underlie this process. There is no single feature that can discriminate between cell death that occurs via apoptosis or necrosis. Furthermore, it is important to note that not every cell type will display all of the classic features of apoptosis. Therefore, studies designed to measure multiple aspects of apoptosis must be conducted in order to confirm the mechanism of cell death as being either apoptotic or necrotic. For this reason, we chose three major techniques: morphological assessment, PARP cleavage and TUNEL assay, which measure different aspects or stages of apoptosis to assess taxol-induced apoptosis in MCF-7 and MDA-MB-231 cells.

Additionally, many studies have indicated that apoptosis is regulated through numerous cellular genes, including inducers (p53, Bax, Bcl-x<sub>s</sub>, Bad, Bak and Bik) and inhibitors (Bcl-2, Bcl-x<sub>L</sub>, Mcl-1) of apoptosis. (Tudor, G., *et al.*, 2000). Consequently, it has been hypothesized that defects in apoptosis-regulating genes may cause human cancers (Thompson, C.B., 1995; Williams, G.T., 1991). Thus, the second objective of our study was to elucidate the role of the expression of apoptosis regulating genes in taxol-induced apoptosis using western blot analysis. This would be expected to reveal more details about mechanisms of taxol-induced apoptosis in human breast adenocarcinomas.

## CHAPTER 3: MATERIALS AND METHODS

### 3.1 Materials

Dulbecco's modified Eagle's medium (DMEM) and 1x trypsin-ethylenediamine tetraacetic acid (EDTA) was purchased from Sigma-Aldrich Canada Ltd. Hyclone was the supplier of the fetal bovine serum (FBS) and penicillin/streptomycin. MCF-7 and MDA-MB-231 cells were kindly provided by Dr. Alan Pater, Division of Basic Medical Sciences, Faculty of Medicine, Memorial University of Newfoundland.

Taxol was purchased from Shanghai Fudan Taxusal New Technology Corporation, whereas 3-(4,5,-dimethylthiazol-2-yl)-2,5-diphenyl tetrazolium bromide (MTT) and dimethyl sulfoxide (DMSO) were obtained from Sigma-Aldrich Canada Ltd.

VWR supplied the 0.20  $\mu\text{m}$  Corning® syringe filters, 6- and 96-well cell culture plates and 8-well Lab-Tek chamber slides. Sigma-Aldrich Canada Ltd., Vector Laboratories Inc. and Roche Diagnostics provided the Hoechst 33342 dye, VectaShield mounting medium, and the *In Situ* Cell Death Detection Kit, tetra-methyl rhodamine (TMR) red, respectively.

Sodium azide, hydrochloric acid, methanol, potassium chloride, sodium chloride, sodium phosphate, potassium phosphate and glycine were purchased from Fisher Scientific. Furthermore, Sigma-Aldrich Canada Ltd. was the supplier of the Trizma® base, sodium dodecyl sulfate (SDS), DL-dithiothreitol (DTT), phenylmethylsulfonyl fluoride (PMSF), aprotinin, igepal CA-630 and sodium deoxycholate.

Bio-Rad Laboratories Ltd. supplied the DC Protein Assay kit, bovine serum albumin (BSA) standard, ammonium persulfate (APS), acrylamide/bis 29:1 premixed

powder and N, N, N', N'-tetramethylethylenediamine (TEMED). Bromophenol blue, Ponceau S and mouse anti- $\beta$ -actin monoclonal antibody (mAb) were purchased from Sigma. BD PharMingen supplied purified mouse anti-human mAbs for PARP and cytochrome c. Novocastra Laboratories and Santa Cruz Biotechnology Inc. supplied the mouse anti-human mAbs for p53 and Bcl-2, respectively. Enhanced chemiluminescence (ECL<sup>TM</sup>) horseradish peroxidase-conjugated anti-mouse immunoglobulin G (IgG) antibody, ECL<sup>TM</sup> detection system, Hyperfilm<sup>TM</sup> ECL<sup>TM</sup> nitrocellulose membrane, Hyperfilm<sup>TM</sup> ECL<sup>TM</sup> and the electrode paper were purchased from Amersham Biosciences. Invitrogen Canada Inc. and Carnation were the suppliers of the BenchMark<sup>TM</sup> Prestained protein ladder and skim milk powder, respectively.

## 3.2 Methods

### 3.2.1 Cell Culture

MCF-7 and MDA-MB-231 cells are human breast adenocarcinoma cell lines derived from the pleural effusion of women with metastatic breast cancer (Cailleau, R., *et al.*, 1974; Soule, H.D., *et al.*, 1973). Both MCF-7 and MDA-MB-231 were maintained as a monolayer in DMEM supplemented with 10% FBS and 1% penicillin/streptomycin. They were routinely cultured in 75 cm<sup>2</sup> flasks at 37°C in a humidified incubator with an atmosphere of 5% CO<sub>2</sub>.

During subculturing, once the cells reached subconfluence, the medium was removed from the flasks and the monolayers were washed with approximately 10 mL of phosphate-buffered saline (PBS, pH 7.4) (2.67 mM KCl, 1.47 mM KH<sub>2</sub>PO<sub>4</sub>, 138 mM

NaCl, 8.10 mM  $\text{Na}_2\text{HPO}_4 \cdot 7\text{H}_2\text{O}$ ). Cells were left in PBS for at least 30 seconds to remove as much of the extracellular protein as possible. The PBS was then removed and 3 mL of 1x trypsin-EDTA solution (which had been pre-warmed to 37°C) was added. The flasks were placed back in the 37°C humidified incubator for approximately 2-3 minutes and were then checked under an inverted light microscope to ensure that the cell monolayers were lifting off the flasks. Once the majority of cells had detached from the flasks, approximately 8 mL of PBS was added to each flask and the cell suspensions were transferred to a sterile 15 mL conical centrifuge tube. The cells were then spun down at 1200 rpm for 5 minutes using a Thermo IEC tabletop centrifuge. Following centrifugation, the supernatants were carefully removed using sterile, disposable 10 mL pipettes. The cell pellets were then resuspended with DMEM and were subsequently reseeded at a 1:3 or 1:4, or were counted with a hemocytometer in order to achieve specific concentrations of cells.

Cells were maintained in the logarithmic phase of growth at the time of drug treatment throughout all experimental assays.

### **3.2.2 Preparation of Taxol Working Solutions**

One hundred  $\mu\text{M}$  and 10,000  $\mu\text{M}$  stock solutions of taxol were prepared in DMSO and were sterilized using a 0.20  $\mu\text{m}$  Corning® syringe filter. The stock solutions were then aliquotted aseptically into autoclaved 1.5 mL Eppendorf tubes and were stored at -20°C. Immediately prior to an experiment, working solutions were prepared by diluting taxol stock solutions in DMEM to the appropriate concentration. At no time throughout

the experimental assays did the final DMSO concentration in the taxol working solutions exceed 0.1%.

### 3.2.3 Assessment of Cytotoxicity

#### 3.2.3.1 Assessment of Cytotoxicity of DMSO in MCF-7 and MDA-MB-231 Cells

Since taxol solutions were prepared in DMSO, it was essential to demonstrate that the amount of DMSO used was not toxic and all cell death observed with taxol solutions was attributed to taxol alone. The cytotoxicity of DMSO in MCF-7 and MDA-MB-231 cells was assessed using the MTT assay. This assay is based on the reduction of a tetrazolium salt, MTT, to a colored formazan product by mitochondrial dehydrogenase present only in living, metabolically active cells (Sladowski, D., *et al.*, 1993; Mosmann, T., 1983). In brief,  $2 \times 10^4$  cells/100  $\mu\text{L}$ / well were seeded in eight replicates into 96-well microtitre plates and were incubated for 24 hours at 37°C in a 5% CO<sub>2</sub> humidified incubator to allow adherence of cells. The medium was then removed and medium containing 0.5%, 1.0%, 1.5% and 2.0% DMSO was added to the wells. The plates were returned to the incubator for 72 hours. Cells containing no DMSO were also cultured under the same conditions as control.

After 72 hours, 100  $\mu\text{L}$  of a 5 mg/mL solution of MTT in PBS was added to each well. The MTT solution had been filtered using a sterile 0.20  $\mu\text{m}$  Corning® syringe filter to remove any insoluble residue that may be present in some batches of MTT. Following 4 hours of incubation with MTT at 37°C, the supernatant was carefully removed and 100  $\mu\text{L}$  of DMSO was added to each well to solubilize any formazan crystals generated. The

plates were then agitated on a plate shaker for 20 minutes at room temperature to ensure that all the crystals had been dissolved. The plates were then read on a Bio-Rad Model 550 microplate reader interfaced with an EM PaC 386 computer, using a test wavelength of 570 nm and a reference wavelength of 630 nm. The reference wavelength was used in order to detect any artifacts in the plates and was subtracted from the 570 nm values. Data analysis was carried out using the Bio-Rad Microplate Manager®/ PC version 4 software program. Percentage of cell survival was expressed as:

$$\frac{\text{mean absorbance for each DMSO concentration}}{\text{mean control absorbance}} \times 100\%$$

Percentage of cell survival was then plotted versus percentage of DMSO.

Experiments were repeated at least three times and the results were expressed as mean +/- standard deviation (SD).

### 3.2.3.2 Assessment of Cytotoxicity of Taxol in MCF-7 and MDA-MB-231 Cells

The MTT assay was also used to assess the cytotoxicity of taxol in MCF-7 and MDA-MB-231 cells. Taxol solutions ( $6.4 \times 10^{-4}$   $\mu$ M,  $3.2 \times 10^{-3}$   $\mu$ M,  $1.6 \times 10^{-2}$   $\mu$ M, 0.08  $\mu$ M, 0.4  $\mu$ M, 2  $\mu$ M and 10  $\mu$ M) were prepared from a stock solution (10,000  $\mu$ M) that had been further diluted in DMSO and subsequently in DMEM, such that the final DMSO concentration was 0.01% or less. In brief,  $2 \times 10^4$  cells/100  $\mu$ L/ well were seeded in eight replicates into a 96-well microtitre plate and were incubated for 24 hours at 37°C in a 5% CO<sub>2</sub> humidified incubator to allow adherence of cells. The medium was then removed and taxol solutions ( $6.4 \times 10^{-4}$   $\mu$ M,  $3.2 \times 10^{-3}$   $\mu$ M,  $1.6 \times 10^{-2}$   $\mu$ M, 0.08  $\mu$ M, 0.4

$\mu\text{M}$ , 2  $\mu\text{M}$  and 10  $\mu\text{M}$ ) were added to the wells. The cells were returned to the incubator for 72 hours. Cells containing no taxol were also cultured under the same conditions as control.

After 72 hours, 100  $\mu\text{L}$  of a 5 mg/mL solution of MTT in PBS was added to each well. Following 4 hours of incubation with MTT at 37°C, the supernatant was carefully removed and 100  $\mu\text{L}$  of DMSO was added to each well to solubilize any formazan crystals generated. The plates were agitated on a plate shaker for 20 minutes at room temperature to ensure that all the crystals had been dissolved. The plates were then read on a Bio-Rad Model 550 microplate reader interfaced with an EM PaC 386 computer, using a test wavelength of 570 nm and a reference wavelength of 630 nm. The reference wavelength was used in order to detect any artifacts in the plates and was subtracted from the 570 nm values. Data analysis was carried out using the Bio-Rad Microplate Manager®/ PC version 4 software program. Percentage of cell survival was expressed as:

$$\frac{\text{mean absorbance for each taxol concentration}}{\text{mean control absorbance}} \times 100\%$$

Percentage of cell survival was then plotted versus taxol concentration. The taxol concentration causing 50% inhibition of cell growth ( $\text{IC}_{50}$ ) was determined from the curve. Experiments were repeated at least three times and the results were expressed as mean  $\pm$  SD.

### 3.2.4 Morphological Examination

Apoptosis is characterized by a distinct set of morphological features. In order to assess whether MCF-7 and MDA-MB-231 cells exhibit these features upon exposure to 100 nM taxol for 3, 8, 24, 48 and 72 hours, cells were examined using light and fluorescence microscopy.

One hundred thousand cells per 400  $\mu\text{L}$ /well were seeded in triplicate into 8-well Lab-Tek chamber slides and were incubated for 24 hours at 37° C in a 5% CO<sub>2</sub> humidified incubator to allow adherence of cells. After 24 hours in culture, the medium was replaced and medium containing 100 nM taxol was added to the culture. The cells were incubated for 3, 8, 24, 48 and 72 hours, respectively. Cells containing no taxol were assessed under the same conditions as control.

#### 3.2.4.1 Evaluation of Apoptotic Morphology by Light Microscopy

Morphological changes were assessed using differential interference contrast (DIC) microscopy. Following 3, 8, 24, 48 and 72 hours exposure to 100 nM taxol, the gasket and chamber frame of the 8-well Lab-Tek chamber slides were removed, and cells were coverslipped, examined and photographed at 20 X magnification using an Olympus X WI microscope with Spot RT Slider Digital camera. Cells containing no taxol were also assessed under the same conditions as control. Experiments were repeated at least three times to ensure that all pictures obtained were representative of the conditions.

### 3.2.4.2 Analysis of Chromatin Condensation By Fluorescence Microscopy

Chromatin condensation, one of the hallmarks of apoptosis, was examined using Hoechst staining. Following 3, 8, 24, 48 and 72 hours exposure to 100 nM taxol, the chamber frame of the 8-well Lab-Tek chamber slides were removed and individual wells of the slides were washed in approximately 400  $\mu$ L of PBS. The PBS was then removed and cells were fixed in ice-cold methanol (400  $\mu$ L/well) for 10 minutes at room temperature. The slides were then washed three times (5 minutes per wash) by placing slides in coplin jars filled with PBS and were then stained for 10 minutes with 200  $\mu$ L/well of 0.5  $\mu$ g/mL Hoechst 33342 in PBS. The slides were then washed again three times with PBS (5 minutes per wash) and were mounted with 90% glycerol for MDA-MB-231 and VectaShield mounting medium for MCF-7. The cells were then coverslipped, examined and photographed at 40 X magnification using an Olympus BX 50 microscope at an excitation wavelength of 360-730 nm and an emission wavelength of 460 nm. The Hoechst dye stains morphologically normal nuclei dimly blue, whereas apoptotic nuclei demonstrate condensed, smaller and very intensely bright blue nuclei (Eguchi, Y., *et al.*, 1997).

Cells containing no taxol were assessed under the same conditions as control. Experiments were repeated at least three times to ensure that all photographs obtained were representative of the conditions.

### 3.2.5 TUNEL Assay

Degradation of chromosomal DNA into nucleosome-sized fragments is one of the characteristics of apoptotic cell death. To assess whether MCF-7 and MDA-MB-231 cells exhibit this feature upon exposure to 100 nM taxol, the *In Situ* Cell Death Detection kit, TMR red, utilizing TUNEL technology was employed.

One hundred thousand cells per 400  $\mu$ L/well were seeded in triplicate into 8-well Lab-Tek chamber slides and were incubated at 37° C in a 5% CO<sub>2</sub> humidified incubator for 24 hours to allow adherence of cells. After 24 hours in culture, the medium was replaced and medium containing 100 nM taxol was added to the culture for 3, 8, 24, 48 and 72 hours, respectively. Cells containing no taxol were assessed under the same conditions as control.

Following 3, 8, 24, 48, and 72 hours exposure to 100 nM taxol, the gasket and chamber frame of the 8-well Lab-Tek chamber slides were removed and individual wells of the slides were washed in approximately 400  $\mu$ L of PBS. The PBS was then removed and cells were fixed in 1:1 acetone:methanol (400  $\mu$ L/well) for 10 minutes at -20°C. The slides were then washed again three times (5 minutes per wash) by placing slides in coplin jars filled with PBS and were then stained in 75  $\mu$ L/well of TUNEL reaction mixture (containing terminal deoxynucleotidyl transferase and TMR-labeled dUTP) for 1 hour at 37° C in a 5% CO<sub>2</sub> humidified incubator. Following staining, the cells were then washed again three times (5 minutes per wash) by placing slides in coplin jars filled with PBS and slides were mounted in VectaShield mounting medium. The cells were then coverslipped, examined and photographed at 40 X magnification using an Olympus BX

50 microscope at an excitation wavelength of 530-550 nm and an emission wavelength of 570-620 nm. Apoptotic cells were easily identified as they were stained bright red. The number of apoptotic cells out of 300 randomly selected cells was then determined in each of the triplicate wells and the results were expressed as mean +/- SD. Experiments were repeated at least three times to ensure that all results obtained were representative of the conditions.

### **3.2.6 Extraction of Protein from MCF-7 and MDA-MB-231 Cells**

Protein from MCF-7 and MDA-MB-231 was extracted according to a published method (Yang, X., *et al.*, 1998). Briefly,  $1 \times 10^6$  cells/2 mL were seeded into 6-well plates and were grown to 80-85% confluency. Once cells reached this confluency level, the medium was replaced with medium containing 100 nM taxol. After 3, 8, 24, 48, and 72 hours, taxol present in the cell culture was removed by aspiration of the medium and the cells were washed twice with approximately 2-3 mL of ice-cold PBS. Then, 250  $\mu$ L of ice-cold lysis buffer [50 mM Tris-HCl, pH 8.0; 150 mM NaCl; 0.02% sodium azide; 1% NP-40; 0.1% SDS; 0.5% sodium deoxycholate; dH<sub>2</sub>O; PMSF dissolved in 100% ethanol (10 mg/ml), and aprotinin dissolved in dH<sub>2</sub>O (2 mg/mL)] was added to each well. The lysated cells were then scraped using a Costar® cell scraper, transferred into an ice chilled 1.5 mL Eppendorf tube, and kept on ice for 30 minutes. Following this, the mixture was centrifuged using an IEC MicoMax centrifuge at 12,000 g at 4°C for 10 minutes. The supernatant was then collected and aliquotted out into portions of 50  $\mu$ L/1.5 mL Eppendorf tubes. The lysate was then stored at -80°C until protein quantification

using the Bio-Rad DC Protein assay kit was performed. Cells containing no taxol were assessed under the same conditions as control.

### 3.2.7 Bio-Rad DC Protein Assay

To determine protein concentration, the Bio-Rad DC protein assay was performed using a commercially available kit, according to manufacturer's instructions. This colorimetric assay allows determination of protein concentration following detergent solubilization and is based on the reaction of protein with an alkaline copper tartrate solution and folin reagent (Peterson, G.L., 1979; Lowry, O. H., *et al.*, 1951). As with the Lowry assay, there are two steps that lead to color development: the reaction between protein and copper in an alkaline medium, and the subsequent reduction of folin reagent by the copper-treated protein.

Prior to the determination of protein content in the extracts, a standard curve was generated using BSA as the standard. For optimal results, the BSA solutions were prepared in the same lysis buffer [50 mM Tris-HCL, pH 8.0; 150 mM NaCl; 0.02% sodium azide; igepal CA-630; 0.1% SDS; 0.5% sodium deoxycholate; dH<sub>2</sub>O; PMSF dissolved in ethanol (10mg/ml); and aprotinin dissolved in dH<sub>2</sub>O (2 mg/mL)] as that of the samples. At that time, the working reagent (A') was also prepared. Because the samples contained detergent, the working reagent (A') was prepared by adding 40  $\mu$ L of reagent S (surfactant) to 2 mL of reagent A (alkaline copper tartrate solution). This is done in order to make the assay more detergent compatible.

Once the working reagent (A') and BSA standard solutions were prepared, 5  $\mu\text{L}$  of standards and samples were pipetted into a clean, dry 96-well microtitre plate. Each standard and sample was prepared in triplicate. Next, 25  $\mu\text{L}$  of reagent A', followed by 200  $\mu\text{L}$  of reagent B (folin reagent) was added to each well. The plates were then agitated gently and were left to sit for 15 minutes to allow color development. During this time, any bubbles that may have formed during pipetting and agitation were popped using a clean, dry pipet tip, as they can interfere with absorbance readings. The plates were read on a Bio-Rad Model 550 microplate reader interfaced with an EM PaC 386 computer, using a test wavelength of 630 nm. Data analysis was then carried out using the Bio-Rad Microplate Manager®/ PC version 4 software program at which time the protein concentration was determined.

### **3.2.8 Western Blot**

To elucidate the role of apoptotic regulatory proteins in taxol-induced apoptosis in MCF-7 and MDA-MB-231 cells, western blot analysis was performed. Briefly, MCF-7 and MDA-MB-231 cells were exposed to 100 nM taxol and protein extracts were prepared as described in Section 3.2.6. The protein extracts were then resolved in a discontinuous polyacrylamide gel consisting of a resolving or separating (lower) gel and a stacking (upper) gel. The stacking gel served to concentrate large sample volumes, resulting in better band resolution, whereas the resolving gel separated the molecules. The resolving gel was prepared with 10-15% acrylamide; 375 mM Tris/HCL, pH 8.8; 0.1% SDS; 0.1% APS and 4 $\mu\text{L}$  of TEMED. The stacking gel was composed of 5%

acrylamide; 125 mM Tris/HCL, pH 6.8; 0.1% SDS, 0.1% APS and 5 $\mu$ L of TEMED.

While the stacking gel was polymerizing, the protein extracts, ranging from 5-60  $\mu$ g, were boiled in 2x SDS-polyacrylamide gel electrophoresis (PAGE) gel loading buffer (0.125 M Tris/HCL, pH 6.8; 4% SDS; 0.3 mM bromophenol blue; 20% glycerol and 0.2 mM DTT) or 6x SDS-PAGE gel loading buffer (0.35 M Tris/HCL, pH 6.8; 10% SDS; 0.175 mM bromophenol blue; 30% glycerol; and 0.6 M DTT) for 4 minutes. The protein extracts were then loaded into the sample wells and electrophoresis was conducted at 200V in SDS-PAGE running buffer (24.6 mM Tris, 191 mM Glycine, 3.46 mM SDS) using the Mini-Protean<sup>®</sup> II apparatus (Bio-Rad Laboratories, Ltd.).

Following electrophoresis, the Mini-Protean<sup>®</sup> II apparatus (Bio-Rad) was dismantled and the gel was equilibrated in transfer buffer (25 mM Tris, 192 mM Glycine, 20% methanol) for 30 minutes. Equilibration facilitates the removal of electrophoresis buffer salts and detergents, which is necessary to prevent an increase in the conductivity of the transfer buffer. During the 30-minute equilibration period, the transfer buffer was changed every 10 minutes in order to prevent the diffusion of low molecular weight proteins. Also during this time, the Hybond<sup>™</sup> ECL<sup>™</sup> Nitrocellulose membrane (Amersham Biosciences) was soaked in transfer buffer for 15-30 minutes. Once the equilibration was completed, the transfer sandwich (consisting of filter paper, membrane, gel and fiber pads) was assembled into the transfer cassette and placed in a buffer tank containing transfer buffer. Subsequently, the proteins were transferred to the Hybond<sup>™</sup> ECL<sup>™</sup> Nitrocellulose membrane at 100V for 90 minutes using the Mini Trans-Blot<sup>®</sup> apparatus (Bio-Rad Laboratories, Ltd.). To ensure transfer was successful, the membrane

was stained with Ponceau S Staining solution (0.5% (w/v) Ponceau S, 1 % (v/v) glacial acetic acid) for approximately 30 seconds and destained in distilled water until bands were visible.

Following this, non-specific binding sites were blocked by immersing the membrane in 5% skim milk powder in TBST (20 mM Tris/HCL, 137 mM NaCl, 0.1% Tween-20) for 1 hour at room temperature on a shaker. Subsequently, the membrane was incubated with the primary antibody (purified mouse anti-human mAbs for PARP, cytochrome c, p53 or Bcl-2) diluted in 5 % skim milk powder in TBST overnight at room temperature with shaking. After briefly rinsing the membrane using two changes of TBST and then washing once for 15 minutes and twice for 5 minutes, the membrane was incubated with horseradish peroxidase-conjugated anti-mouse secondary antibody diluted 1:1500 in 5% skim milk powder and TBST for 1 hour at room temperature. The membrane was then washed as previously described and signals were detected using the ECL™ system (Amersham Biosciences). To do this, the membrane was incubated in equal volumes of detection reagent 1 and detection reagent 2 for exactly 1 minute. Excess detection reagent was then drained off and the membrane was exposed to Hyperfilm™ ECL™, as instructed by the manufacturer.

In order to ensure that any observed changes in protein expression was not due to differences in the amount of protein loaded, the membrane was stripped of the primary signal and reprobed with anti- $\beta$ -actin mAb. To do this, the membrane was incubated in stripping buffer (100 mM 2-mercaptoethanol; 2 % SDS; 62.5 mM Tris/HCL, pH 6.8) at 50°C for 15-30 minutes with occasional agitation. The membrane was then washed twice

with TBST for 10 minutes at room temperature and was then blocked in 7% skim milk powder in TBST for 2 hours at room temperature. Subsequently, the membrane was incubated with anti- $\beta$ -actin mAb diluted 1:10,000 in 5% skim milk powder and TBST overnight at room temperature on a shaker. The signals were then detected as described for the primary signal. In some cases, the membrane was stored wet and wrapped in plastic at 4°C after each immunodetection. These membranes were then reprobated at a later date.

The resulting immunoblot signals were quantified by densitometry using the chemiImager 4000 software program. The densitometric value for each of the  $\beta$ -actin bands corresponding to 3, 8, 24, 48 and 72 hours was divided into the value of the  $\beta$ -actin band at 0 hours. The resulting ratios were then multiplied by the corresponding densitometric value for the cytochrome c, p53, or Bcl-2 bands in order to normalize to the  $\beta$ -actin control. Protein levels were then expressed as cytochrome c, p53, or Bcl-2/ $\beta$ -actin optical density (O.D.) ratio. Experiments were repeated at least three times and the values were represented as the mean  $\pm$  SD.

### **3.2.9 Statistical Analysis**

Statistical analysis was conducted using the student's t-test in the SigmaPlot® 8.0 software program. Differences with a value of \*,  $p < 0.05$  were considered to be statistically significant, while those with a value of \*\*,  $p < 0.001$  were considered statistically very significant.

## CHAPTER 4: RESULTS

### 4.1 Cytotoxicity of DMSO and Taxol in MCF-7 and MDA-MB-231 Cells

Cytotoxicity studies of DMSO and taxol in MCF-7 and MDA-MB-231 cells were conducted using the colorimetric MTT assay. Because taxol solutions were prepared in DMSO, it was imperative that the percentage of DMSO used to dissolve taxol was not toxic and all cell death observed was attributed to taxol alone. Hence, we initially examined the cytotoxicity of 0.5%, 1.0%, 1.5% and 2.0% DMSO in these cell lines. As shown in Figure 4.1 and Figure 4.2, the percentage of cell survival in both cell lines decreased dose-dependently in response to the varying concentrations of DMSO. Furthermore, 0.5% DMSO was observed to have little antiproliferative effect on both cell lines. Based on these observations and those in the literature, stock solutions of taxol were made in DMSO, so that the highest concentration of DMSO used for cell treatment was 0.1% or less (Tudor, G., *et al.*, 2000).

Cytotoxicity of taxol in MCF-7 and MDA-MB-231 cells was also evaluated by the MTT assay. Both cell lines were incubated in medium containing 5-fold serial dilutions of taxol ( $6.4 \times 10^{-4}$   $\mu\text{M}$ -10  $\mu\text{M}$ ) for 72 hours. Figure 4.3 and Figure 4.4 show representative graphs of cell survival percentages for MCF-7 and MDA-MB-231 cells treated with varying concentrations of taxol for 72 hours. The  $\text{IC}_{50}$  or concentration of taxol causing 50% growth inhibition was generated from these graphs. The  $\text{IC}_{50}$  values for MCF-7 and MDA-MB-231 cells were 0.040  $\mu\text{M}$  and 0.013  $\mu\text{M}$ , respectively (Table 4.1). These results suggest an increased sensitivity of MDA-MB-231 cells to taxol vs. MCF-7 cells.

By comparison, our IC<sub>50</sub> values are different with that of a similar study with MCF-7 and MDA-MB-231 cells treated with taxol, where they reported an IC<sub>50</sub> value of 0.0047μM in both cell lines (Beech, D.J., *et al.*, 2001). However, these differences may reflect the use of different methodologies and exposure times to taxol.

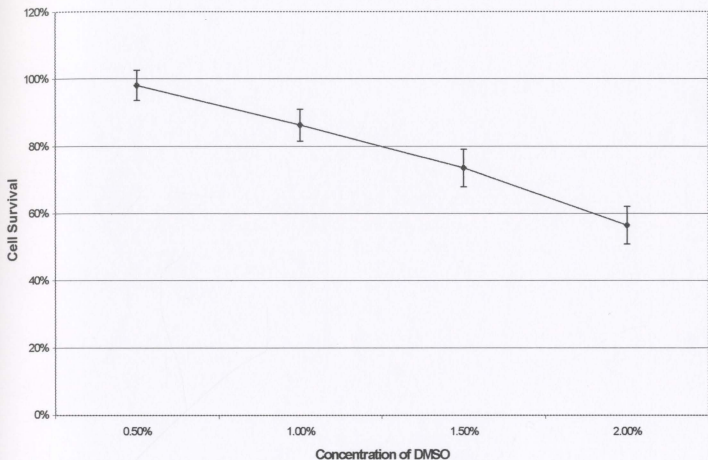


**Figure 4.1. Cytotoxicity of DMSO in MCF-7 Cells**

A 3-day MTT colorimetric assay was used to determine the cytotoxicity of 0.5%, 1.0%, 1.5% and 2.0% DMSO in MCF-7 cells, as described in Materials and Methods.

Percentage of cell survival was plotted against the concentration of DMSO. Each point represents the mean from at least three independent experiments  $\pm$  SD.

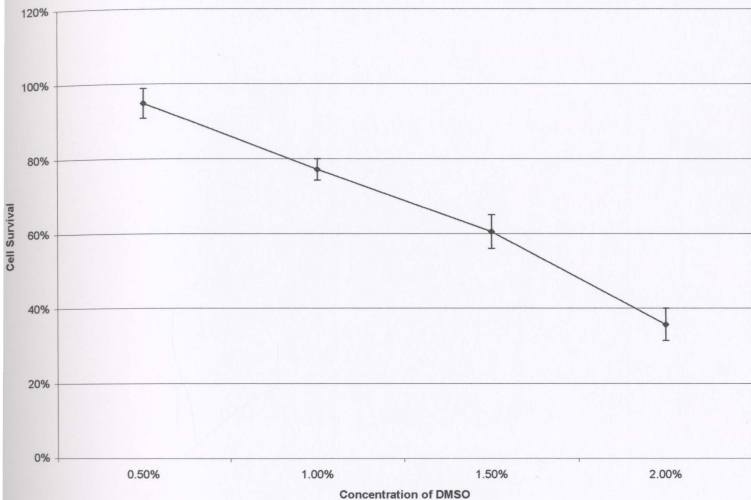


**Figure 4.2. Cytotoxicity of DMSO in MDA-MB-231 Cells**

A 3-day MTT colorimetric assay was used to determine the cytotoxicity of 0.5%, 1.0%, 1.5% and 2.0% DMSO in MDA-MB-231 cells, as described in Materials and Methods. Percentage of cell survival was plotted against the concentration of DMSO. Each point represents the mean from at least three independent experiments  $\pm$  SD.

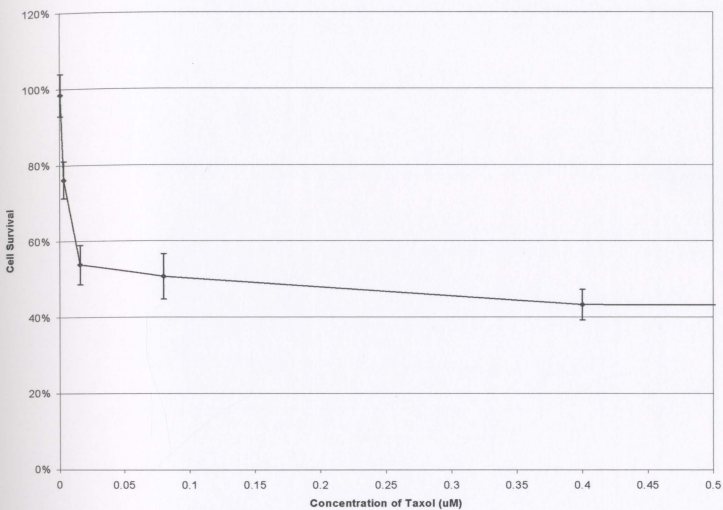


**Figure 4.3. Cytotoxicity of Taxol in MCF-7 Cells**

A 3-day MTT colorimetric assay was used to determine the cytotoxicity of taxol in MCF-7 cells, as described in Materials and Methods. Percentage of cell survival was plotted against the concentration of taxol. Each point represents the mean from at least three independent experiments +/- SD.

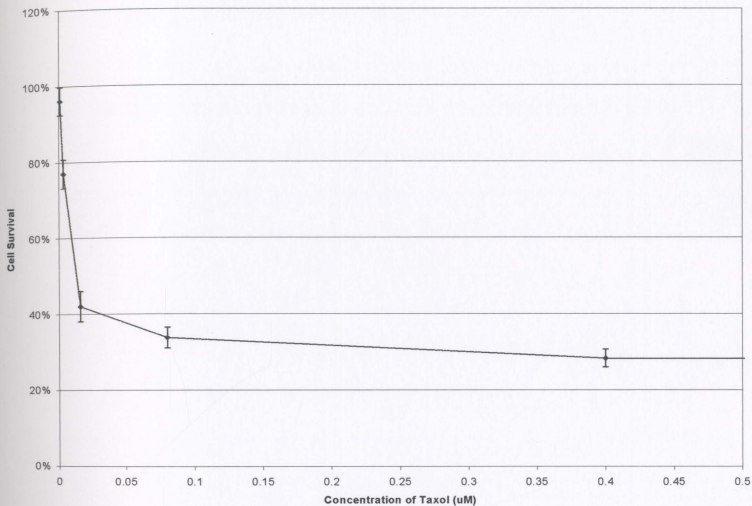


**Figure 4.4. Cytotoxicity of Taxol in MDA-MB-231 Cells**

A 3-day MTT colorimetric assay was used to determine the cytotoxicity of taxol in MDA-MB-231 cells, as described in Materials and Methods. Percentage of cell survival was plotted against the concentration of taxol. Each point represents the mean from at least three independent experiments +/- SD.

**Table 4.1. IC<sub>50</sub> Values of Taxol in MCF-7 and MDA-MB-231 Cells**

A 3-day MTT colorimetric assay was used to determine the cytotoxicity of taxol in MCF-7 and MDA-MB-231 cells, as described in Materials and Methods. Percentage of cell survival was plotted against the concentration of taxol. From this, the IC<sub>50</sub> or concentration of taxol causing 50% growth inhibition was calculated.

Cells	IC <sub>50</sub> (μM)
MCF-7	0.040
MDA-MB-231	0.013

## 4.2 Morphological Changes Evaluated by Light Microscopy

Morphological changes often serve as markers of apoptotic cell death (Wen, L-P., *et al.*, 1997). To evaluate whether taxol induces apoptosis in MCF-7 and MDA-MB-231 cells exposed to 100 nM taxol for 3, 8, 24, 48 and 72 hours, DIC microscopy was employed. Control cells containing no taxol were also cultured under the same conditions and represented the 0 hours time point. As shown in Figure 4.5 and Figure 4.6, the most conspicuous changes observed in taxol-treated cells included cell shrinkage and extensive detachment of the cells from the cell culture substratum. These changes are characteristic of apoptotic cell death and became visible after 3 hours treatment with 100 nM taxol. Other characteristic features of the apoptotic process, such as rounding up of cells, apoptotic body formation and membrane blebbing were also observed. These morphological changes became more remarkable with increased exposure time. Furthermore, these observations suggest that MCF-7 and MDA-MB-231 cells, treated with 100 nM taxol, detached from the substratum and died by apoptosis. Experiments were repeated at least three times to ensure that all photographs obtained were representative of the conditions.

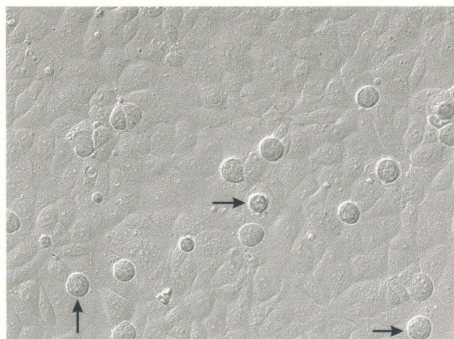


**Figure 4.5. Representative Photomicrographs Demonstrating Morphological Changes of MCF-7 Cells Undergoing Apoptosis Induced by 100 nM Taxol**

Apoptotic morphology was assessed by the use of DIC microscopy. Following 3, 8, 24, 48, and 72 hours exposure to 100 nM taxol, cells were examined and photographed at 20 X magnification, as described in Materials and Methods. Control cells containing no taxol were also cultured under the same conditions and represented the 0 hours time point. Arrows indicate examples of apoptotic cells. These data are representative of at least three independent experiments.



**0-Hours**



**3-Hours**

Figure 4.2. Representative Transmission Electron Micrographs Demonstrating Morphological

Changes of PCE-7 Cells Undergoing Apoptosis Induced by 100 nM Taxol

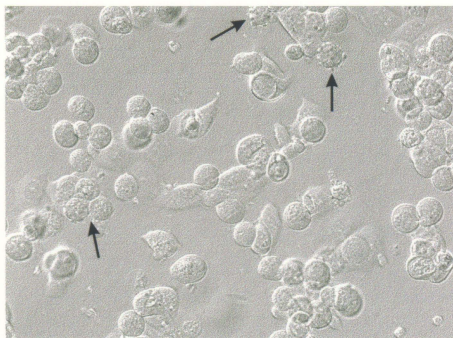
Apoptotic morphology was assessed by the use of DIC microscopy. Following 2, 24, 48, and 72 hours exposure to 100 nM taxol, cells were examined and photographed. A morphological assessment is provided in Materials and Methods. Control cells (untreated) and cells were also cultured under the same conditions and represented the 0 hours time point. Arrows indicate examples of apoptotic cells. These data are representative of at least three independent experiments.

**Figure 4.5. Representative Photomicrographs Demonstrating Morphological Changes of MCF-7 Cells Undergoing Apoptosis Induced by 100 nM Taxol**

Apoptotic morphology was assessed by the use of DIC microscopy. Following 3, 8, 24, 48, and 72 hours exposure to 100 nM taxol, cells were examined and photographed at 20 X magnification, as described in Materials and Methods. Control cells containing no taxol were also cultured under the same conditions and represented the 0 hours time point. Arrows indicate examples of apoptotic cells. These data are representative of at least three independent experiments.



**8-Hours**

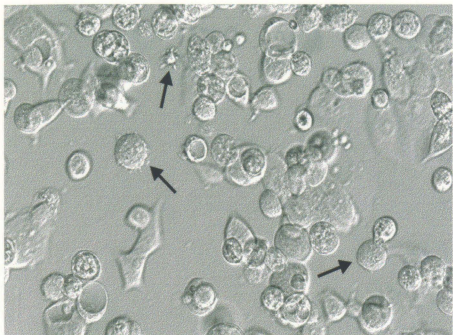


**24-Hours**

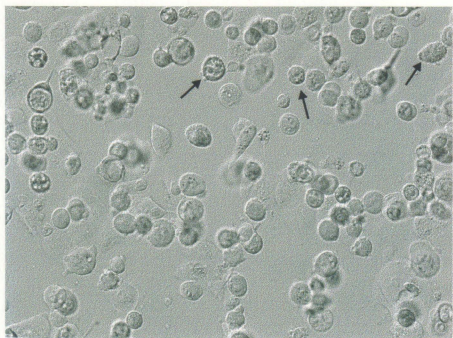


**Figure 4.5. Representative Photomicrographs Demonstrating Morphological Changes of MCF-7 Cells Undergoing Apoptosis Induced by 100 nM Taxol**

Apoptotic morphology was assessed by the use of DIC microscopy. Following 3, 8, 24, 48, and 72 hours exposure to 100 nM taxol, cells were examined and photographed at 20 X magnification, as described in Materials and Methods. Control cells containing no taxol were also cultured under the same conditions and represented the 0 hours time point. Arrows indicate examples of apoptotic cells. These data are representative of at least three independent experiments.



**48-Hours**

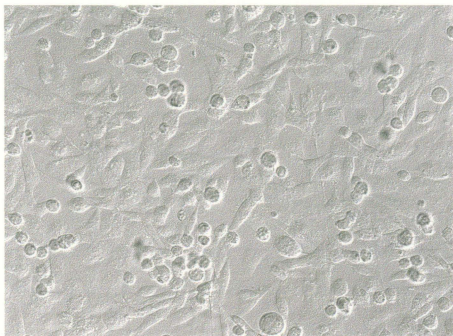


**72-Hours**

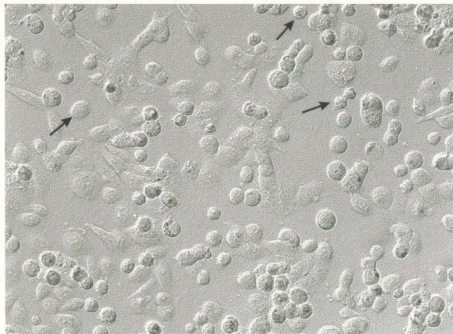


**Figure 4.6. Representative Photomicrographs Demonstrating Morphological Changes in MDA-MB-231 Cells Undergoing Apoptosis Induced by 100 nM Taxol**

Apoptotic morphology was assessed by the use of DIC microscopy. Following 3, 8, 24, 48, and 72 hours exposure to 100 nM taxol, cells were examined and photographed at 20 X magnification, as described in Materials and Methods. Control cells containing no taxol were also cultured under the same conditions and represented the 0 hours time point. Arrows indicate examples of apoptotic cells. These data are representative of at least three independent experiments.



**0-Hours**

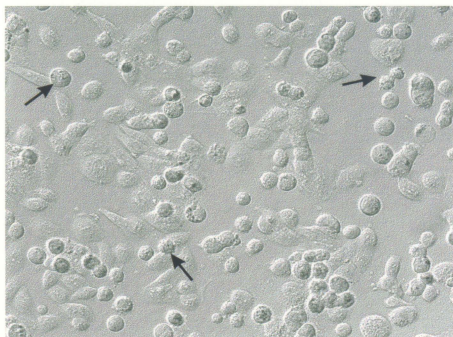


**3-Hours**

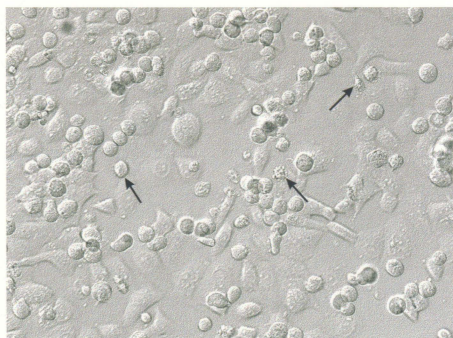
Figure 4.8: Representative Fluorescence Spectroscopy Spectra of the  
Change in WGA-210-211 Cells Undergoing Apoptosis Induced by 100 nM Taxol  
Apoptotic morphology was assessed by the use of DAPI staining. Following 2 h  
of 100 nM Taxol exposure to 100 nM Taxol, cells were stained and photographed  
X magnification as detailed in Materials and Methods. Control cells containing no  
Taxol were also obtained under the same conditions and represented the 0 hours time  
point. Arrows indicate examples of apoptotic cells. These data are representative of  
four independent experiments.

**Figure 4.6. Representative Photomicrographs Demonstrating Morphological Changes in MDA-MB-231 Cells Undergoing Apoptosis Induced by 100 nM Taxol**

Apoptotic morphology was assessed by the use of DIC microscopy. Following 3, 8, 24, 48, and 72 hours exposure to 100 nM taxol, cells were examined and photographed at 20 X magnification, as described in Materials and Methods. Control cells containing no taxol were also cultured under the same conditions and represented the 0 hours time point. Arrows indicate examples of apoptotic cells. These data are representative of at least three independent experiments.



**8-Hours**

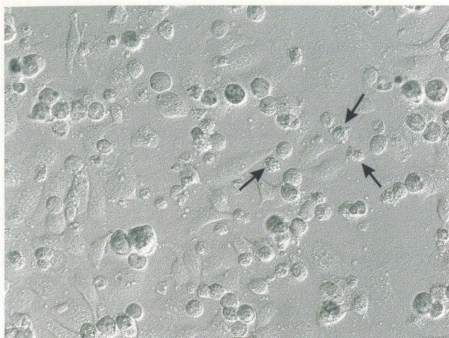


**24-Hours**

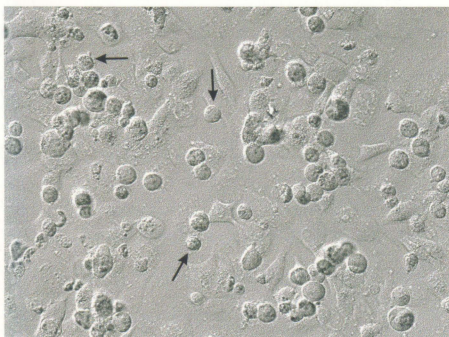
Figure 4. A representative fluorescence micrograph demonstrating the morphology of 3T3-L1 cells undergoing adipogenic differentiation. The cells were cultured in the presence of 100 nM TPA and 100 nM dexamethasone for 7 days. The cells were then stained with Oil Red O and visualized under a fluorescence microscope. The cells exhibit a characteristic foamy morphology, characteristic of adipogenic differentiation. The cells were cultured in the presence of 100 nM TPA and 100 nM dexamethasone for 7 days. The cells were then stained with Oil Red O and visualized under a fluorescence microscope. The cells exhibit a characteristic foamy morphology, characteristic of adipogenic differentiation. The cells were cultured in the presence of 100 nM TPA and 100 nM dexamethasone for 7 days. The cells were then stained with Oil Red O and visualized under a fluorescence microscope. The cells exhibit a characteristic foamy morphology, characteristic of adipogenic differentiation.

**Figure 4.6. Representative Photomicrographs Demonstrating Morphological Changes in MDA-MB-231 Cells Undergoing Apoptosis Induced by 100 nM Taxol**

Apoptotic morphology was assessed by the use of DIC microscopy. Following 3, 8, 24, 48, and 72 hours exposure to 100 nM taxol, cells were examined and photographed at 20 X magnification, as described in Materials and Methods. Control cells containing no taxol were also cultured under the same conditions and represented the 0 hours time point. Arrows indicate examples of apoptotic cells. These data are representative of at least three independent experiments.



**48-Hours**



**72-Hours**

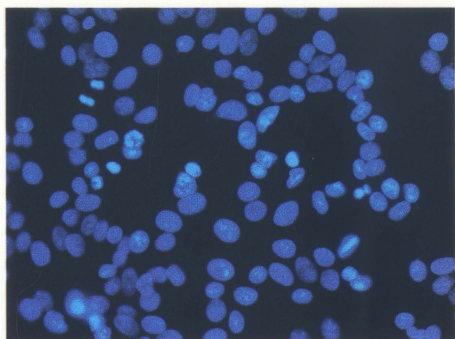
### 4.3 Chromatin Condensation Analyzed by Fluorescence Microscopy

Chromatin condensation, one of the hallmarks of apoptosis, was assessed using Hoechst staining, a dye that stains morphologically normal nuclei dimly blue, whereas apoptotic nuclei demonstrate condensed, smaller and very intensely bright blue nuclei (Eguchi, Y., *et al.*, 1997). To do this, MCF-7 and MDA-MB-231 cells were treated with 100 nM taxol for 3, 8, 24, 48, and 72 hours and stained using Hoechst 33342, as described in Materials and Methods. Control cells containing no taxol were also cultured under the same conditions and represented the 0 hours time point. As shown in Figure 4.7 and Figure 4.8, some differences were observed in the nuclei of 100 nM taxol-treated and untreated MCF-7 and MDA-MB-231 cells. These differences in nuclear morphology, initially observed at 8 hours of 100 nM taxol treatment and most apparent at 24 hours, reflected chromatin condensation and nuclear shrinkage. Experiments were repeated at least three times to ensure that all photographs obtained were representative of the conditions.

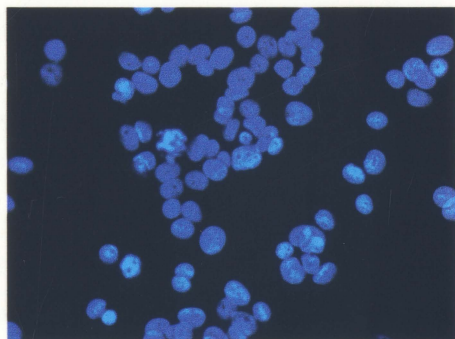


**Figure 4.7. Representative Fluorescence Photomicrographs of MCF-7 Cells Stained with Hoechst 33342**

Cells were treated with 100 nM taxol for 3, 8, 24, 48 and 72 hours, stained with Hoechst 33342 and photographed at 40 X magnification, as described in Materials and Methods. Control cells containing no taxol were also cultured under the same conditions and represented the 0 hours time point. The Hoechst 33342 dye stains morphologically normal nuclei dimly blue whereas apoptotic nuclei demonstrate condensed, intensely bright blue and smaller nuclei. These data are representative of at least three independent experiments.



**0-Hours**



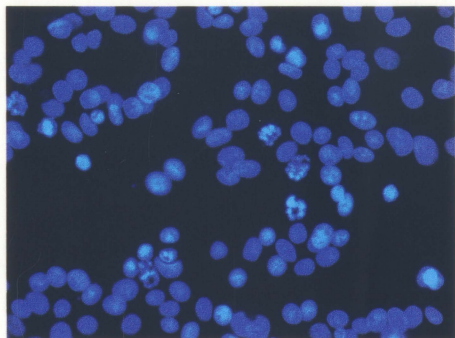
**3-Hours**

Figure 4.3. Representative Fluorescence Photomicrographs of MCF-7 Cells Stained with Hoechst 33258. Cells were treated with 100 nM total for 3, 8, 24, 48 and 72 hours, stained with Hoechst 33258 and photographed at 40 X magnification, as described in Materials and Methods. Control cells containing no total were also cultured under the same conditions and photographed the 0 hour time point. The Hoechst 33258 dye stains morphologically normal nuclei dark blue whereas necrotic nuclei demonstrate condensed, intensely bright blue and smaller nuclei. These data are representative of at least three independent experiments.

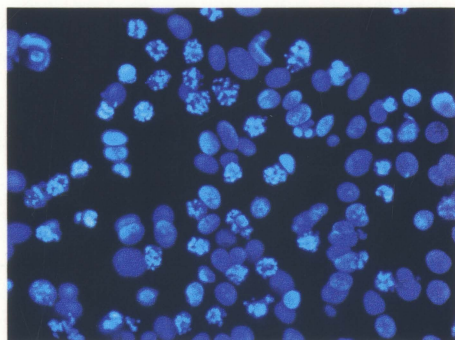
**Figure 4.7. Representative Fluorescence Photomicrographs of MCF-7 Cells Stained with Hoechst 33342**

Cells were treated with 100 nM taxol for 3, 8, 24, 48 and 72 hours, stained with Hoechst 33342 and photographed at 40 X magnification, as described in Materials and Methods.

Control cells containing no taxol were also cultured under the same conditions and represented the 0 hours time point. The Hoechst 33342 dye stains morphologically normal nuclei dimly blue whereas apoptotic nuclei demonstrate condensed, intensely bright blue and smaller nuclei. These data are representative of at least three independent experiments.



**8-Hours**



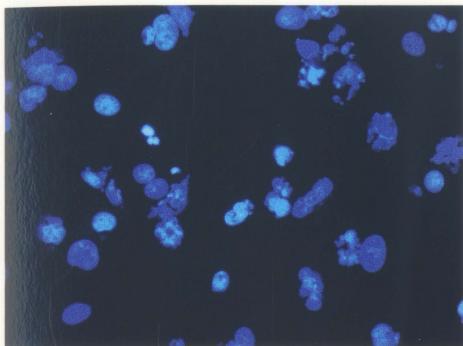
**24-Hours**

Figure 1. Representative fluorescence photomicrographs of HCP-7 Cells stained with Hoechst 33342.

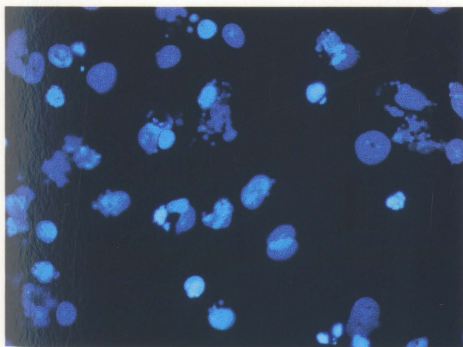
Cells were treated with 100 nM taxol for 1, 5, 24, 48 and 72 hours, stained with Hoechst 33342 and photographed at 40 X magnification, as described in Materials and Methods. Control cells containing no taxol were also cultured under the same conditions and represented the 0 hours time point. The Hoechst 33342 dye stains microtubules, microfilaments and nuclei. Only those cells containing microtubules are shown. Taxol treatment causes microtubule depolymerization and cell death. These data are representative of at least three independent experiments.

**Figure 4.7. Representative Fluorescence Photomicrographs of MCF-7 Cells Stained with Hoechst 33342**

Cells were treated with 100 nM taxol for 3, 8, 24, 48 and 72 hours, stained with Hoechst 33342 and photographed at 40 X magnification, as described in Materials and Methods. Control cells containing no taxol were also cultured under the same conditions and represented the 0 hours time point. The Hoechst 33342 dye stains morphologically normal nuclei dimly blue whereas apoptotic nuclei demonstrate condensed, intensely bright blue and smaller nuclei. These data are representative of at least three independent experiments.



**48-Hours**



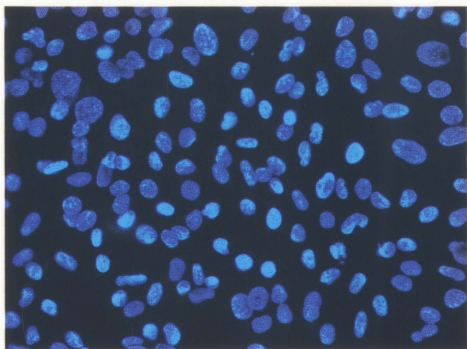
**72-Hours**

Figure 4.3. Representative Fluorescence Photomicrographs of NDA-MF-251 Cells Stained with Hoechst 33342.

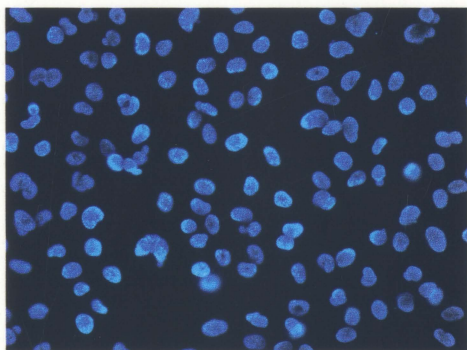
Cells were treated with 100 nM (left) or 1, 2, 5, 10, 20, 50, and 100 nM (right) of NDA-MF-251 for 2, 4, 8, 16, and 32 hours. Cells were stained with Hoechst 33342 and photographed at 40 X magnification, as described in Materials and Methods. Control cells (containing no toxin) were also cultured under the same conditions and photographed at 0 hours time point. The Hoechst 33342 dye stains morphologically normal nuclei (blue) but whereas apoptotic nuclei demonstrate condensed, intensely bright blue and smaller nuclei. These data are representative of three independent experiments.

**Figure 4.8. Representative Fluorescence Photomicrographs of MDA-MB-231 Cells Stained with Hoechst 33342**

Cells were treated with 100 nM taxol for 3, 8, 24, 48 and 72 hours, stained with Hoechst 33342 and photographed at 40 X magnification, as described in Materials and Methods. Control cells containing no taxol were also cultured under the same conditions and represented the 0 hours time point. The Hoechst 33342 dye stains morphologically normal nuclei dimly blue whereas apoptotic nuclei demonstrate condensed, intensely bright blue and smaller nuclei. These data are representative of three independent experiments.



**0-Hours**



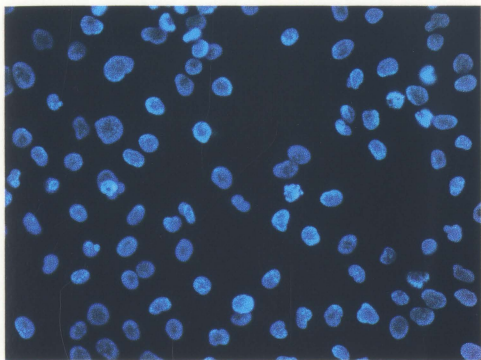
**3-Hours**

Figure 4.8. Representative Fluorescence Photomicrographs of MDA-MB-231 Cells  
 treated with Hoechst 33258.

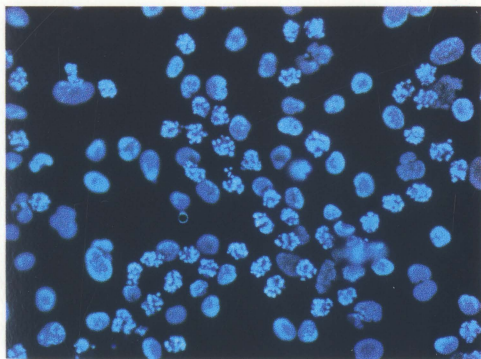
Cells were treated with 100 nM Hoechst 33258 for 1, 2, 4, 8, 16, 32, 48, 72, 96, and 120 hours. The  
 cells were then stained with 100 nM Hoechst 33258 for 15 minutes and imaged  
 using a fluorescence microscope. The images show the nuclei of the cells, which  
 are stained blue. The Hoechst 33258 dye stains nucleic acids, and the  
 fluorescence intensity of the dye is proportional to the amount of DNA in the  
 nuclei. The images show that the Hoechst 33258 dye is able to penetrate the  
 cells and stain the nuclei, even after 120 hours of treatment. This suggests  
 that the dye is not being excluded by the cell membrane and is able to reach  
 the nuclei. The fluorescence intensity of the dye is also relatively stable over  
 time, suggesting that the dye is not being degraded or washed out of the cells.

**Figure 4.8. Representative Fluorescence Photomicrographs of MDA-MB-231 Cells Stained with Hoechst 33342**

Cells were treated with 100 nM taxol for 3, 8, 24, 48 and 72 hours, stained with Hoechst 33342 and photographed at 40 X magnification, as described in Materials and Methods. Control cells containing no taxol were also cultured under the same conditions and represented the 0 hours time point. The Hoechst 33342 dye stains morphologically normal nuclei dimly blue whereas apoptotic nuclei demonstrate condensed, intensely bright blue and smaller nuclei. These data are representative of three independent experiments.



**8-Hours**

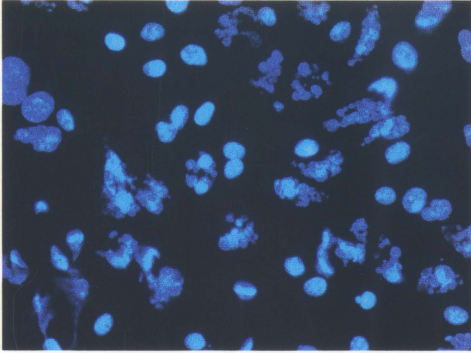


**24-Hours**

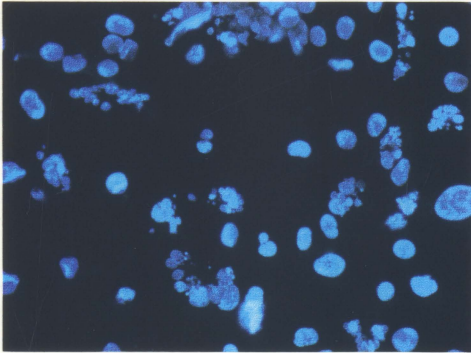
Figure 4.8. Representative Fluorescence Photomicrographs of MDA-MB-231 Cells Stained with Hoechst 33342. Cells were treated with 100 nM taxol for 2, 5, 24, 48 and 72 hours, stained with the 33342 and photographed at 40 X magnification, as described in Materials and Methods. Control cells containing no taxol were also cultured under the same conditions and processed the 0 hours time point. The Hoechst 33342 dye stains nuclei and reveals nuclei that are where specific nuclei demonstrate condensed, hypercompact chromatin and smaller nuclei. These data are representative of three independent experiments.

**Figure 4.8. Representative Fluorescence Photomicrographs of MDA-MB-231 Cells Stained with Hoechst 33342**

Cells were treated with 100 nM taxol for 3, 8, 24, 48 and 72 hours, stained with Hoechst 33342 and photographed at 40 X magnification, as described in Materials and Methods. Control cells containing no taxol were also cultured under the same conditions and represented the 0 hours time point. The Hoechst 33342 dye stains morphologically normal nuclei dimly blue whereas apoptotic nuclei demonstrate condensed, intensely bright blue and smaller nuclei. These data are representative of three independent experiments.



**48-Hours**



**72-Hours**

#### 4.4 DNA Fragmentation Assessed by TUNEL assay

DNA fragmentation is a common biochemical hallmark of apoptosis (Sikorska, M., *et al.*, 1997; Walker, P.R., *et al.*, 1997). Therefore, this phenomenon provides a strong indication of apoptotic cell death. To assess the DNA fragmentation induced by taxol in MCF-7 and MDA-MB-231, cells were treated with 100 nM taxol for 3, 8, 24, 48, and 72 hours and stained using the TUNEL procedure, as described in Materials and Methods. Control cells containing no taxol were also cultured under the same conditions and represented the 0 hours time point. Based on the TUNEL assay, MCF-7 and MDA-MB-231 cells exhibiting DNA strand breaks, a consequence of apoptosis, will incorporate the TMR red (fluorochrome) tagged deoxynucleotides, whereas non-apoptotic cells will not. Thus, apoptotic cells are easily identifiable as they stain intensely bright red. As shown in the representative photomicrographs in Figure 4.9 and Figure 4.10, the incidence of cells staining positive for DNA strand breaks and hence being apoptotic, increased with increasing exposure time to 100 nM taxol.

The percentage of apoptotic cells was then determined by counting the number of apoptotic cells out of 300 randomly selected cells for each condition and the results were expressed as mean  $\pm$  SD. As shown in Figure 4.11 and Figure 4.12, the percentage of apoptotic cells increased time-dependently in response to 100 nM taxol. Furthermore, a statistically significant ( $*p < 0.05$ ) increase in the percentage of apoptotic cells, when compared to untreated cells, was detected in MDA-MB-231 and MCF-7 cells treated with 100 nM taxol following 3 and 8 hours exposure, respectively. By 24, 48 and 72 hours

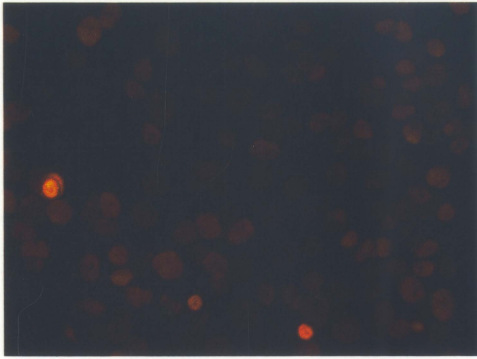
treatment with 100 nM taxol, there was a very statistically significant increase (\*\* $p < 0.001$ ) in the percentage of apoptotic cells vs. control in both cell lines. Experiments were repeated at least three times to ensure that all photographs obtained were representative of the conditions.

Figure 4. Representative fluorescence photomicrographs of MCF-7 cells stained using the TUNEL procedure.

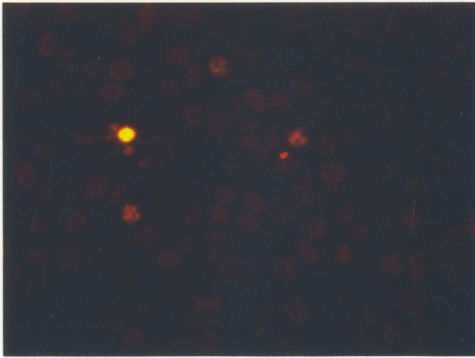
Cells were treated with 100 nM (a) or 1  $\mu$ M (b) of 2, 4, 6, 8-tetrahydro-2H-pyridin-2-one (THPE) and photographed at 40 X magnification, as described in Materials and Methods. Control cells containing no drug were also cultured under the same conditions and represented the 0 hours time point. Apoptosis MCF-7 cells were easily identifiable as they were stained bright red. These data are representative of at least 10 independent experiments.

**Figure 4.9. Representative Fluorescence Photomicrographs of MCF-7 Cells Stained Using the TUNEL Procedure**

Cells were treated with 100 nM taxol for 3, 8, 24, 48, and 72 hours, stained using the TUNEL procedure and photographed at 40 X magnification, as described in Materials and Methods. Control cells containing no taxol were also cultured under the same conditions and represented the 0 hours time point. Apoptotic MCF-7 cells were easily identifiable as they were stained bright red. These data are representative of at least three independent experiments.



**0-Hours**



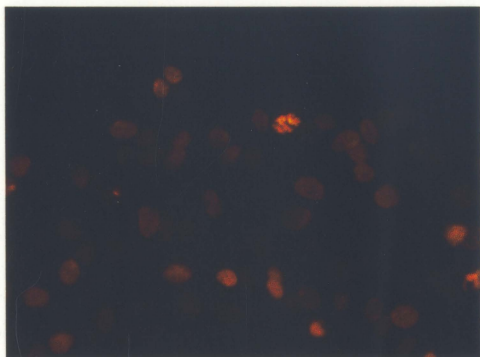
**3-Hours**

Figure 4.3. Representative Fluorescence Photomicrographs of MCF-7 Cells Stained Using the TUNEL Procedure

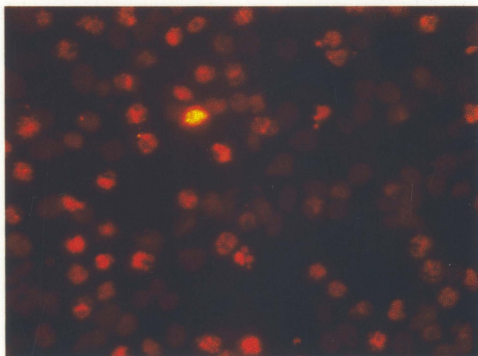
Cells were treated with 100 nM for 1, 24, 48, and 72 hours, stained using the TUNEL procedure and photographed at 40 X magnification, as described in Materials and Methods. Control cells containing no toxin were also cultured under the same conditions and represented the 0 hour time point. Apoptotic MCF-7 cells were easily identifiable as they were stained bright red. These data are representative of at least three independent experiments.

**Figure 4.9. Representative Fluorescence Photomicrographs of MCF-7 Cells Stained Using the TUNEL Procedure**

Cells were treated with 100 nM taxol for 3, 8, 24, 48, and 72 hours, stained using the TUNEL procedure and photographed at 40 X magnification, as described in Materials and Methods. Control cells containing no taxol were also cultured under the same conditions and represented the 0 hours time point. Apoptotic MCF-7 cells were easily identifiable as they were stained bright red. These data are representative of at least three independent experiments.



**8-Hours**



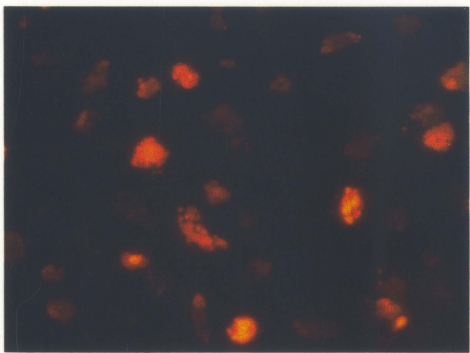
**24-Hours**

Figure 4. Representative Fluorescence Micrographs of MCF-7 Cells Stained Using the TUNEL Procedure

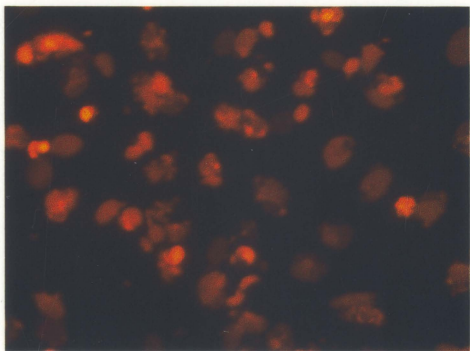
Cells were treated with 100 nM docetaxel for 0, 24, 48, and 72 hours, stained using the TUNEL procedure and photographed at 40 X magnification, as described in Materials and Methods. Control cells containing no label were also cultured under the same conditions and represented the 0 hour time point. Apoptotic MCF-7 cells were easily identifiable as they were stained bright red. These data are representative of at least three independent experiments.

**Figure 4.9. Representative Fluorescence Photomicrographs of MCF-7 Cells Stained Using the TUNEL Procedure**

Cells were treated with 100 nM taxol for 3, 8, 24, 48, and 72 hours, stained using the TUNEL procedure and photographed at 40 X magnification, as described in Materials and Methods. Control cells containing no taxol were also cultured under the same conditions and represented the 0 hours time point. Apoptotic MCF-7 cells were easily identifiable as they were stained bright red. These data are representative of at least three independent experiments.



**48-Hours**



**72-Hours**

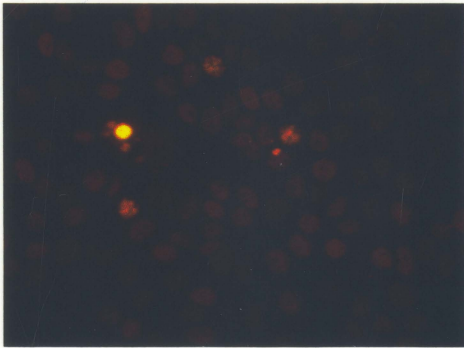


**Figure 4.10. Representative Fluorescence Photomicrographs of MDA-MB-231 Cells Stained Using the TUNEL Procedure**

Cells were treated with 100 nM taxol for 3, 8, 24, 48, and 72 hours, stained using the TUNEL procedure and photographed at 40 X magnification, as described in Materials and Methods. Control cells containing no taxol were also cultured under the same conditions and represented the 0 hours time point. Apoptotic MDA-MB-231 cells were easily identifiable as they were stained bright red. These data are representative of at least three independent experiments.



**0-Hours**

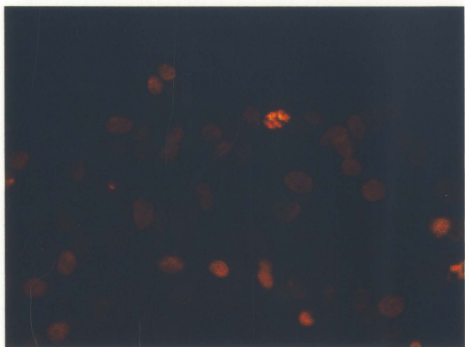


**3-Hours**

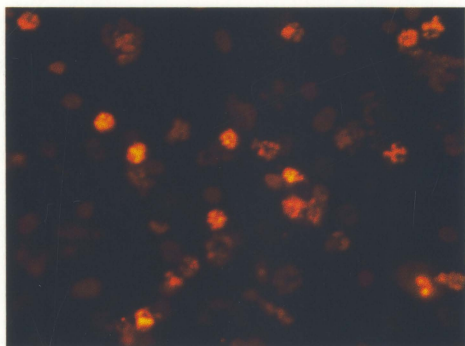


**Figure 4.10. Representative Fluorescence Photomicrographs of MDA-MB-231 Cells Stained Using the TUNEL Procedure**

Cells were treated with 100 nM taxol for 3, 8, 24, 48, and 72 hours, stained using the TUNEL procedure and photographed at 40 X magnification, as described in Materials and Methods. Control cells containing no taxol were also cultured under the same conditions and represented the 0 hours time point. Apoptotic MDA-MB-231 cells were easily identifiable as they were stained bright red. These data are representative of at least three independent experiments.



**8-Hours**

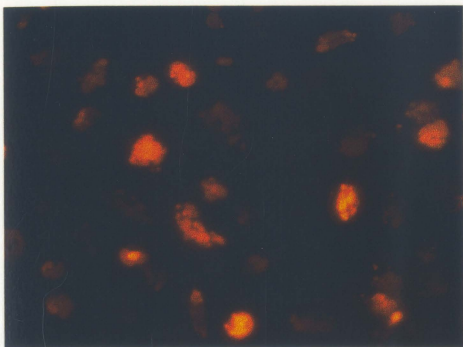


**24-Hours**

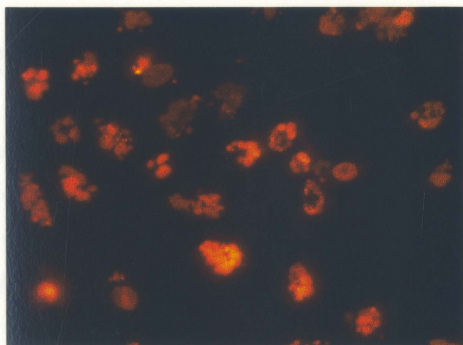


**Figure 4.10. Representative Fluorescence Photomicrographs of MDA-MB-231 Cells Stained Using the TUNEL Procedure**

Cells were treated with 100 nM taxol for 3, 8, 24, 48, and 72 hours, stained using the TUNEL procedure and photographed at 40 X magnification, as described in Materials and Methods. Control cells containing no taxol were also cultured under the same conditions and represented the 0 hours time point. Apoptotic MDA-MB-231 cells were easily identifiable as they were stained bright red. These data are representative of at least three independent experiments.



**48-Hours**



**72-Hours**

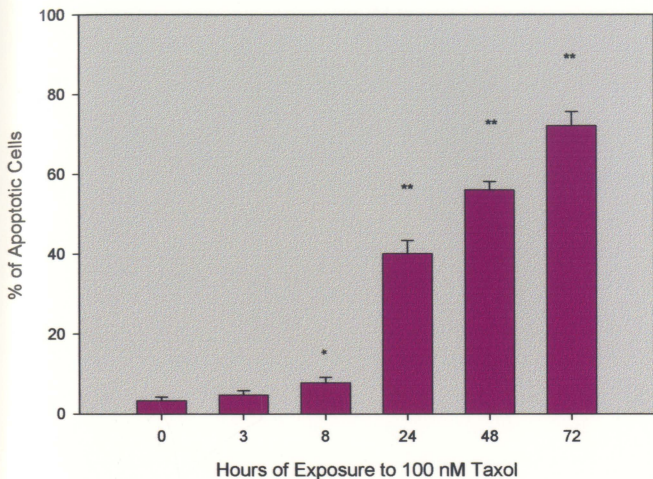


**Figure 4.11. Percentage of Apoptotic MCF-7 Cells Determined Utilizing the TUNEL Procedure**

Cells were treated with 100 nM taxol for 3, 8, 24, 48, and 72 hours, stained using the TUNEL procedure and photographed at 40 X magnification, as described in Materials and Methods. Control cells containing no taxol were also cultured under the same conditions and represented the 0 hours time point. The number of apoptotic cells out of 300 randomly selected cells was determined for each condition and the results were expressed as mean +/- SD from at least three independent experiments. \*P<0.05 and \*\*P<0.001 are the statistical significance of the difference in the percentage of apoptotic cells between control and treated cells.

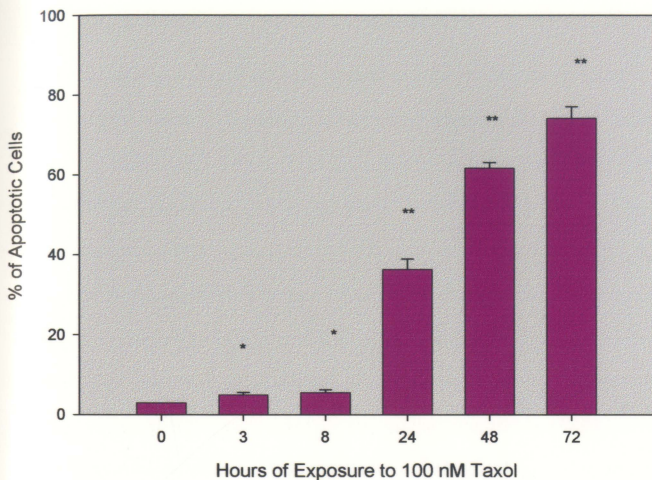


**Figure 4.12. Percentage of Apoptotic MDA-MB-231 Cells Determined Utilizing the TUNEL Procedure**

Cells were treated with 100 nM taxol for 3, 8, 24, 48, and 72 hours, stained using the TUNEL procedure and photographed at 40 X magnification, as described in Materials and Methods. Control cells containing no taxol were also cultured under the same conditions and represented the 0 hours time point. The number of apoptotic cells out of 300 randomly selected cells was determined for each condition and the results were expressed as mean  $\pm$  SD from at least three independent experiments. \* $P < 0.05$  and \*\* $P < 0.001$  are the statistical significance of the difference in the percentage of apoptotic cells between control and treated cells.

#### 4.5 Apoptosis-Related Proteolytic Cleavage of PARP

Another prominent feature during apoptosis is the selective cleavage of PARP by caspase-3 and caspase-7 to generate 85- and 25-kDa fragments (Duriez, P.J., *et al.*, 1997). To assess whether taxol induces PARP cleavage, protein lysate preparations from MCF-7 and MDA-MB-231 cells, which had been treated with 100 nM taxol for 3, 8, 24, 48 and 72 hours were resolved on a 10% SDS-polyacrylamide gel. Subsequently, the protein was transferred to Hybond™ ECL™ nitrocellulose membranes and immunoblots were analyzed, as described in Materials and Methods. Control cells containing no taxol were also cultured under the same conditions and represented the 0 hours time point. As shown in Figure 4.13, PARP cleavage was detected, with the concomitant reduction of full size (116 kDa) molecule and accumulation of the 85 kDa fragment, in MCF-7 cells after 24, 48 and 72 hours exposure to 100 nM taxol. In contrast, PARP was not cleaved in MDA-MB-231 cells at any of the time points tested, as shown in Figure 4.14. Experiments were repeated at least three times to ensure all results obtained were representative of the conditions.

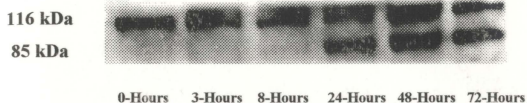


**Figure 4.13. Assessment of PARP Cleavage in MCF-7 Cells**

Total proteins (60  $\mu\text{g}/\text{lane}$ ) from MCF-7 cells treated with 100 nM taxol for 3, 8, 24, 48 and 72 hours were resolved on a 10% SDS-polyacrylamide gel and transferred to Hybond<sup>TM</sup> ECL<sup>TM</sup> nitrocellulose membranes. The protein levels were then assessed by immunoblot analysis, as described in Materials and Methods. Control cells containing no taxol were also cultured under the same conditions and represented the 0 hours time point. The results shown are representative of at least three independent experiments.

116 kDa

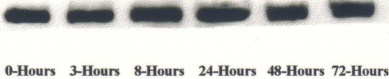


**Figure 4.14. Assessment of PARP Cleavage in MDA-MB-231 Cells**

Total proteins (60  $\mu\text{g}/\text{lane}$ ) from MDA-MB-231 cells treated with 100 nM taxol for 3, 8, 24, 48 and 72 hours were resolved on a 10% SDS-polyacrylamide gel and transferred to Hybond<sup>TM</sup> ECL<sup>TM</sup> nitrocellulose membranes. The protein levels were then assessed by immunoblot analysis, as described in Materials and Methods. Control cells containing no taxol were also cultured under the same conditions and represented the 0 hours time point. The results shown are representative of at least three independent experiments.

#### 4.6 Expression of p53 in MCF-7 and MDA-MB-231 Cells

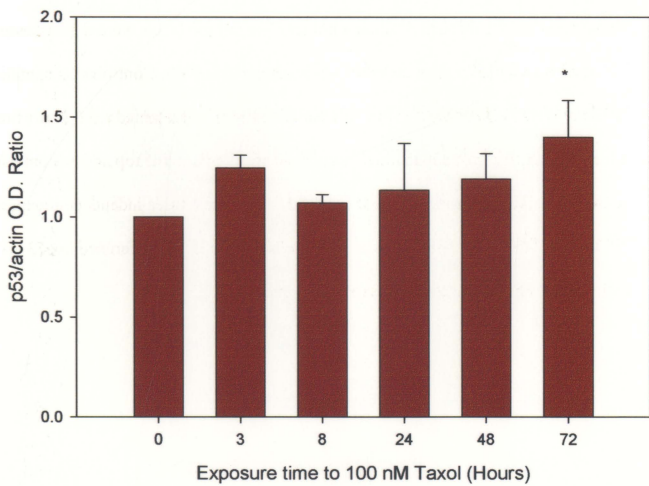
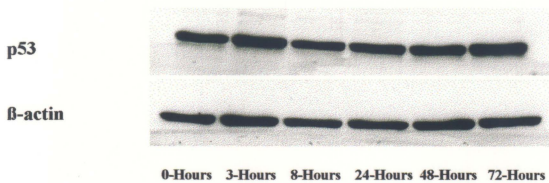
The p53 tumor suppressor gene regulates a number of cellular responses to DNA damage, including cell cycle arrest, some aspects of DNA damage and apoptosis (O'Connor, P. M., *et al.*, 1997; Hartwell, L.H., *et al.*, 1994; Zambetti, G.P., *et al.*, 1993). To assess p53 expression, protein lysate preparations from MCF-7 and MDA-MB-231 cells, which had been treated with 100 nM taxol for 3, 8, 24, 48 and 72 hours were resolved on a 10% SDS-polyacrylamide gel. Subsequently, the protein was transferred to Hybond™ ECL™ nitrocellulose membranes and immunoblots were analyzed, as described in Materials and Methods. Control cells containing no taxol were also cultured under the same conditions and represented the 0 hours time point. As shown in Figure 4.15, there was a statistically significant up-regulation in the expression of p53 protein in MCF-7 cells when exposed to 100 nM taxol for 72 hours, whereby the level of p53 was 142% of the control. In contrast, there was a very statistically significant down-regulation in the expression of p53 protein in MDA-MB-231 cells when exposed to 100 nM taxol for 72 hours. Specifically, the level of p53 at this time point was 39% of the control, as shown in Figure 4.16. Experiments were repeated at least three times to ensure that all results obtained were representative of the conditions.

### Figure 4.12. Expression of p25 in MCF-7 Cells

Tal protein (20 µg/lane) from MCF-7 cells treated with 100 nM taxol for 3, 6, 24, 48, and 72 hours were resolved on a 10% SDS-polyacrylamide gel and transferred to Hybond<sup>TM</sup> ECL<sup>TM</sup> nitrocellulose membrane. The protein levels were then analyzed immunoblot analysis as described in Materials and Methods. Control cells containing taxol were also cultured under the same conditions and represented the 0 hours time point. Western blot and densitometric analysis are shown in the top and bottom panels, respectively. Values represent the mean  $\pm$  SD of at least three independent experiments. \* $P < 0.05$  and \*\* $P < 0.001$  are the statistical significance of the difference in p25 expression between control and taxol-treated cells.

#### **Figure 4.15. Expression of p53 in MCF-7 Cells**

Total proteins (20 µg/lane) from MCF-7 cells treated with 100 nM taxol for 3, 8, 24, 48 and 72 hours were resolved on a 10% SDS-polyacrylamide gel and transferred to Hybond™ ECL™ nitrocellulose membranes. The protein levels were then assessed by immunoblot analysis, as described in Materials and Methods. Control cells containing no taxol were also cultured under the same conditions and represented the 0 hours time point. Western blot and densitometric analysis are shown in the top and bottom panel, respectively. Values represent the mean +/- SD of at least three independent experiments. \*P<0.05 and \*\*P< 0.001 are the statistical significance of the difference in p53 expression between control and taxol-treated cells.



\*  $P < 0.05$

Figure 4.14. Expression of p53 in MDA-MB-231 Cells

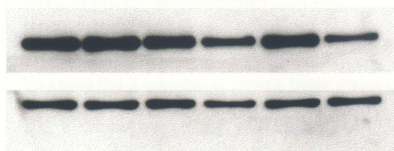
Total protein (2  $\mu$ g/lane) from MDA-MB-231 cells treated with 100 nM taxol for 2, 24, 48 and 72 hours were resolved on a 10% SDS polyacrylamide gel and transferred to Immobilon-P<sup>®</sup> nitrocellulose membrane. The protein levels were then assayed by immunoblot analysis as described in Materials and Methods. Control cells containing no taxol were also subjected under the same conditions and represented the 0 hours time point. Western blot and densitometric analysis are shown in the top and bottom panels, respectively. Values represent the mean  $\pm$  SD of at least three independent experiments. \* $P < 0.05$  and \*\* $P < 0.001$  are the statistical significance of the difference in p53 expression between control and taxol-treated cells.

#### **Figure 4.16. Expression of p53 in MDA-MB-231 Cells**

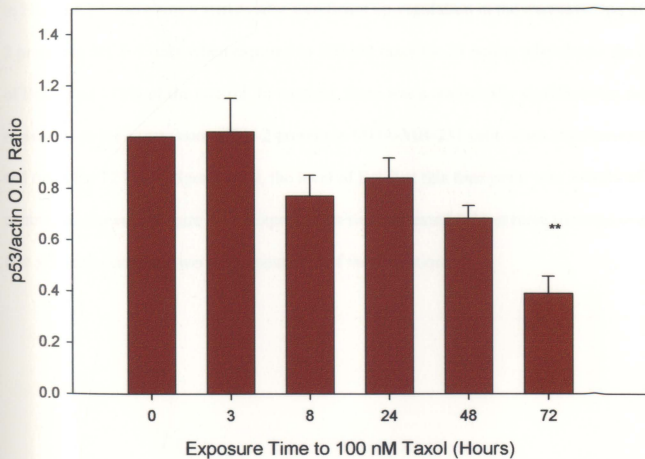
Total proteins (5  $\mu\text{g}/\text{lane}$ ) from MDA-MB-231 cells treated with 100 nM taxol for 3, 8, 24, 48 and 72 hours were resolved on a 10% SDS-polyacrylamide gel and transferred to Hybond<sup>TM</sup> ECL<sup>TM</sup> nitrocellulose membranes. The protein levels were then assessed by immunoblot analysis, as described in Materials and Methods. Control cells containing no taxol were also cultured under the same conditions and represented the 0 hours time point. Western blot and densitometric analysis are shown in the top and bottom panel, respectively. Values represent the mean  $\pm$  SD of at least three independent experiments. \* $P < 0.05$  and \*\* $P < 0.001$  are the statistical significance of the difference in p53 expression between control and taxol-treated cells.

p53

$\beta$ -actin



0-Hours 3-Hours 8-Hours 24-Hours 48-Hours 72-Hours



\*\* P < 0.001

#### **4.7 Expression of Bcl-2 in MCF-7 and MDA-MB-231 Cells**

In recent years, it has been well established that Bcl-2 prevents most forms of apoptotic cell death. To assess Bcl-2 expression, protein lysate preparations from MCF-7 and MDA-MB-231 cells, which had been treated with 100 nM taxol for 3, 8, 24, 48 and 72 hours were resolved on a 10% SDS-polyacrylamide gel. Subsequently, the protein was transferred to Hybond™ ECL™ nitrocellulose membranes and immunoblots were analyzed, as described in Materials and Methods. Control cells containing no taxol were also cultured under the same conditions and represented the 0 hours time point. As shown in Figure 4.17, there was a statistically significant up-regulation in the expression of Bcl-2 protein in MCF-7 cells when exposed to 100 nM taxol for 24 hours, whereby the level of Bcl-2 was 173% of the control. In contrast, there was a statistically significant down-regulation in the expression of Bcl-2 protein in MDA-MB-231 cells when exposed to 100 nM taxol for 72 hours. Specifically, the level of Bcl-2 at this time point was 34% of the control, as shown in Figure 4.18. Experiments were repeated at least three times to ensure that all results obtained were representative of the conditions.



**Figure 4.17. Expression of Bcl-2 in MCF-7**

Total proteins (60  $\mu$ g/lane) from MCF-7 cells treated with 100 nM taxol for 3, 8, 24, 48 and 72 hours were resolved on a 15% SDS-polyacrylamide gel and transferred to Hybond<sup>TM</sup> ECL<sup>TM</sup> nitrocellulose membranes. The protein levels were then assessed by immunoblot analysis, as described in Materials and Methods. Control cells containing no taxol were also cultured under the same conditions and represented the 0 hours time point. Western blot and densitometric analysis are shown in the top and bottom panel, respectively. Values represent the mean  $\pm$  SD of at least three independent experiments. \* $P < 0.05$  and \*\* $P < 0.001$  are the statistical significance of the difference in Bcl-2 expression between control and taxol-treated cells.

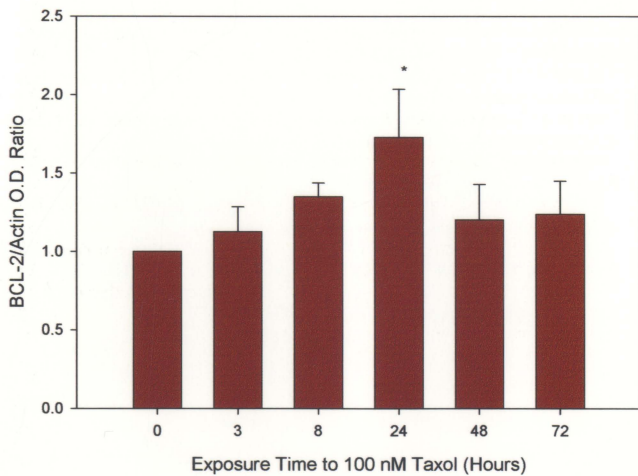
Bcl-2



$\beta$ -actin



0-Hours 3-Hours 8-Hours 24-Hours 48-Hours 72-Hours



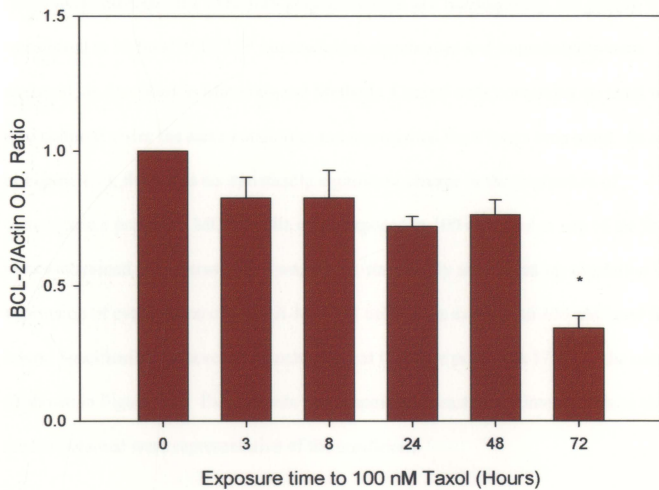
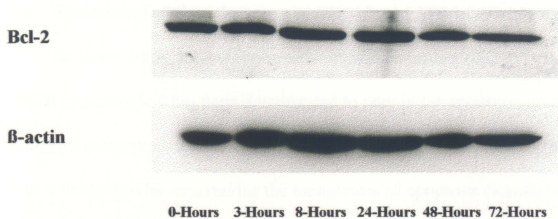
\*  $P < 0.05$

Figure 1. Expression of Bcl-2 in MDA-MB-231 Cells

Total protein (40 µg/lane) from MDA-MB-231 cells treated with 100 nM taxol for 2, 4, 8, 16, 32, 48 and 72 hours were resolved on a 15% SDS polyacrylamide gel and transferred to Hybond<sup>TM</sup> ECL<sup>TM</sup> nitrocellulose membrane. The protein levels were then assessed by immunoblot analysis, as described in Materials and Methods. Control cells containing no taxol were also cultured under the same conditions and represented the 0 hours time point. Western blot and densitometric results are shown in the top and bottom panels, respectively. Values represent the mean  $\pm$  SD of at least three independent experiments. \* $P < 0.05$  and \*\* $P < 0.001$  vs the untreated significance of the difference in Bcl-2 expression between control and taxol-treated cells.

#### **Figure 4.18. Expression of Bcl-2 in MDA-MB-231 Cells**

Total proteins (40  $\mu\text{g}/\text{lane}$ ) from MDA-MB-231 cells treated with 100 nM taxol for 3, 8, 24, 48 and 72 hours were resolved on a 15% SDS-polyacrylamide gel and transferred to Hybond<sup>TM</sup> ECL<sup>TM</sup> nitrocellulose membranes. The protein levels were then assessed by immunoblot analysis, as described in Materials and Methods. Control cells containing no taxol were also cultured under the same conditions and represented the 0 hours time point. Western blot and densitometric analysis are shown in the top and bottom panel, respectively. Values represent the mean  $\pm$  SD of at least three independent experiments. \* $P < 0.05$  and \*\* $P < 0.001$  are the statistical significance of the difference in Bcl-2 expression between control and taxol-treated cells.



\*  $P < 0.05$

#### 4.8 Expression of Cytochrome c in MCF-7 and MDA-MB-231 Cells

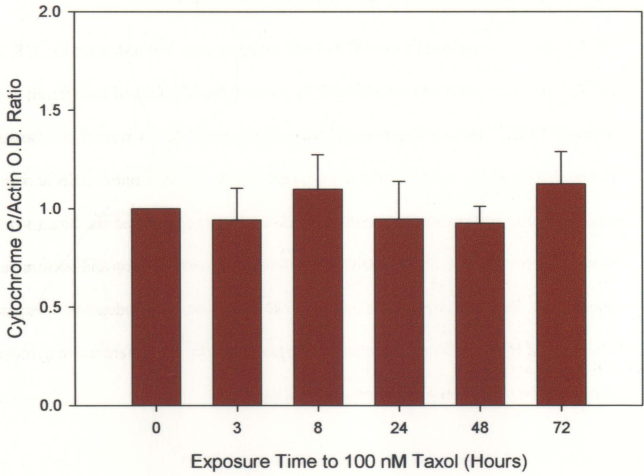
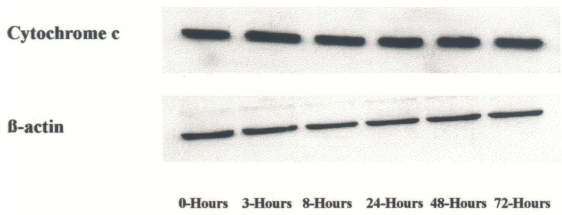
In recent years, an increasing amount of interest has been directed toward the role which cytochrome c has been documented to play in the apoptotic processes. Following exposure to apoptotic stimuli, cytochrome c is rapidly released into the cytosol, an event that is thought to be required for the completion of apoptosis (Kaufmann, SH., *et al.*, 2000). To assess cytochrome c expression, protein lysate preparations from MCF-7 and MDA-MB-231 cells, which had been treated with 100 nM taxol for 3, 8, 24, 48 and 72 hours were resolved on a 15% SDS-polyacrylamide gel. Subsequently, the protein was transferred to Hybond™ ECL™ nitrocellulose membranes and immunoblots were analyzed, as described in Materials and Methods. Control cells containing no taxol were also cultured under the same conditions and represented the 0 hours time point. As shown in Figure 4.19, there was no statistically significant change in the expression of cytochrome c protein in MCF-7 cells when exposed to 100 nM taxol at any of the time points examined. In contrast, there was a very statistically significant up-regulation in the expression of cytochrome c in MDA-MB-231 cells when exposed to 100 nM taxol for 72 hours. Specifically, the level of cytochrome c at this time point was 173% of the control, as shown in Figure 4.20. Experiments were repeated at least three times to ensure that all results obtained were representative of the conditions.

Figure 3.17. Expression of Cytokeratins 7 in SKC 5-7 Cells

Total protein (10 µg/lane) from SKC 5-7 cells treated with 100 nM taxol for 2, 8, 24, 48, and 72 hours was transferred on a 10% SDS-polyacrylamide gel and transferred to Hybond<sup>®</sup> ECL<sup>™</sup> nitrocellulose membrane. The protein levels were then assessed by immunoblot analysis as described in Materials and Methods. Control cells containing no taxol were also cultured under the same conditions and represented the 0 hours time point. Western blot and densitometry analysis are shown in the top and bottom panel, respectively. Values represent the mean  $\pm$  SD of at least three independent experiments. \* $P < 0.05$  and \*\* $P < 0.001$  are the statistical significance of the difference in cyokeratin expression between control and taxol-treated cells.

#### **Figure 4.19. Expression of Cytochrome c in MCF-7 Cells**

Total proteins (10 µg/lane) from MCF-7 cells treated with 100 nM taxol for 3, 8, 24, 48 and 72 hours were resolved on a 15% SDS-polyacrylamide gel and transferred to Hybond™ ECL™ nitrocellulose membranes. The protein levels were then assessed by immunoblot analysis, as described in Materials and Methods. Control cells containing no taxol were also cultured under the same conditions and represented the 0 hours time point. Western blot and densitometric analysis are shown in the top and bottom panel, respectively. Values represent the mean +/- SD of at least three independent experiments. \*P<0.05 and \*\*P< 0.001 are the statistical significance of the difference in cytochrome c expression between control and taxol-treated cells.





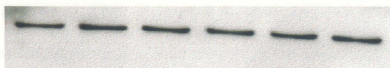
**Figure 4.20. Expression of Cytochrome c in MDA-MB-231 Cells**

Total proteins (10  $\mu\text{g}/\text{lane}$ ) from MCF-7 cells treated with 100 nM taxol for 3, 8, 24, 48 and 72 hours were resolved on a 15% SDS-polyacrylamide gel and transferred to Hybond<sup>TM</sup> ECL<sup>TM</sup> nitrocellulose membranes. The protein levels were then assessed by immunoblot analysis, as described in Materials and Methods. Control cells containing no taxol were also cultured under the same conditions and represented the 0 hours time point. Western blot and densitometric analysis are shown in the top and bottom panel, respectively. Values represent the mean  $\pm$  SD of at least three independent experiments. \* $P < 0.05$  and \*\* $P < 0.001$  are the statistical significance of the difference in cytochrome c expression between control and taxol-treated cells.

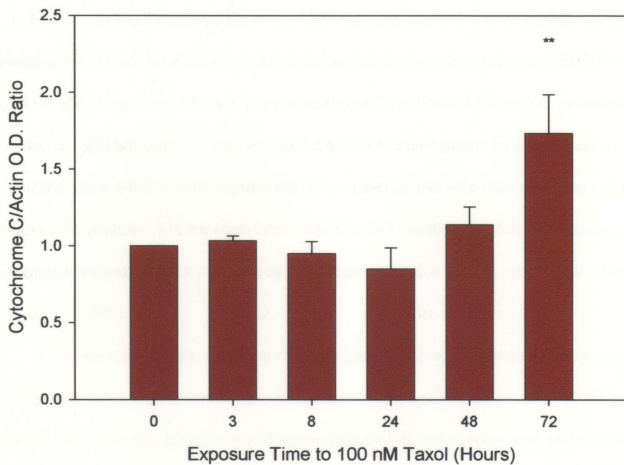
Cytochrome c



$\beta$ -actin



0-Hours 3-Hours 8-Hours 24-Hours 48-Hours 72-Hours



\*\* P < 0.001

## CHAPTER 5: DISCUSSION AND CONCLUSIONS

Taxol is one of the most promising agents used for the clinical treatment of breast cancer (Rowinsky, E.K., *et al.*, 1995; Holmes, F.A., *et al.*, 1991). It is known for its unique ability to stabilize microtubules, thus preventing the completion of mitosis. Studies have also shown that taxol exerts its cytotoxic effects via the induction of apoptosis (Kaufmann, S.H., *et al.*, 2000; Fan, W., 1999; McCloskey, D.E., *et al.*, 1996; Bhalla, K., *et al.*, 1993). Specifically, research groups have reported that 100 nM taxol can induce apoptosis in human breast cancer cell lines (Kottke, T.J., *et al.*, 2002; Kottke, T. J., *et al.*, 1999; Samejima, K., *et al.*, 1999; McCloskey, D.E., *et al.*, 1996). As an expansion of such previous work, taxol-induced apoptosis was assessed in MCF-7 and MDA-MB-231 human breast adenocarcinoma cells. These cell lines were chosen in an effort to highlight potential differences in the induction of apoptosis in response to 100 nM taxol. MCF-7 cells express estrogen receptors and wild-type p53 gene and are minimally invasive. On the other hand, MDA-MB-231 cells are estrogen receptor negative, express mutant p53 gene and are highly invasive (Liu, Z., *et al.*, 1997; Elstner, E., *et al.*, 1995).

To assess apoptosis, a number of techniques, designed to measure multiple aspects of apoptosis, were examined. These included morphological assessment, TUNEL assay and PARP cleavage. Morphological assessment by DIC microscopy and analysis of chromatin condensation by Hoechst 33342 staining provided evidence of taxol-induced apoptosis in MCF-7 and MDA-MB-231 cells. Upon exposure to 100 nM taxol, both cell lines exhibited typical morphological features associated with apoptotic cell death,

including cell shrinkage, membrane blebbing, formation of apoptotic bodies and chromatin condensation. These observations are consistent with a similar study of MCF-7 cells, where 24 hours treatment with 100 nM taxol induced typical apoptotic-related morphological features, such as chromatin condensation (Kottke, T.J., *et al.*, 2002).

Occurrence of taxol-induced apoptosis of MCF-7 and MDA-MB-231 cells was further verified by DNA fragmentation. Because of the rarity of detecting DNA strand breaks in MCF-7 cells by agarose gel electrophoresis, the TUNEL assay was employed. Analysis of DNA fragmentation revealed a time-dependent increase in DNA strand breaks in taxol-treated MCF-7 and MDA-MB-231 cells. Because DNA fragmentation are common features of apoptotic cells, this result provides further evidence of taxol-induced apoptosis in MCF-7 and MDA-MB-231 cells.

Another prominent feature during apoptosis is the selective cleavage of PARP by caspase-3 and caspase-7 to generate 85- and 25-kDa fragments. Using protein lysate preparations, PARP cleavage was detected, with the concomitant reduction of full size (116 kDa) molecule and accumulation of the 85-kDa fragment in MCF-7 cells after 24, 48 and 72 hours exposure to 100 nM taxol. Interestingly, MCF-7 cells lack procaspase-3 polypeptide due to a 47-bp deletion within exon 3 of the procaspase-3 gene that alters the reading frame of the message and results in an unstable truncated polypeptide (Janicke, R.U., *et al.*, 1998). Hence, this result suggests that caspase-3 is not required for the proteolytic cleavage of PARP during taxol-induced apoptosis in MCF-7 cells. In contrast, PARP cleavage was not detected in MDA-MB-231 cells at any of the time points tested, an observation that is consistent with other literature reports (Blagosklonny, M.V., *et al.*,

2002). Because all of the previous parameters we have discussed are indicative of taxol-induced apoptosis in MDA-MB-231 cells, these data suggest that PARP itself is dispensable in the apoptotic pathway. This observation is supported by recent studies that have demonstrated that PARP<sup>-/-</sup> cells exhibit a normal apoptotic response to various stimuli, including TNF- $\alpha$  and anti-Fas treatment (Leist, M., *et al.*, 1997; Wang, Z.-Q., *et al.*, 1997).

To further elucidate these findings, MCF-7 and MDA-MB-231 cells were continuously exposed to taxol for different periods of time and the expression of various apoptotic regulatory proteins were examined by western blot. Because the p53 tumor suppressor gene is thought to mediate apoptosis, the expression of p53 in taxol-treated MCF-7 and MDA-MB-231 cells was assessed. Upon exposure to 100 nM taxol, the expression of p53 was significantly up-regulated in MCF-7 cells, suggesting that taxol-induced apoptosis in this cell line occurs via a p53-dependent pathway. Conversely, taxol decreased the expression of p53 in MDA-MB-231 cells following 72 hours treatment. Interestingly, the p53 gene in MDA-MB-231 cells is deleted in one allele and mutated at lys<sup>280</sup> in exon 8 in the other allele, resulting in non-functional protein (Ronnebaum, I.B., *et al.*, 1994). Hence, this result suggests that taxol-induced apoptosis in MDA-MB-231 cells occurs via a p53-independent pathway. This observation is supported by studies that have reported that taxol is capable of partly mediating apoptosis in a p53-independent pathway, although the exact mechanism for this phenomenon is not clear (Fisher, D.E., *et al.*, 1994). Perhaps, taxol can induce apoptosis in MDA-MB-231 cells, independently of p53, through other mechanisms; at the nuclear level through its endonuclease activities, at

the cell membrane through the activation of caspases, or at the mitochondria through the release of cytochrome c. Further experiments would be required to further ascertain the mechanism by which taxol induces apoptosis in MDA-MB-231 cells.

The expression level of Bcl-2 was also evaluated in MCF-7 and MDA-MB-231 cells treated with 100 nM taxol. Unexpectedly, expression of Bcl-2 was significantly up-regulated in MCF-7 cells following 24 hours exposure to taxol. Because Bcl-2 is a potent inhibitor of apoptosis, this result is not consistent with the previous results (morphological assessment, chromatin condensation and TUNEL assay) suggesting the induction of apoptosis in MCF-7 cells following 24 hours exposure to 100 nM taxol. In order to better understand this discrepancy, the constitutive levels and ratios of Bcl-2 and other anti- and pro-apoptotic members of the Bcl-2 family should be ascertained, as they are a determining factor in the control of apoptosis. However, it is possible that taxol-induced apoptosis in MCF-7 cells may have occurred via a "Bcl-2 insensitive pathway", such as that triggered by tumor necrosis factor or Fas ligand (Strasser, A., *et al.*, 2000). Additionally, Bcl-2 may have other functions that are distinct from its ability to inhibit apoptosis. Studies have suggested that overexpression of Bcl-2 may promote the exit of cells from the cell cycle, as well as prevent quiescent G<sub>0</sub>-phase cells from re-entering the cell cycle (Strasser, A., *et al.*, 1997). Hence, the increased expression of Bcl-2 in MCF-7 cells following 24 hours exposure to 100 nM taxol may help prevent cells from re-entering the cell cycle. In contrast, there was a significant down-regulation in the expression of Bcl-2 protein in MDA-MB-231 cells exposed to 100 nM taxol for 72 hours. Because Bcl-2 is a suppressor of apoptosis, this result suggests that the down-regulation

of Bcl-2 might contribute to the induction of apoptosis in taxol-treated MDA-MB-231 cells. This finding is consistent with previous studies that have demonstrated that taxol-induced cell death is associated with phosphorylation and subsequent degradation of the Bcl-2 protein (Chadebech, P., *et al.*, 1999; Kottke, T.J., *et al.*, 1999; Srivastava, R.K., *et al.*, 1999; Wang, W., *et al.*, 1999).

Studies have indicated that chemotherapeutic agent-induced apoptosis is often associated with the release of cytochrome c from the mitochondria into the cytosol, which is a critical event in the activation of caspase-9 and the induction of apoptosis (Kaufmann, S.H., *et al.*, 2000). Hence, the expression level of cytochrome c was also evaluated in MCF-7 and MDA-MB-231 cells treated with 100 nM taxol. In MCF-7 cells, there was no statistically significant change in the expression of cytochrome c when exposed to 100 nM taxol at any of the time points examined. In contrast, there was a very statistically significant up-regulation in the expression of cytochrome c in MDA-MB-231 cells when exposed to 100 nM taxol for 72 hours. Unfortunately, these results do not provide any evidence suggesting the release of cytochrome c from the mitochondria. In order to assess cytochrome c release, cell lysates should have undergone fractionation and subsequent centrifugation in order to separate mitochondrial and cytosolic fractions of cytochrome c and then western blot analysis should have been performed. Furthermore, immunohistochemistry could have also been performed to determine the localization of cytochrome c. Thus, these experiments would need to be performed in the future to assess cytochrome c release.

In conclusion, our project suggests that taxol induced apoptosis in MCF-7 and MDA-MB-231 human breast adenocarcinoma cells. Treatment of these cells with 100 nM taxol led to chromatin condensation, DNA fragmentation, and apoptosis-associated morphological changes after 3-24 hours exposure. Additionally, proteolytic cleavage of PARP was detected in MCF-7 but not MDA-MB-231 cells. To further elucidate these findings, the expression of certain apoptotic regulatory genes was also examined by western blot analysis. In MCF-7 cells, levels of Bcl-2 and p53 increased after 24 hours and 72 hours, respectively, whereas no significant change in levels of cytochrome c was found. Conversely, in MDA-MB-231 cells, levels of Bcl-2 and p53 decreased after 72 hours, whereas cytochrome c levels increased after 72 hours. These data suggest that 100 nM taxol induces apoptosis in MCF-7 and MDA-MB-231 cells, probably via a p53-dependent and independent pathway, respectively. Bcl-2 and cytochrome c, however, did not play clear roles. The information from this project may increase understanding of taxol-induced apoptosis and may aid the development of more effective taxol-based chemotherapy regimens and improved clinical responses.

## CHAPTER 6: REFERENCES

- Adjei, P.N., Kaufmann, S.H., Leung, W.Y., Mao, F. and Gores, G.J. Selective induction of apoptosis in Hep 3B cells by topoisomerase I inhibitors: evidence for a protease-dependent pathway that does not activate cysteine protease P32. *Journal of Clinical Investigation*, **98(11)**: 2588-2596 (1996).
- Agarwala, S.S. Chapter 6 Plant-Derived agents In *Current Cancer Therapeutics* First Edition. John M. Kirkwood, Michael T. Lotze and Joyce M. Yasko. Philadelphia. Princeton Academic Press, Inc. pp. 74-76 (1994).
- Al-Rubeai, M. Apoptosis and cell culture technology. *Advances in Biochemical Engineering/Biotechnology*, **59**: 225-249 (1998).
- Amato, S.F., Swart, J.M., Berg, M., Wanebo, H.J., Mehta, S.R. and Chiles, T.C. Transient stimulation of the c-Jun-NH<sub>2</sub>-terminal kinase/activator protein 1 pathway and inhibition of extracellular signal-regulated kinase are early effects in paclitaxel-mediated apoptosis in human B lymphoblasts. *Cancer Research*, **58(2)**: 241-247 (1998).
- Aoufouchi, S., Yélamos and Milstein, C. Inhibition of apoptosis of a PARP<sup>-/-</sup> cell line transfected with PARP DNA-binding domain mutants. *Journal of Molecular Biology*, **290(5)**: 943-949 (1999).
- Arends, M.J. and Wyllie, A.H. Apoptosis: mechanisms and roles in pathology. *International review of experimental pathology*, **32**: 223-254 (1991).
- Arends, M.J., Morris, R.G. and Wyllie, A.H. Apoptosis: The role of the endonuclease. *American Journal of Pathology*, **136(3)**: 593-608 (1990).
- Arver, B., Du, Q., Chen, J., Luo, L. and Lindblom, A. Hereditary breast cancer: a review. *Seminars in Cancer Biology*, **10(4)**: 271-288 (2000).
- Au, J.L.S., Panchal, N., Li, D. and Gan, Y. Apoptosis: A new pharmacodynamic endpoint. *Pharmaceutical Research*, **14(12)**: 1659-1671 (1997).
- Beech, D.J., Parekh, N. and Pang, Y. Insulin-like growth factor-I receptor antagonism results in increased cytotoxicity of breast cancer cells to doxorubicin and taxol. *Oncology Reports*, **8(2)**:325-329 (2001).
- Belotti, D., Vergani, V., Drudis, T., Borsotti, P., Pitelli, M.R., Viale, G., Giavazzi, R. and Taraboletti, G. The microtubule-affecting drug paclitaxel has antiangiogenic activity. *Clinical Cancer Research*, **2(11)**: 1843-1849 (1996).

Bhalla, K., Ibrado, A.M., Tourkina, E., Tang, C., Mahoney, M.E. and Huang, Y. Taxol induces internucleosomal DNA fragmentation associated with programmed cell death in human myeloid leukemia cells. *Leukemia*, **7(4)**: 563-568 (1993).

Bissery, M.C., Guenard, D., Gueritte-Voegelein, F. and Lavelle, F. Experimental antitumor activity of taxotere (RP 56976, NSC 628503), a taxol analogue. *Cancer Research*, **51(18)**: 4845-4852 (1991).

Bissett, D. and Kaye, S.B. Taxol and taxotere-current status and future prospects. *European Journal of Cancer*, **29A(9)**: 1228-1231 (1993).

Blagosklonny, M.V., Robey, R., Sheikh, M.S. and Fojo, T. Paclitaxel-induced FasL-independent apoptosis and slow (non-apoptotic) cell death. *Cancer Biology and Therapy*, **1(2)**: 113-117 (2002).

Blagosklonny, M.V. Unwinding the loop of Bcl-2 phosphorylation. *Leukemia*: **15(6)**: 869-874 (2001).

Blagosklonny, M.V., Schulte, T., Nguyen, P., Trepel, J. and Neckers, L.M. Taxol-induced apoptosis and phosphorylation of Bcl-2 protein involves c-Raf-1 and represents a novel c-Raf-1 signal transduction pathway. *Cancer Research*, **56(8)**: 1851-1854 (1996).

Blajeski, A.L., Kottke, T.J. and Kaufmann, S.H. A multistep model for paclitaxel-induced apoptosis in human breast cancer cell lines. *Experimental Cell Research*, **270(2)**: 277-288 (2001).

Blankenberg, F.G., Tait, J., Ohtsuki, K. and Strauss, H.W. Apoptosis: the importance of nuclear medicine. *Nuclear Medicine Communications*, **21(3)**: 241-250 (2000).

Blume, E. Government moves to increase taxol supply. *Journal of the National Cancer Institute*, **83(15)**: 1054-1056 (1991).

Blume, E. Investigators seek to increase taxol supply. *Journal of the National Cancer Institute*, **81(15)**: 1122-1123 (1989).

Bossy-Wetzel, E. and Green, D.R. Apoptosis: checkpoint at the mitochondrial frontier. *Mutation Research*, **434(3)**: 243-251 (1999).

Boyer, P.D., Chance, B., Ernster, L., Mitchell, P., Racker, E. and Slater, E.C. Oxidative phosphorylation and photophosphorylation. *Annual Review of Biochemistry*, **46**: 955-966 (1977).

- Budihardjo, I.I., Poirier, G.G. and Kaufmann, S.H. Apparent cleavage of poly(ADP-ribose) polymerase in non-apoptotic mouse LTA cells: an artifact of cross-reactive secondary antibody. *Molecular and Cellular Biochemistry*, **178(1-2)**: 245-249 (1998).
- Burkhart, C.A., Berman, J.W., Swindell, C.S. and Horwitz, S.B. Relationship between the structure of taxol and other taxanes on induction of tumor necrosis factor- $\alpha$  gene expression and cytotoxicity. *Cancer Research*, **54(22)**: 5779-5782 (1994).
- Burris, H.A. 3<sup>rd</sup> Pharmaceutical issues of paclitaxel. Preclinical pharmacology and phase I clinical trials. *The Annals of Pharmacotherapy*, **28(5 Suppl)**: S7-S10 (1994).
- Cailleau, R., Young, R., Olivé, M. and Reeves, W.J., Jr. Breast tumor cell lines from pleural effusion. *Journal of the National Cancer Institute*, **53(3)**: 661-667 (1974).
- Campbell, J.B. Breast cancer-race, ethnicity, and survival: a literature review. *Breast Cancer Research and Treatment*, **74(2)**: 187-192 (2002).
- Canman, C.E. and Kastan, M.B. Induction of apoptosis by tumor suppressor genes and oncogenes. *Seminars in Cancer Biology*, **6(1)**: 17-25 (1995).
- Carolin, K.A. and Pass. H.A. Prevention of breast cancer. *Critical Reviews in Oncology/Hematology*, **33(3)**: 221-238 (2000).
- Carson, D.A. and Ribeiro, J.M. Apoptosis and disease. *Lancet*, **341(8855)**: 1251-1254 (1993).
- Cella, D.F. Chapter 7 Using quality-of-life and cost-utility assessments in Cancer Treatment Decisions In Handbook of Cancer Chemotherapy Fourth Edition. R.T. Skeel and N.A. Lachant. New York. Little, Brown and Company. pp 80-94 (1995).
- Chadebech, P., Bricchese, L., Baldin, V., Vidal, S. and Valette, A. Phosphorylation and proteasome-dependent degradation of Bcl-2 in mitotic-arrested cells after microtubule damage. *Biochemical and Biophysical Research Communications*, **262(3)**: 823-827 (1999).
- Chen, Q., Gong, B. and Almasan, A. Distinct stages of cytochrome c release from mitochondria: evidence for a feedback amplification loop linking caspase activation to mitochondrial dysfunction in genotoxic stress induced apoptosis. *Cell Death and Differentiation*, **7(2)**: 227-233 (2000).
- Cheng, S.C., Luo, D. and Xie, Y. Taxol induced Bcl-2 protein phosphorylation in human hepatocellular carcinoma QGY-7703 cell line. *Cell Biology International*, **25(3)**: 261-265 (2001).

- Cohen, G.M., Sun, X.M., Snowden, R.T., Dinsdale, D. and Skilleter, D.N. Key morphological features of apoptosis may occur in the absence of internucleosomal DNA fragmentation. *Biochemical Journal*, **286**(pt2): 331-334 (1992).
- Darzynkiewicz, Z., Bedner, E. and Smolewski, P. Flow cytometry in analysis of cell cycle and apoptosis. *Seminars in Hematology*, **38**(2): 179-193 (2001).
- Darzynkiewicz, Z., Juan, G. and Traganos, F. Assaying drug-induced apoptosis. *Methods in Molecular Biology*, **95**: 241-254 (2001).
- Darzynkiewicz, Z. and Traganos, F. Measurement of apoptosis. *Advances in Biochemical Engineering/Biotechnology*, **62**: 33-73 (1998).
- Darzynkiewicz, Z., Juan, G., Li, X., Gorczyca, W., Murakami, T. and Traganos, F. Cytometry in cell necrobiology: analysis of apoptosis and accidental cell death (necrosis). *Cytometry* **27**(1): 1-20 (1997).
- Darzynkiewicz, Z., Bruno, S., DelBino, G., Gorczyca, W., Hotz, M.A., Lassota, P. and Traganos, F. Features of apoptotic cells measured by flow cytometry. *Cytometry*, **13**(8): 795-808 (1992).
- DeLap, R.J. Chapter 3 Antimetabolic agents In Current Cancer Therapeutics First Edition. John M. Kirkwood, Michael T. Lotze and Joyce M. Yasko. Philadelphia. Princeton Academic Press, Inc. pp. 32-47 (1994).
- Denecker, G., Dooms, H., Van Loo, G., Vercammen, D., Grooten, J., Fiers, W., Declercq, W. and Vandenaebelle, P. Phosphatidylserine exposure during apoptosis precedes release of cytochrome c and decrease in mitochondrial transmembrane potential. *FEBS Letters*, **465**(1): 47-52 (2000).
- Devaux, P.F. Static and dynamic lipid asymmetry in cell membranes. *Biochemistry*, **30**(5): 1163-1173 (1991).
- Dixon, S.C., Soriano, B.J., Lush, R.M., Borner, M.M. and Figg, W.D. Apoptosis: its role in the development of malignancies and its potential as a novel therapeutic target. *The Annals of Pharmacotherapy*, **31**(1): 76-82 (1997).
- Dorr, R.T. Pharmacology and toxicology of Cremophor EL diluent. *The Annals of Pharmacotherapy*, **28**(5 suppl): S11-S14 (1994).
- Duriez, P.J. and Shah, G.M. Cleavage of poly(ADP-ribose) polymerase: a sensitive parameter to study cell death. *Biochemistry and Cell Biology*, **75**(4): 337-349 (1997).

- Duvall, E., Wyllie, A.H. and Morris, R.G. Macrophage recognition of cells undergoing programmed cell death (apoptosis). *Immunology*, **56**(2): 351-358 (1985).
- Eguchi, Y., Shimizu, S. and Tsujimoto, Y. Intracellular ATP levels determine cell fate by apoptosis or necrosis. *Cancer Research*, **57**(10): 1835-1840 (1997).
- Elstein, K.H. and Zucker, R.M. Comparison of cellular and nuclear flow cytometric techniques for discriminating apoptotic subpopulations. *Experimental Cell Research*, **211**(2): 322-331 (1994).
- Elstner, E., Linker-Israeli, M., Said, J., Umiel, T., deVos, S., Shintaku, I.P., Heber, D., Binderup, L., Uskokovic, M. and Koeffler, H.P. 20-epi-vitamin D3 analogues: a novel class of potent inhibitors of proliferation and inducers of differentiation of human breast cancer cell lines. *Cancer Research*, **55**(13): 2822-2830 (1995).
- Fadok, V.A., Bratton, D.L., Frasch, S.C., Warner, M.L. and Henson, P.M. The role of phosphatidylserine in recognition of apoptotic cells by phagocytes. *Cell Death and Differentiation*, **5**(7): 551-562 (1998).
- Fadok, V.A., Voelker, D.R., Campbell, P.A., Cohen, J.J., Bratton, D.L. and Henson, P.M. Exposure of phosphatidylserine on the surface of apoptotic lymphocytes triggers recognition and removal by macrophages. *Journal of Immunology*, **148**(7): 2207-2216 (1992).
- Fan, W. Possible mechanisms of paclitaxel-induced apoptosis. *Biochemical Pharmacology*, **57**(11): 1215-1221 (1999).
- Fisher, D.E. Apoptosis in cancer therapy: crossing the threshold. *Cell*, **78**(4): 539-542 (1994).
- Fisher, D.E., Bodis, S., Lowe, S., Takemoto, C., Housman, D. and Jacks, T. *Blood*, **84**: 111a (abstract) (1994).
- Fojo, T. and Giannakakou, P. Taxol and other microtubule-interactive agents. *Current Opinion in Oncologic, Endocrine and Metabolic Investigational Drugs*, **2**(3): 293-304 (2000).
- Goldspiel, B.R. Pharmaceutical issues: preparation, administration, stability, and compatibility with other medications. *The Annuals of Pharmacotherapy*, **28**(5 suppl): S23-S26 (1994).

- Goldstein, J.C., Waterhouse, N.J., Juin, P., Evan, G.I. and Green, D.R. The coordinate release of cytochrome c during apoptosis is rapid, complete and kinetically invariant. *Nature Cell Biology*, **2(3)**: 156-162 (2000).
- Gong, J., Traganos, F. and Darzynkiewicz, Z. A selective procedure for DNA extraction from apoptotic cells applicable for gel electrophoresis and flow cytometry. *Analytical Biochemistry*, **218(2)**: 314-319 (1994).
- Gorczyca, W., Melamed, M.R. and Darzynkiewicz, Z. Analysis of apoptosis by flow cytometry. *Methods in Molecular Biology*, **91**: 217-238 (1998).
- Graham, S.H., Chen, J. and Clark, R.S.B. Bcl-2 family gene products in cerebral ischemia and traumatic brain injury. *Journal of Neurotrauma*, **17(10)**: 831-841 (2000).
- Green, D.R. and Reed, J.C. Mitochondria and apoptosis. *Science*, **281(5381)**: 1309-1312 (1998).
- Gregory, R.E. and DeLisa, A.F. Paclitaxel: a new antineoplastic agent for refractory ovarian cancer. *Clinical Pharmacy*, **12(6)**: 401-415 (1993).
- Guéritte-Voegelein, F., Guénard, D., Lavelle, F., Le Goff, M.T., Mangatal, L. and Potier, P. Relationships between the structure of taxol analogues and their antimitotic activity. *Journal of Medicinal Chemistry*, **34(3)**: 992-998 (1991).
- Hainaut, P. and Hollstein, M. p53 and human cancer: the first ten thousand mutations. *Advances in Cancer Research*, **77**:81-137 (2000).
- Haldar, S., Chintapalli, J. and Croce, C.M. Taxol induces Bcl-2 phosphorylation and death of prostate cancer cells. *Cancer Research*, **56(6)**: 1253-1255 (1996).
- Hall, P.A. Assessing apoptosis: a critical survey. *Endocrine-Related Cancer*, **6(1)**: 3-8 (1999).
- Hannun, Y.A. Apoptosis and the dilemma of cancer chemotherapy. *Blood*, **89(6)**: 1845-1853 (1997).
- Hartwell, L.H. and Kastan, M.B. Cell cycle control and cancer. *Science*, **266(5192)**: 1821-1828 (1994).
- He, L., Orr, G.A. and Horwitz, S.B. Novel molecules that interact with microtubules and have functional activity similar to taxol™. *Drug Discovery Today*, **6(22)**: 1153-1164 (2001).

- Hengartner, M.O. The biochemistry of apoptosis. *Nature*, **407(6805)**: 770-776 (2000).
- Herr, I. and Debatin, K-M. Cellular stress response and apoptosis in cancer therapy. *Blood*, **98(9)**: 2603-2614 (2001).
- Higgins, C.F. Flip-flop: the transmembrane translocation of lipids. *Cell*, **79**: 393-395 (1994).
- Holmes, F.A., Walters, R.S., Theriault, R.L., Forman, A.D., Newton, L.K., Raber, M.N., Buzdar, A.U., Frye, D.K., and Hortobagyi, G.N. Phase II trial of taxol, an active drug in the treatment of metastatic breast cancer. *Journal of the National Cancer Institute*, **83(24)**: 1797-1805 (1991).
- Horwitz, S.B. Mechanism of action of taxol. *Trends in Pharmacological Sciences*, **13(4)**: 134-136 (1992).
- Hsieh, T., Burfeind, P., Laud, K., Backer, J.M., Traganos, F., Darzynkiewicz, Z. and Wu, J. Cell cycle effects and control of gene expression by resveratrol in human breast carcinoma cell lines with different metastatic potentials. *International Journal of Oncology*, **15(2)**: 245-252 (1999).
- Janicke, R.U., Sprengart, M.L., Wati, M.R. and Porter, A.G. Caspase-3 is required for DNA fragmentation and morphological changes associated with apoptosis. *Journal of Biological Chemistry*, **273(16)**:9357-9360 (1998).
- Jiang, X. and Wang, X. Cytochrome c promotes caspase-9 activation by inducing nucleotide binding to apaf-1. *Journal of Biological Chemistry*, **275(40)**: 31199-31203 (2000).
- Jordan, M.A., Toso, R.J., Thrower, D. and Wilson, L. Mechanism of mitotic block and inhibition of cell proliferation by taxol at low concentrations. *Proceedings of the National Academy of Sciences USA*, **90(20)**: 9552-9556 (1993).
- Kaufmann, S.H. Induction of endonucleolytic DNA cleavage in human acute myelogenous leukemia cells by etoposide, camptothecin, and other cytotoxic anticancer drugs: a cautionary note. *Cancer Research*, **49(21)**: 5870-5878 (1989).
- Kaufmann, S.H. and Earnshaw, W.C. Induction of apoptosis by cancer chemotherapy. *Experimental Cell Research*, **256(1)**: 42-49 (2000).
- Kerr, J.F.R., Wyllie, A.H. and Currie, A.R. Apoptosis: a basic biological phenomenon with wide-ranging implications in tissue kinetics. *British Journal of Cancer*, **26(4)**: 239-257 (1972).

Kingston, D.G.I. The chemistry of taxol. *Pharmacology and Therapeutics*, **52(1)**: 1-34 (1991).

Kingston, D.G.I. Taxol: the chemistry and structure-activity relationships of a novel anticancer agent. *Trends in Biotechnology*, **12(6)**: 222-227 (1994)

Kitamura, Y., Shimohama, S., Kamoshima, W., Ota, T., Matsuoka, Y., Nomura, Y., Smith, M.A., Perry, G., Whitehouse, P.J. and Taniguchi, T. Alteration of proteins regulating apoptosis, Bcl-2, Bcl-x, Bax, Bak, Bad, Ich-1 and CPP32, in Alzheimer's disease. *Brain Research*, **780(2)**: 260-269 (1998).

Klauber, N., Parangi, S., Flynn, E., Hamel, E. and D'Amato, R.J. Inhibition of angiogenesis and breast cancer in mice by the microtubule inhibitors 2-methoxyestradiol and taxol. *Cancer Research*, **57(1)**: 81-86 (1997).

Kobayashi, K., and Vogelzang, N.J. Chapter 2 Antibiotic agents In Current Cancer Therapeutics First Edition. John M. Kirkwood, Michael T. Lotze and Joyce M. Yasko. Philadelphia. Princeton Academic Press, Inc. pp. 19-31(1994).

Kockx, M.M., Muhring, J., Knaapen, M.W. and de Meyer, G.R. RNA synthesis and splicing interferes with DNA in situ end labeling techniques used to detect apoptosis. *American Journal of Pathology*, **152(4)**: 885-888 (1998).

Kohler, D.R. and Goldspiel, B.R. Paclitaxel (Taxol). *Pharmacotherapy*, **14(1)**: 3-34 (1994).

Koopman, G., Reutelingsperger, C.P.M., Kuijten, G.A.M., Keehnen, R.M.J., Pals, S.T. and van Oers, M.H.J. Annexin v for flow cytometric detection of phosphatidylserine expression on B cells undergoing apoptosis. *Blood*, **84(5)**: 1415-1420 (1994).

Kottke, T.J., Blajeski, A.L., Meng, X.W., Svingen, P.A., Ruchaud, S., Mesner, P.W., Jr., Boerner, S.A., Samejima, K., Henriquez, N.V., Chilcote, T.J., Lord, J., Salmon, M., Earnshaw, W.C. and Kaufmann, S.H. Lack of correlation between caspase activation and caspase activity assays in paclitaxel-treated MCF-7 breast cancer cells. *Journal of Biological Chemistry*, **277(1)**: 804-815 (2002).

Kottke, T.J., Blajeski, A.L., Martins, L.M., Mesner, P.W., Jr., Davidson, N.E., Earnshaw, W.C., Armstrong, D.K. and Kaufmann, S.H. The comparison of paclitaxel-, 5-fluoro-2'-deoxyuridine-, and epidermal growth factor (EGF)-induced apoptosis. Evidence for EGF-induced anoikis. *Journal of Biological Chemistry*, **274(22)**: 15927-15936 (1999).

- Kuhn, J.G. Pharmacology and pharmacokinetics of paclitaxel. *The Annals of Pharmacotherapy*, **28(5 suppl)**: S15-S17 (1994).
- Lau, D.H., Xue, L., Young, L.J., Burke, P.A. and Cheung, A.T. Paclitaxel (Taxol): An inhibitor of angiogenesis in a highly vascularized transgenic breast cancer. *Cancer Biotherapy and Radiopharmaceuticals*, **14(1)**: 31-36 (1999).
- Leist, M., Single, B., Kunstle, G., Volbracht, C., Hentze, H. and Nicotera, P. Apoptosis in the absence of poly-(ADP-ribose) polymerase. *Biochemical and Biophysical Research Communications*, **233(2)**: 518-522 (1997).
- Levine, A.J. p53, the cellular gatekeeper for growth and division. *Cell*, **88(3)**: 323-331 (1997).
- Li, X., Melamed, M.R. and Darzynkiewicz, Z. Detection of apoptosis and DNA replication by differential labeling of DNA strand breaks with fluorochromes of different color. *Experimental Cell Research*, **222(1)**: 28-37 (1996).
- Lin, T., Brunner, T., Tietz, B., Madsen, J., Bonfoco, E., Reaves, M., Huflejt, M. and Green, D.R. Fas ligand-mediated killing by intestinal intraepithelial lymphocytes. Participation in intestinal graft-versus-host disease. *Journal of Clinical Investigation*, **101(3)**: 570-577 (1998).
- Liu, D. and Huang, Z. Synthetic peptides and non-peptidic molecules as probes of structure and function of Bcl-2 family proteins and modulators of apoptosis. *Apoptosis*, **6(6)**: 453-462 (2001).
- Liu, Y., Bhalla, K., Hill, C. and Priest, D.G. Evidence for involvement of tyrosine phosphorylation in taxol-induced apoptosis in a human ovarian tumor cell line. *Biochemical Pharmacology*, **48(6)**: 1265-1272 (1994).
- Liu, Z., Brattain, M.G. and Appert, H. Differential display of reticulocalbin in the highly invasive cell line, MDA-MB-435, versus the poorly invasive cell line, MCF-7. *Biochemical and Biophysical Research Communications*, **231(2)**: 283-289 (1997).
- Lorenzen, J., Thiele, J. and Fischer, R. The mummified Hodgkin cell: cell death in Hodgkin's disease. *Journal of Pathology*, **182(3)**: 288-298 (1997).
- Lowry, O. H., Rosebrough, N.J., Farr, A.L. and Randall, R. J. Protein measurement with the folin phenol reagent. *Journal of Biological Chemistry*, **193**: 265-275 (1951).
- MacDonald, F. and Ford, C.H.J. Chapter 1 General principles In *Molecular Biology of Cancer*, BIOS Scientific Publishers Ltd., Oxford, pp 1-11 (1997).

- Majno, G. and Joris, I. Apoptosis, oncosis and necrosis. An overview of cell death. *American Journal of Pathology*, **146(1)**: 3-15 (1995).
- Manfredi, J.J. and Horwitz, S.B. Taxol: an antimitotic agent with a new mechanism of action. *Pharmacology and Therapeutics*. **25(1)**: 83-125 (1984).
- May, D.M. and Morgan, B. Chapter 1 Alkylating agents In Current Cancer Therapeutics First Edition. John M. Kirkwood, Michael T. Lotze and Joyce M. Yasko. Philadelphia. Princeton Academic Press, Inc. pp. 1-18 (1994).
- McCloskey, D.E., Kaufmann, S.H., Prestigiacomo, L.J. and Davidson, N.E. Paclitaxel induces programmed cell death in MDA-MB-468 human breast cancer cells. *Clinical Cancer Research*, **2(5)**: 847-854 (1996).
- McKenna, S.L., McGowan, A.J. and Cotter, T.G. Molecular mechanisms of programmed cell death. *Advances in Biochemical Engineering Biotechnology*, **62**: 1-31 (1998).
- Merrick, H.W. Principles of Surgery in Cancer Management In Handbook of Cancer Chemotherapy Fourth Edition. R.T. Skeel and N.A. Lachant. New York. Little, Brown and Company. pp.46-51 (1995).
- Miyashita, T. and Reed, J.C. Tumor suppressor p53 is a direct transcriptional activator of the human Bax gene. *Cell*, **80(2)**: 293-299 (1995).
- Moos, P.J. and Fitzpatrick, F.A. Taxane-mediated gene induction is independent of microtubule stabilization: induction of transcription regulators and enzymes that modulate inflammation and apoptosis. *Proceedings of the National Academy of Sciences USA*, **95(7)**: 3896-3901 (1998).
- Morris, R.G., Hargreaves, A.D., Duval, E. and Wyllie, A.H. Hormone-induced cell death surface changes in thymocytes undergoing apoptosis. *American Journal of Pathology*, **115(3)**: 426-436 (1984).
- Mosmann, T. Rapid colorimetric assay for cellular growth and survival: Application to proliferation and cytotoxicity assays. *Journal of Immunological Methods*, **65(1-2)**: 55-63 (1983).
- Mowat, M.R.A. p53 in tumor progression: life, death, and everything. *Advances in Cancer Research*, **74**: 25-48 (1998).
- Mower, D.A. Jr., Peckham, D.W., Illera, V.A., Fishbaugh, J.K., Stunz, L.L. and Ashman, R.F. Decreased membrane phospholipid packing and decreased cell size precede DNA

cleavage in mature mouse B cell apoptosis. *Journal of Immunology*, **152(10)**: 4832-4842 (1994).

National Cancer Institute of Canada: Canadian Cancer Statistics 2003, Toronto, Canada, 2003.

Nicolaou, K.C., Yang, Z., Liu, J.J., Ueno, H., Biediger, R.J. and Guy, R.K. Total synthesis of taxol. *Nature*, **367(6464)**: 630-634 (1994).

Nowell, P.C. The clonal evolution of tumor cell populations. *Science*, **194(4260)**: 23-28 (1976).

O'Connor, P.M. Mammalian G<sub>1</sub> and G<sub>2</sub> phase checkpoints. *Cancer Surveys*, **29**: 151-182 (1997).

Oberhammer, F., Fritsch, G., Pavelka, M., Froschi, G., Tiefenbacher, R., Purchio, T. and Schulte-Hermann, R. Induction of apoptosis in cultured hepatocytes and in the regressing liver by transforming growth factor-beta 1 occurs without activation of an endonuclease. *Toxicology Letters*, **64-65**: 701-704 (1992).

Panchagnula, R. Pharmaceutical aspects of paclitaxel. *International Journal of Pharmaceutics*, **172**: 1-15 (1998).

Parone, P.A., James, D. and Martinou, J.C. Mitochondria: regulating the inevitable. *Biochimie*, **84(2-3)**: 105-111 (2002).

Patel, T., Gores, G.J. and Kaufmann, S.H. The role of proteases during apoptosis. *FASEB*, **10(5)**: 587-597 (1996).

Peterson, G.L. Review of the folin phenol protein quantitation method of Lowry, Rosebrough, Farr and Randall. *Analytical Biochemistry*, **100**: 201-220 (1979).

Pinton, P., Ferrari, D., Di Virgilio, F., Pozzan, T. and Rizzuto, R. Molecular machinery and signaling events in apoptosis. *Drug Development Research* **52**: 558-570 (2001).

Rao, S., Krauss, N.E., Heerding, J.M., Swindell, C.S., Ringel, I., Orr, G.A. and Horwitz, S.B. 3'-(p-azidobenzamido)taxol photolabels the N-terminal 31 amino acids of  $\beta$ -tubulin. *Journal of Biological Chemistry*, **269(5)**: 3132-3134 (1994).

Ringel, I. and Horwitz, S.B. Studies with RP 56976 (Taxotere): a semisynthetic analogue of taxol. *Journal of the National Cancer Institute*, **83(4)**: 288-291 (1991).

- Rowinsky, E.K. The development and clinical utility of the taxane class of antimicrotubule chemotherapy agents. *Annual Review of Medicine*, **48**: 353-374 (1997).
- Rowinsky, E.K. and Donehower, R.C. Paclitaxel (Taxol). *New England Journal of Medicine*, **332(15)**: 1004-1014 (1995).
- Rowinsky, E.K. Clinical Pharmacology of taxol. *Journal of the National Cancer Institute Monographs*, **(15)**: 25-37 (1993).
- Rowinsky, E.K., Eisenhauer, E.A., Chaudhry, V., Arbusk, S.G. and Donehower, R.C. Clinical toxicities encountered with paclitaxel (Taxol). *Seminars in Oncology*, **20(4 suppl 3)**: 1-15 (1993).
- Runnebaum, I.B., Yee, J.K., Kieback, D.G., Sukumar, S. and Friedmann, T. Wild-type p53 suppresses the malignant phenotype in breast cancer cells containing mutant p53 alleles. *Anticancer Research*, **14(3A)**: 1137-1144 (1994).
- Sallmann, F.R., Bourassa, S., Saint-Cyr, J. and Poirier, G.G. Characterization of antibodies specific for the caspase cleavage site on poly(ADP-ribose)polymerase: specific detection of apoptotic fragments and mapping of the necrotic fragments of poly(ADP-ribose)polymerase. *Biochemistry and Cell Biology*, **75(4)**: 451-456 (1997).
- Samejima, K., Svingen, P.A., Basi, G.S., Kottke, T.J., Mesner, P.W., Jr., Stewart, L., Durrieu, F., Poirier, G.G., Alnemri, E.S., Champoux, J.J., Kaufmann, S.H. and Earnshaw, W.C. Caspase-mediated cleavage of DNA topoisomerase I at unconventional sites during apoptosis. *Journal of Biological Chemistry*, **274(7)**: 4335-4340 (1999).
- Saunders, D.E., Lawrence, W.D., Christensen, C., Wappler, N.L., Ruan, H. and Deppe, G. Paclitaxel-induced apoptosis in MCF-7 breast-cancer cells. *International Journal of Cancer*, **70(2)**: 214-220 (1997).
- Savill, J.S., Henson, P.M. and Haslett, C. Phagocytosis of aged human neutrophils by macrophages is mediated by a novel "charge sensitive" recognition mechanism. *The Journal of Clinical Investigation*, **84(5)**: 1518-1527 (1989).
- Shall, S. and de Murcia, G. Poly(ADP-ribose)polymerase-1: what have we learned from the deficient mouse model? *Mutation Research*, **460(1)**: 1-15 (2000).
- Shen, Y. and White, E. p53-dependent apoptosis pathways. *Advances in Cancer Research*: **82**: 55-84 (2001).
- Shtil, A.A., Mandlikar, S., Yu, R., Walter, R.J., Hagen, K., Tan, T-H., Roninson, I.B. and Kong, A-N.T. Differential regulation of mitogen-activated protein kinases by

microtubule-binding agents in human breast cancer cells. *Oncogene*, **18(2)**: 377-384 (1999).

Sikorska, M, and Walker, P.R. Endonuclease activities and apoptosis. In *Physiological Cell Death*. R.A. Lockshin, J.L. Tilly and Z. Zakeri. New York. Wiley-Liss, Inc. pp.211-242 (1997).

Singh, N.P. A simple method for accurate estimation of apoptotic cells. *Experimental Cell Research*, **256(1)**: 328-337 (2000).

Skeel (a), R.T. Selection of treatment for the patient with cancer In *Handbook of Cancer Chemotherapy Fourth Edition*. R.T. Skeel and N.A. Lachant. New York. Little, Brown and Company. pp. 116-120 (1995).

Skeel (b), R.T. Antineoplastic drugs and biologic response modifiers: classification, use, and toxicity of clinically useful agents In *Handbook of Cancer Chemotherapy Fourth Edition*. R.T. Skeel and N.A. Lachant. New York. Little, Brown and Company. pp. 123-126 (1995).

Skeel (c), R.T. Antineoplastic drugs and biologic response modifiers: classification, use, and toxicity of clinically useful agents In *Handbook of Cancer Chemotherapy Fourth Edition*. R.T. Skeel and N.A. Lachant. New York. Little, Brown and Company. pp.126-127 (1995).

Skeel (d), R.T. Antineoplastic drugs and biologic response modifiers: classification, use, and toxicity of clinically useful agents In *Handbook of Cancer Chemotherapy Fourth Edition*. R.T. Skeel and N.A. Lachant. New York. Little, Brown and Company. pp.128 (1995).

Sladowski, D., Steer, S.J., Clothier, R.H. and Balls, M. An improved MTT assay. *Journal of Immunological Methods*, **157(1-2)**: 203-207 (1993).

Soldani, C. and Scovassi, A.I. Poly (ADP-ribose) polymerase-1 cleavage during apoptosis: an update. *Apoptosis*, **7(4)**: 321-328 (2002).

Soldani, C., Lazzè, M.C., Bottone, M.G., Tognon, G., Biggiogera, M., Pellicciari, C.E. and Scovassi, A.I. Poly(ADP-ribose) polymerase cleavage during apoptosis: when and where? *Experimental Cell Research*, **269(2)**: 193-201 (2001).

Soldatenkov, V.A. and Smulson, M. Poly(ADP-ribose)polymerase in DNA damage-response pathway: implications for radiation oncology. *International Journal of Cancer (Radiation Oncology Investigations)*, **90(2)**: 59-67 (2000).

Soule, H.D., Vazquez, J., Long, A., Albert, S. and Brennan, M. A human cell line from a pleural effusion derived from a breast carcinoma. *Journal of the National Cancer Institute*, **51(5)**: 1409-1413 (1973).

Soussi, T. p53 antibodies in the sera of patients with various types of cancer: a review. *Cancer Research*, **60(7)**: 1777-1788 (2000).

Srivastava, R.K., Sasaki, C.Y., Hardwick, J.M. and Longo, D.L. Bcl-2 mediated drug resistance: inhibition of apoptosis by blocking nuclear factor of activated T lymphocytes (NFAT)-induced Fas ligand transcription. *Journal of Experimental Medicine*, **190(2)**: 253-265 (1999).

Strasser, A., O'Connor, L. and Dixit, V.M. Apoptosis signaling. *Annual Review of Biochemistry*, **69**: 217-245 (2000).

Strasser, A., Huang, D.C.S. and Vaux, D.L. The role of the bcl-2/ced-9 gene family in cancer and general implications of defects in cell death control for tumorigenesis and resistance to chemotherapy. *Biochimica et Biophysica Acta*, **1333(2)**: F151-F178 (1997).

Stierle, A., Strobel, G. and Stierle, D. Taxol and taxane production by *Taxomyces andreanae*, an endophytic fungus of pacific yew. *Science*, **260(1505)**: 214-216 (1993).

Strobl, J.S., Melkounian, Z., Peterson, V.A., and Hylton, H. The cell death response to  $\gamma$ -radiation in MCF-7 cells is enhanced by a neuroleptic drug, pimozide. *Breast Cancer Research and Treatment*, **51(1)**: 83-95 (1998).

Theodoropoulos, P.A., Polioudaki, H., Kostaki, O., Derdas, S.P., Georgoulas, V., Dargemont, C. and Georgatos, S.D. Taxol affects nuclear lamina and pore complex organization and inhibits import of karyophilic proteins into the cell nucleus. *Cancer Research*, **59(18)**: 4625-4633 (1999).

Thompson, C.B. Apoptosis in the pathogenesis and treatment of disease. *Science*, **267(5203)**: 1456-1462 (1995).

Tsujimoto, Y. and Shimizu, S. Bcl-2 family: life-or-death switch. *FEBS Letters*, **466(1)**: 6-10 (2000).

Tudor, G., Aguilera, A., Halverson, D.O., Laing, N.D. and Sausville, E.A. Susceptibility to drug-induced apoptosis correlates with differential modulation of Bad, Bcl-2 and Bcl-X<sub>1</sub> protein levels. *Cell Death and Differentiation*, **7(6)**: 574-586 (2000).

Tzima, E. and Walker, J.H. Platelet annexin v: the ins and outs. *Platelets*, **11(5)**: 245-251 (2000).

- van Engeland, M., Schutte, B, Hopman, A.H.N., Ramaekers, F.C.S. and Reutelingsperger, C.P.M. In Apoptosis A practical approach. G.P. Studzinski. New York. Oxford University Press Inc. pp.125-140 (1999).
- van Engeland, M., Nieland, L.J.W., Ramaekers, F.C.S., Schutte, B. and Reutelingsperger, C.P.M. Annexin V-affinity assay: a review on an apoptosis detection system based on phosphatidylserine exposure. *Cytometry*, **31(1)**: 1-9 (1998).
- van Engeland, M., Ramaekers, F.C.S., Schutte, B. and Reutelingsperger, C.P.M. A novel assay to measure loss of plasma membrane asymmetry during apoptosis of adherent cells in culture. *Cytometry*, **24(2)**: 131-139 (1996).
- van Heerde, W.L., Robert-Offerman, S., Dumont, E., Hofstra, L., Doevendans, P.A., Smits, J.F.M., Daemem, M.J.A.P. and Reutelingsperger, C.P.M. Markers of apoptosis in cardiovascular tissues: focus on annexin V. *Cardiovascular Research*, **45(3)**: 549-559 (2000).
- Vermes, I., Haanen, C., Steffens-Nakken, H. and Reutelingsperger, C.P.M. A novel assay for apoptosis. Flow cytometric detection of phosphatidylserine expression on early apoptotic cells using fluorescein labeled annexin V. *Journal of Immunological Methods*, **184(1)**: 39-51 (1995).
- Von Ahsen, O., Waterhouse, N.J., Kuwana, T., Newmeyer, D.D. and Green, D.R. The 'harmless' release of cytochrome c. *Cell Death and Differentiation*, **7(12)**: 1192-1199 (2000).
- Walker, P.R. and Sikorska, M. New Aspects of the mechanism of DNA fragmentation in apoptosis. *Biochemistry and Cell Biology*, **75(4)**: 287-299 (1997).
- Walker, P.R., LeBlanc, J., Carson, C., Ribocco, M. and Sikorska, M. Neither caspase-3 nor DNA fragmentation factor is required for high molecular weight DNA degradation in apoptosis. *Annals of the New York Academy of Sciences*, **887**: 48-59 (1999).
- Walker, P.R., Weaver, V.M., Lach, B., LeBlanc, J. and Sikorska, M. Endonuclease activities associated with high molecular weight and internucleosomal DNA fragmentation in apoptosis. *Experimental Cell Research*, **213(1)**: 100-106 (1994).
- Wang, L., Klimpel, G.R., Planas, J.M., Li, H. and Cloyd, M.W. Apoptotic killing of CD4<sup>+</sup> T lymphocytes in HIV-1-infected PHA-stimulated PBL cultures is mediated by CD8<sup>+</sup> LAK cells. *Journal of Virology*. **241(2)**: 169-180 (1998).

- Wang, W. and Passaniti, A. Extracellular matrix inhibits apoptosis and enhances endothelial cell differentiation by a NFKappaB-dependent mechanism. *Journal of Cellular Biochemistry*, **73(3)**: 321-331 (1999).
- Wang, Z.-Q., Stingl, L., Morrison, C., Jantsch, M., Los, M., Schulze-Osthoff, K. and Wagner, E.F. PARP is important for genomic stability but dispensable in apoptosis. *Genes and Development*, **11(18)**: 2347-2358 (1997).
- Weiss, R.B., Donehower, R.C., Wiernik, P.H., Ohnuma, T., Gralla, R.J., Trump, D.L., Baker, J.R. Jr., van Echo, D.A., von Hoff, D.D. and Leyland-Jones, B. Hypersensitivity reactions from taxol. *Journal of Clinical Oncology, Official Journal of the American Society of Clinical Oncology*, **8(7)**: 1263-1268 (1990).
- Wen, L-P., Fahrni, J.A., Troie, S., Guan, J.L., Orth, K. and Rosen, G.P. Cleavage of focal adhesion kinase by caspases during apoptosis. *Journal of Biological Chemistry*, **272(41)**: 26056-26061 (1997).
- Williams, G.T. Programmed cell death: apoptosis and oncogenesis. *Cell*, **65(7)**: 1097-1098 (1991).
- Wilson, J.W. and Potten, C.S. In Apoptosis A practical approach. G.P. Studzinski. New York. Oxford University Press Inc. pp. 23-27 (1999).
- Wingo, P.A., Tong, T. and Bolden, S. Cancer Statistics, 1995. *CA A Cancer Journal for Clinicians*, **45(1)**: 8-30 (1995).
- Wyllie, A.H., Kerr, J.F.R. and Currie, A.R. Cell death: the significance of apoptosis. *International Review of Cytology*, **68**: 251-306 (1980).
- Yang, X., Hao, Y., Pater, M.M., Tang, S-C. and Pater, A. Enhanced expression of anti-apoptotic proteins in human papillomavirus-immortalized and cigarette smoke condensate-transformed human endocervical cells: correlation with resistance to apoptosis induced by DNA damage. *Molecular Carcinogenesis*, **22(2)**: 95-101 (1998).
- Yeh, E.T.H. Life and death of the cell. *Hospital Practice*, **33(8)**: 85-87, 91-92 (1998).
- Zambetti, G.P. and Levine, A. J., A comparison of the biological activities of wild-type and mutant p53. *FASEB Journal*, **7(10)**: 855-865 (1993).
- Zörnig, M., Hueber, A-O., Baum, W. and Evan, G. Apoptosis regulators and their role in tumorigenesis. *Biochimica et Biophysica Acta*, **1551(2)**: F1-F37 (2001).





